Application to Food Standards Australia New Zealand for the Inclusion of Canola MON 94100 in *Standard 1.5.2 - Food Derived from Gene Technology*

Submitted by:

Bayer CropScience Proprietary Limited
Level 1, 8 Redfern Road
Hawthorn East, Victoria 3123

28 September, 2020

TABLE OF CONTENTS

LIST OF FIGURES

LIST OF TABLES

UNPUBLISHED REPORTS BEING SUBMITTED

Appendix 1. [redacted]. 2020. Amended from MSL0030076: Molecular Characterization of Dicamba Tolerant Canola (MON 94100). **TRR0000306**. Monsanto Company. (CBI)

Appendix 2. [redacted]. 2019. Bioinformatics Evaluation of the T-DNA in MON 94100 Utilizing the AD_2019, TOX_2019, and PRT_2019 Databases. **MSL0030274.** Monsanto Company.

Appendix 3. [redacted]. 2019. Bioinformatics Evaluation of Putative Flank-Junction Peptides in MON 94100 Utilizing the AD_2019, TOX_2019, and PRT_2019, Databases. **MSL0030273.** Monsanto Company.

Appendix 4. [redacted] 2019. Segregation Analysis of the T-DNA Insert in Herbicide Tolerant Canola MON 94100 Across Three Generations. **MSL0030193.** Monsanto Company.

Appendix 5. [redacted] 2019. Demonstration of the Presence of DMO Protein in Canola Grain Samples Across Multiple Generations of MON 94100. **MSL0030222.** Monsanto Company.

Appendix 6. [redacted] 2019. Characterization of the MON 94100-Produced DMO Protein Purified from the Canola Seed and Comparison of the Physicochemical and Functional Properties of the MON 94100-produced and MON 87708-produced DMO Proteins. **MSL0030875.** Monsanto Company.

Appendix 7. [redacted] 2019. Amended from MSL0030665: Assessment of DMO Protein Levels in Treated Canola Tissues Collected from MON 94100 Produced in United States and Canadian Field Trials During 2018. **MSL0030937.** Monsanto Company.

Appendix 8. [redacted] 2019. Updated Bioinformatics Evaluation of DMO+27 Utilizing the AD_2019, TOX_2019, and PRT_2019 Databases. **MSL0030271.** Monsanto Company.

Appendix 9. [redacted]. 2020. Summary of the Magnitude of Residues of Dicamba in Grain Following Applications to Dicamba-Tolerant Canola, MON 94100. **MSL0030924**. Monsanto Company.

Appendix 10. [redacted] 2019. Compositional Analyses of Canola Seed from MON 94100 Grown in the United States and Canada During the 2018 Season. **MSL0030455.** Monsanto Company.

CHECKLIST

General Requirements (3.1.1)	Reference
A Form of application	
☑ *Application in English*	*Available*
☑ *Executive Summary (separated from main application electronically)*	*Separate document prepared*
☑ *Relevant sections of Part 3 clearly identified*	*Completed*
☑ *Pages sequentially numbered*	*Completed*
☑ *Electronic copy (searcahable)*	*Prepared*
☑ *All references provided*	*Prepared*
B Applicant details	*Page 1*
C Purpose of the application	*Page 1*
D Justification for the application	
☑ *Regulatory impact information*	*Page 3*
☑ *Impact of international trade*	*Page 4**Error! Bookmark not defined.***
E Information to support the application	
☑ *Data requirement*	*Appendices 1 - 10*
F Assessment procedure	
☑ *General*	*Page 4*
☐ *Major*	
☐ *Minor*	
☐ *Hight level heath claim variation*	
G Confidential Commercial Information	
☑ *CCI material separated from other application material*	*Completed*
☐ *Formal request including reasons*	
☐ *Non-confidential summary provided*	
H Other confidential information	
☑ *Confidential material separated from other application material*	*Completed*
☐ *Formal request including reasons*	
I Exclusive Capturable Commercial Benefit	

☑ *Justification provided*	*Page 4*
J International and Other National Standards	
☑ *International standards*	*Page 4*
☑ *Other national standards*	*Page 4*
K Statutory Declaration	*Page 116*
L Checklist/s provided with Application	
☑ *3.1.1 Checklist*	*Page viii*
☑ *All page number references from application included*	*Completed*
☑ Any other relevant checklists for Sections 3.2 – 3.7	*Checklist 3.5.1*

Foods Produced using Gene Technology (3.5.1)	
☑ A.1 Nature and identity of the GM food	*Page 5*
☑ A.2 History of use of host and donor organisms	*Page 6*
☑ A.3 Nature of genetic modification	*Page 10*
☑ B.1 Characterisation and safety assessment	*Page 49*
☑ B.2 New proteins	*Page 70*
☑ B.3 Other (non-protein) new sustances	*Page 94*
☑ B.4 Novel herbicide metabolites in GM herbicide-tolerant plants	*Page 95*
☑ B.5 Compositional analyse	*Page 100*
☑ C Nutritional impact of GM food	*Page 115*
☑ D Other information	*Page 115*

ABBREVIATIONS AND DEFINITIONS[1]

AA	Amino Acid
ADF	Acid Detergent Fiber
APHIS	Animal and Plant Health Inspection Service
BBCH	Biologische Bundesanstalt, Bundessortenamt und CHemische Industrie
BP	Basepair
COMPARE	COMprehensive Protein Allergen Resource
CTP	Chloroplast Transit Peptide
DCSA	3,6-Dichlorosalycilic Acid
DMO	Dicamba Mono-Oxygenase
DNA	Deoxyribonucleic Acid
dw	Dry Weight
E. coli	*Escherichia coli*
ELISA	Enzyme-linked Immunosorbent Assay
EPA	Environmental Protection Agency
EPSPS	5-enolpyruvlshikimate-3-phosphate Synthase Protein
E-score	Expectation score
ETS	Excellence Through Stewardship
FA	Fatty Acid
FDA	Food and Drug Administration (U.S.)
g	Gram
h	Hour
HESI	Health and Environmental Sciences Institute
HPLC	High-Performance Liquid Chromatography
ILSI	International Life Science Institute
kb	Kilobase
LOD	Level of Detection
LOQ	Limit of Quantitation
µg	Microgram
mg	Milligram
mM	Millimolar
mRNA	Messenger RNA
MW	Molecular Weight
ng	Nanogram
NGS	Next Generation Sequencing
OECD	Organization for Economic Co-operation and Development
ORF	Open Reading Frame
PCR	Polymerase Chain Reaction
pH	Quantitative measure of the acidity or basicity of aqueous or other liquid solutions
SE	Standard Error
USDA	United States Department of Agriculture
UTR	Untranslated Region

[1] Alred, G.J., C.T. Brusaw, and W.E. Oliu. 2003. Handbook of Technical Writing, 7th edn., pp. 2-7. Bedford/St. Martin's, Boston, MA.

PART 1 GENERAL INFORMATION

1.1 Applicant Details

(a) Applicant's name/s	[redacted]Ph.D.
(b) Company/organisation name	Bayer CropScience Pty Ltd
(c) Address (street and postal)	Level 1, 8 Redfern Road, Hawthorn East, Victoria 3123
(d) Telephone number	[redacted]
(e) Email address	[redacted]
(f) Nature of applicant's business	Technology Provider to the Agricultural and Food Industries
(g) Details of other individuals, companies or organisations associated with the application	

1.2 Purpose of the Application

This application is submitted to Food Standards Australia New Zealand by Bayer CropScience Proprietary Limited on behalf of Bayer Group.

The purpose of this submission is to make an application to vary **Standard 1.5.2** – *Food Produced Using Gene Technology* of the *Australia New Zealand Food Standards Code* to seek the addition of canola line MON 94100 and products containing herbicide-tolerant canola line MON 94100 (hereafter referred to as MON 94100) to the Table to Clause 2 (see below).

Food derived from gene technology	Special requirements
Food derived from canola line MON 94100	None

1.3 Justification for the Application

1.3(a) The need for the proposed change

Herbicide-tolerant canola, MON 94100, was developed that is tolerant to dicamba (3,6-dichloro-2-methoxybenzoic acid) herbicide. MON 94100 contains a demethylase gene from *Stenotrophomonas maltophilia* that expresses a dicamba mono-oxygenase (DMO) protein to confer tolerance to dicamba herbicide.

MON 94100 will provide canola growers with a tool for effective and sustainable weed management including control of glyphosate resistant weeds. The best management practices for minimizing the development of herbicide-resistant weeds are built on the concepts of implementing diversified weed management programs, which includes using multiple herbicides with different modes of action either in mixtures, sequences, or in rotation.

MON 94100 may be combined with other authorized biotechnology-derived traits (e.g., Roundup Ready) through traditional breeding methods to create commercial products with tolerance to multiple herbicides. These next-generation combined-trait canola products will continue to offer broader grower choice in herbicide options available to them and support continued weed control durability.

1.3(b) The advantages of the proposed change over the status quo, taking into account any disadvantages

Weed competition can be a major limiting factor in canola production leading to significant yield reductions. Weeds compete with canola for water, nutrients, and light resulting in substantial yield losses when left uncontrolled (CCC, 2019). Weed species in canola vary from region to region and from state to state. Economic thresholds for controlling weeds in canola require some form of weed management practice on all canola acreage. Weed management practices include mechanical tillage, crop rotations, cultural practices, and herbicide application. Numerous selective herbicides are available for preplant, preemergence, and postemergence control of annual and perennial weeds in canola.

MON 94100 canola provides tolerance to the dicamba herbicide and may be combined with other GM or non-GM herbicide tolerant traits to provide growers with more options and flexibility to manage weeds, including tough-to-control and glyphosate-resistant broadleaf and grass weeds. Dicamba provides effective control of over 95 annual and biennial broadleaf weed species, and suppression of over 100 perennial broadleaf and woody plant species in North America. Additionally, dicamba provides control of eleven broadleaf species that have been confirmed to have resistance to glyphosate of which five are troublesome weeds in canola including foxtail species (giant, green, yellow), common ragweed, horseweed (marestail), kochia (*Bassia scoparia*), lambsquarters (*Chenopodium album*) and pigweed species (waterhemp, redroot, smooth, Powell). It is anticipated that no major changes in production management practices will occur beyond the intended benefits of more effective and improved management of common, troublesome and/or herbicide-resistant weeds and the opportunity for growers to rotate and/or use in combination with multiple sites-of-action herbicides for preemergence and in-crop postemergence herbicide applications.

1.4 Regulatory Impact Information

Costs and benefits

If the draft variation to permit the sale and use of food derived from MON 94100 is approved, possible affected parties may include consumers, industry sectors and government. The consumers who may be affected are those that consume food containing ingredients derived from canola. Industry sectors affected may be food importers and exporters, distributors, processors and manufacturers. Lastly, government enforcement agencies may be affected.

A cost/benefit analysis quantified in monetary terms is difficult to determine. In fact, most of the impacts that need to be considered cannot be assigned a dollar value. Criteria would need to be deliberately limited to those involving broad areas such as trade, consumer information and compliance. If the draft variation is approved:

Consumers:

- There would be benefits in the broader availability of canola products.
- There is unlikely to be any significant increase in the prices of foods if manufacturers are able to use comingled canola products.
- Consumers wishing to do so will be able to avoid GM canola products as a result of labeling requirements and marketing activities.

Government:

- Benefit that if canola MON 94100 was detected in food products, approval would ensure compliance of those products with the Code. This would ensure no potential for trade disruption on regulatory grounds.
- Approval of canola MON 94100 would ensure no potential conflict with WTO responsibilities.
- In the case of approved GM foods, monitoring is required to ensure compliance with the labeling requirements, and in the case of GM foods that have not been approved, monitoring is required to ensure they are not illegally entering the food supply. The costs of monitoring are thus expected to be comparable, whether a GM food is approved or not.

Industry:

- Sellers of procesed foods containing canola derivatives would benefit as foods derived from canola MON 94100 would be compliant with the Code, allowing broader market access and increased choice in raw materials. Retailers may be able to offer a broader range of canola products or imported foods manufactured using canola derivatives.
- Possible cost to food industry as some food ingredients derived from canola MON 94100 would be required to be labelled

1.5 Impact of International Trade

If the draft variation to permit the sale and use of food derived from MON 94100 was rejected it would result in the requirement for segregation of any canola derived products containing MON 94100 from those containing approved canola, which would be likely to increase the costs of imported canola derived foods.

It is important to note that if the draft variation is approved, canola MON 94100 will not have a mandatory introduction. The consumer will always have the right to choose not to use/consume this product.

1.6 Assessment Procedure

Bayer CropScience is submitting this application in anticipation that it will fall within the General Procedure category.

1.7 Exclusive Capturable Commercial Benefit

This application is likely to result in an amendment to the Code that provides exclusive benefits and therefore Bayer CropScience intends to pay the full cost of processing the application.

1.8 International and Other National Standards

1.8(a) International standards

Bayer CropScience makes all efforts to ensure that safety assessments are aligned, as closely as possible, with relevant international standards such as the Codex Alimentarius Commission's *Principles for the Risk Analysis of Foods Derived from Modern Biotechnology* and supporting *Guideline for the Conduct of Food Safety Assessment of Foods Derived from Recombinant-DNA Plants* (Codex Alimentarius, 2009).

In addition, the composition analysis is conducted in accordance with OECD guidelines and includes the measurement of OECD-defined canola nutrients and anti-nutrients based on conventional commercial canola varieties (OECD, 2011).

1.8(b) Other national standards or regulations

Bayer CropScience has submitted a food and feed safety and nutritional assessment summary for MON 94100 to the United States Food and Drug Administration (FDA) and has also requested a Determination of Nonregulated Status for MON 94100, including all progenies derived from crosses between MON 94100 and other canola, from the Animal and Plant Health Inspection Service (APHIS) of the U.S. Department of Agriculture (USDA).

Consistent with our commitments to the Excellence Through Stewardship® (ETS) Program[2], regulatory submissions have been or will be made to countries that import significant canola or food and feed products derived from U.S. canola and have functional regulatory review processes in place.

[2] Excellence Through Stewardship is a registered trademark of Excellence Through Stewardship, Washington, DC. (http://www.excellencethroughstewardship.org)

PART 2 SPECIFIC DATA REQUIREMENTS FOR SAFETY ASSESSMENT

A. TECHNICAL INFORMATION ON THE GM FOOD

A.1 Nature and Identity of the Genetically Modified Food

A.1(a) A description of the new GM organism

MON 94100 contains a demethylase gene from *Stenotrophomonas maltophilia* that expresses a dicamba mono-oxygenase (DMO) protein to confer tolerance to dicamba herbicide. MON 94100 will provide canola growers with an additional herbicide/weed control option for effective and sustainable weed management, including control of glyphosate resistant weeds. The best management practices for minimizing the development of herbicide resistant weeds are built on the concepts of implementing diversified weed management programs, which includes using multiple herbicides with different sites-of-action, either in mixtures, sequences or in rotation.

MON 94100 canola may be combined with other authorized introduced traits through traditional breeding methods to create commercial products (e.g., Roundup Ready) with tolerance to multiple herbicides. These next generation combined-trait canola products will continue to offer broader grower choice in herbicide options available to them and support continued weed control durability.

A.1(b) Name, number or other identifier of each new line or strain

In accordance with OECD's "Guidance for the Designation of a Unique Identifier for Transgenic Plants" MON 94100 has been assigned the unique identifier MON-941ØØ-2.

A.1(c) The name the food will be marketed under (if known)

A commercial trade name for the product has not been determined at the time of this submission and will be available prior to commercial launch of the product.

A.1(d) The types of products likely to include the food or food ingredient

MON 94100 will be utilized in the same manner and for the same uses as conventional canola because MON 94100 is not materially different from conventional canola other than the introduction of the herbicide tolerance trait and can be processed into a wide variety of food products as described in Section A.2(b)(iii).

A.2 History of Use of the Host and Donor Organisms

A.2(a) Description of all donor organism(s)

A.2(a)(i) Common and scientific names and taxonomic classification

The *dmo* gene is derived from the bacterium *Stenotrophomonas maltophilia* strain DI-6, isolated from soil at a dicamba manufacturing plant (Krueger *et al.*, 1989). *S. maltophilia* is ubiquitously present in the environment (Mukherjee and Roy, 2016), including in water and dairy products (An and Berg, 2018; Okuno *et al.*, 2018; Todaro *et al.*, 2011). These bacteria have been used as effective biocontrol agents in plant and animal pathogenesis (Mukherjee and Roy, 2016), and have antibacterial activity against both gram-positive and gram-negative bacteria (Dong *et al.*, 2015). These bacteria can form biofilms that become resistant to antibiotics (Berg and Martinez, 2015; Brooke *et al.*, 2017). The taxonomy of *S. maltophilia* is (Palleroni and Bradbury, 1993; Ryan *et al.*, 2009):

Kingdom: Bacteria

Phylum: Proteobacteria

Class: Gammaproteobacteria

Order: Xanthomonadales

Family: Xanthomonadaceae

Genus: *Stenotrophomonas*

PV-BNHT508701 was used for the transformation of conventional canola to produce MON 94100. PV-BNHT508701 contains two separate T-DNAs, each delineated by Left and Right Border regions. The first T-DNA, designated as T-DNA I, contains the *dmo* expression cassette. The *dmo* expression cassette is regulated by the PClSV promoter from peanut chlorotic streak caulimovirus, the 5' UTR leader sequence from the RNA of tobacco etch virus, the chloroplast targeting sequence and the first 24 amino acids from *Pisum sativum* (pea) *rbcS* gene, and the 3' UTR from an expressed gene of *Medicago truncatula* which functions as a terminator for transcription of the *dmo* gene (Genbank Accession MH931406). The second T-DNA, designated as T-DNA II, contains the *splA* expression cassette and the *aadA* expression cassette. The *splA* expression cassette is regulated by the 5' UTR leader, promoter, and enhancer sequence of an unknown seed protein gene from *Vicia faba* (broad bean) and the 3' UTR sequence from *Pisum sativum* (pea) rbcS gene family encoding the small subunit of ribulose bisphosphate carboxylase protein. The *aadA* expression cassette is regulated by FMV enhancer of figwort mosaic virus, EF1α promoter from *Arabidopsis thaliana*, the CTP2 targeting sequence from *A. thaliana*, and E9 3′ UTR from *Pisum sativum*. Section A.3(c) provides a detailed discussion of the genetic elements and Section A.3(d) provides characterization data demonstrating the presence of all intended elements from T-DNA I and the absence of T-DNA II.

A.2(a)(ii) Information on pathogenicity, toxicity, allergenicity

S. maltophilia has been found in healthy individuals without any hazard to human health (Heller *et al.*, 2016; Lira *et al.*, 2017). The opportunistic pathogenicity of *S. maltophilia* is mainly associated with individuals with compromised immune systems rather than with any specific virulence genes of these bacteria. Thus, documented occurrences of *S. maltophilia* infections have been limited to immune-compromised individuals in hospital settings (Lira *et al.*, 2017).

Other than the potential to become an opportunist pathogen in immune-compromised hosts, *S. maltophilia* is not known for human or animal pathogenicity.

A.2(a)(iii) History of use of the organism in food supply or human exposure

The history of safe exposure of S. maltophilia has been repeatedly reviewed during the evaluation of several dicamba-tolerant events with no safety or allergenicity issues identified by FSANZ or other regulatory agencies including MON 87419 maize in 2016 (A1118), MON 88701 cotton in 2014 (A1080), and MON 87708 soybean in 2012 (A1063).

A.2(b) Description of the host organism

A.2(b)(i) Phenotypic information

Brassica napus is a member of the family Brassicaceae, previously known as Crucifereae (OECD, 2012).

Family – Brassicaceae (previously known as Crucifereae)

Tribe – Brassiceae

Genus – *Brassica* L.

Species – *Brassica napus* L.

Subspecies

Brassica napus oleifera (common name: spring/summer oilseed rape, Canola)

Brassica napus f. *biennis* (common name: winter oilseed rape, winter Canola)

Oilseed rape has not historically been desirable for human consumption due to high erucic acid content. In addition, meal derived from oilseed rape had relatively high concentrations of toxicants (glucosinolates), which reduced the animal feed value of the meal. In the 1960s, through intensive breeding programs, Canadian scientists made two important genetic modifications to oilseed rape which led to the first double-low (low erucic acid and low glucosinolate) variety (Brown *et al.*, 2009). In 1978, to distinguish this new edible variety of *B. napus* oil from industrial *B. napus* oil, the Canola Council of Canada chose the word "canola" (Canadian oil, low acid) to become the registered trademark for edible *B. napus* containing oil with less than 2% erucic acid (Brown *et al.*, 2009; CCC, 2020; Codex Alimentarius, 2005).

Canola is grown principally for its oil which is extracted from the seed, and has both food and industrial applications. Canola is approximately 40% oil and 60% meal (OGTR, 2011). Canola grain is traditionally crushed and solvent extracted in order to separate the oil from the meal. Processing usually involves grain cleaning, grain pre-conditioning and flaking, grain cooking/conditioning (including steam-heating between 80 and 105 °C, for 15–20 min), pressing the flake to mechanically remove a portion of the oil, solvent extraction of the press-

cake to remove the remainder of the oil, oil and meal desolventizing, degumming and refining of the oil, and toasting of the meal (OECD, 2012).

Canola oil is considered high quality oil that is used in a variety of foods, including frying and baking oils, salad oils, margarines and shortenings. Oil is the most valuable component of canola grain and is the world's third largest source of vegetable oil, with 14% of world vegetable oil consumption after soybean oil at 28% and palm oil at 36% (ASA, 2019; USDA-FAS, 2019). Canola oil contains a low level (<10% of total fatty acids) of saturated fatty acids, a high level (approximately 60%) of the monounsaturated fatty acid, oleic acid, a moderate level (approximately 20%) of linoleic acid, and an appreciable amount (approximately 10%) of alpha-linolenic acid (CCC, 2016). Dietary guidance calls for limiting saturated fats in the diet in favor of monounsaturated and polyunsaturated fats. Canola oil helps achieve this guidance by replacing saturated fats with unsaturated fats. Furthermore, canola oil provides alpha-linolenic acid, which is essential to human health and must be supplied in the diet. Canola oil has well established heart health benefits and the FDA has issued a qualified health claim based on its ability to reduce the risk of coronary heart disease (U.S. FDA, 2006).

In 2018/2019 Canada, the European Union, China, and India are the largest producers of oilseed rape with 20.3, 20.0, 12.9, and 8.0 million metric tons, respectively. Australia produced approximately 2.1 million metric tons of canola in the same growing season (ABARES[3]).

A.2(b)(ii) How the organism is propagated for food use

Brassica napus is predominantly self-pollinating although interplant (plants are touching one another) outcrossing rates range from 12% to 55% with a mean of 30% (Beckie *et al.*, 2003).

The plant of canola can be grown on a wide range of soil types, but well-drained, clay-loam soils that do not crust are ideal for canola (NDSU, 2005). Canola cannot tolerate standing water or water-logged soils, and has moisture requirements similar to small grains, but is less tolerant to drought conditions. Due to these factors canola fits well into rotations with small grain cereal crops (winter and spring wheat and spring barley).

Reproduction of spring canola is favoured by dry weather conditions, which favours the activity of insect pollinators, and shorter growing seasons. Winter varieties take advantage of longer growing seasons. Water availability is also of particular importance, mainly during the period of seed ripening.

Spring canola, a cool season crop, is grown in Canada, southern Australia, northern China, and in northern portions of the U.S. Great Plains. Spring canola is slow growing and does not compete well with weeds in its early growth stages. Closely related weeds like wild mustard, stinkweed and shepherd's purse are often problematic in commercial spring canola fields, and weeds must be controlled early in the spring canola life cycle to avoid yield loss due to competition (OECD, 1997). Winter canola is planted in the fall, requires vernalization (exposure to winter cold) to flower, and is grown in parts of Europe, Asia, northwestern U.S. and in the central portions of the U.S. Great Plains. Winter canola, once established, suppresses and out-competes most annual weeds (Boyles *et al.*, 2009) and a small amount of these varieties are also grown in Australia.

[3] https://www.agriculture.gov.au/abares

A.2(b)(iii) What part of the organism is used for food

Canola is grown principally for its oil which is extracted from the seed, and has both food and industrial applications. Canola is approximately 40% oil and 60% meal (OGTR, 2011).

A.2(b)(iv) Whether special processing is required to render food safe to eat

Historically, the presence of the naturally occurring toxicants, erucic acid in the oil fraction and glucosinolates in the meal, has made oilseed rape unattractive for human and animal consumption. In the 1960s intensive breeding programs resulted in the development and introduction of low erucic acid varieties of oilseed rape or "canola" (Canadian oil, low acid) (OGTR, 2008; OECD, 2001). Further breeding efforts lowered glucosinolates in oilseed rape varieties to acceptable levels and oilseed rape is now grown both for its high quality vegetable oil and its high quality animal feed.

Currently, canola is grown principally for its oil which is extracted from the grain, and has both food and industrial applications. The solid residue or meal left after oil extraction is also an important product and is used as a high protein animal feedstuff. The canola grain is processed into two major products with typical percent yields of (by weight): oil (40%) and meal (60%).

Canola grain is traditionally crushed and solvent extracted in order to separate the oil from the meal. Processing usually involves grain cleaning, grain pre-conditioning and flaking, grain cooking/conditioning (including steam-heating between 80 and 105 °C, for 15–20 min), pressing the flake to mechanically remove a portion of the oil, solvent extraction of the press-cake to remove the remainder of the oil, oil and meal desolventizing, degumming and refining of the oil, and toasting of the meal (OECD, 2012).

The primary human food produced from canola is refined, bleached, and deodorized (RBD) oil. Canola oil is extensively used in the food industry in products such as cooking and salad oils, salad dressings, shortening, and oleo margarine. Currently, edible oil is the sole product from canola with direct human consumption.

A.2(b)(v) The significance to the diet in Australia and New Zealand of the host organism

Estimates of canola consumption are available from the WHO Global Environmental Monitoring System - Food Contamination Monitoring and Assessment Programme (GEMS/Food) (https://apps.who.int/nutrition/landscape_analysis/nlis_gem_food/en/index.html). The primary human food produced from canola is canola oil. Based on GEMS/Food DB released in 2008, the consumption of canola oil of general population in Australia is 0.97 g/kg bw/day.

A.3 The Nature of the Genetic Modification

A.3(a) Method used to transform host organism

MON 94100 was developed through *Agrobacterium tumefaciens* mediated transformation of canola hypocotyls, based on the method described by Radke *et al.* (1992), utilizing PV-BNHT508701. Hypocotyl segments were excised from etiolated seedlings of germinated 65037 seed. After co-culturing with the *Agrobacterium* carrying the plasmid vector, the hypocotyl segments were placed on medium containing carbenicillin to inhibit the growth of excess *Agrobacterium*. The hypocotyls were then placed on selection media containing spectinomycin and carbenicillin in order to inhibit the growth of untransformed plant cells and excess *Agrobacterium*, respectively. Once transformed callus and shoots were developed, one green shoot from each single explant callus was removed and placed on media conducive to root development. The rooted plants (R0) with normal phenotypic characteristics were selected and transferred to soil for growth and further assessment.

The R0 plants were self-pollinated to produce R1 seed, and the unlinked insertions of T-DNA I and T-DNA II were segregated. The R1 population was screened for the presence of T-DNA I and absence of T-DNA II and vector backbone sequences by PCR assay and sequencing analysis. Only plants that were homozygous for T-DNA I and negative for T-DNA II and vector backbone sequences were selected for further development and their progenies were subjected to further molecular and phenotypic assessments. As is typical of a commercial event production and selection process, hundreds of different transformation events (regenerants) were generated in the laboratory using PV-BNHT508701. After careful selection and evaluation of these events in the laboratory, greenhouse and field, MON 94100 was selected as the lead event based on superior agronomic, phenotypic, and molecular characteristics (Prado *et al.*, 2014). Studies on MON 94100 were initiated to further characterize the genetic insertion and the expressed product, and to establish the food, feed, and environmental safety relative to conventional canola. The major steps involved in the development of MON 94100 are depicted in Figure 1. The result of this process was the production of MON 94100 canola with only the *dmo* expression cassette.

For details, please refer to Appendix 1 ([redacted] 2020, (TRR0000306)).

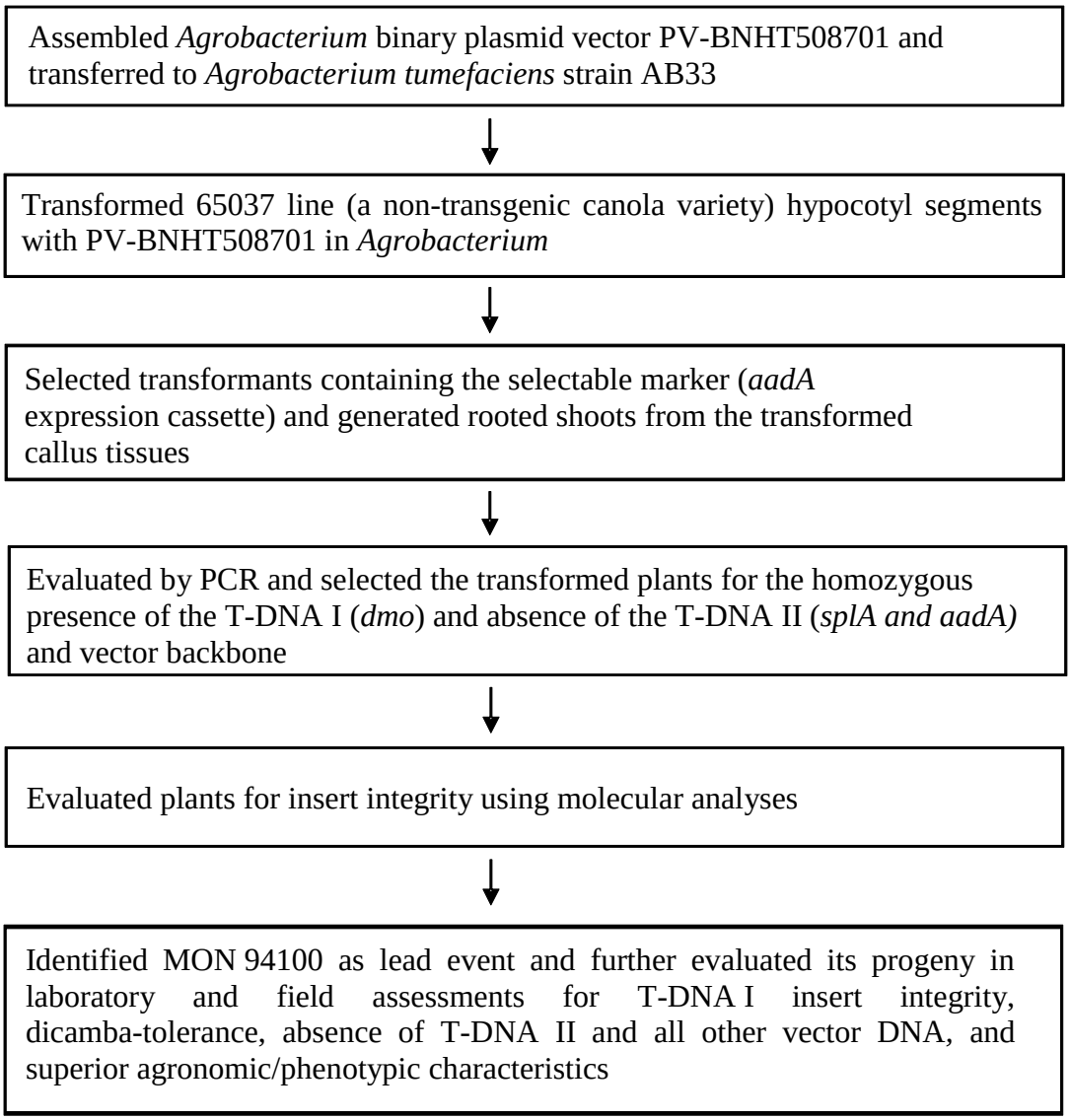

Figure 1. Schematic of the Development of MON 94100

A.3(b) Intermediate hosts (*e.g.* bacteria)

A disarmed strain of *Agrobacterium tumefaciens* was the intermediate host used to transfer the plasmid PV-BNHT508701 into canola cells. PV-BNHT508701 contains one T-DNA containing the *dmo* expression cassette. Following transformation, self-pollination, breeding, and segregation methods were used to produce MON 94100.

A.3(c) Gene construct including size, source and function of all elements

A.3(c)(i) The size, source and function of all the genetic components including marker genes, regulatory and other elements

MON 94100 was developed through *Agrobacterium tumefaciens* mediated transformation of canola hypocotyls, utilizing PV-BNHT508701.

PV-BNHT508701

Plasmid vector PV-BNHT508701 was used in the transformation of conventional canola to produce MON 94100 and its plasmid map is shown in Figure 3. A detailed description of the genetic elements and their prefixes (e.g., B, P, L, TS, CS, T, OR, and E) in PV-BNHT508701 is provided in Table 1. Plasmid vector PV-BNHT508701 is approximately 17.2 kb in length and contains two separate T-DNAs, each delineated by Left and Right Border regions. The first T-DNA, designated as T-DNA I, contains the *dmo* expression cassette. The second T-DNA, designated as T-DNA II, contains the *splA* and *aadA* expression cassettes. During transformation, both T-DNAs were inserted at discrete loci into the canola genome. Following transformation, traditional breeding, segregation analysis, selection and screening were used to isolate those plants that contained the *dmo* expression cassette (T-DNA I) and did not contain the *splA* or *aadA* expression cassettes (T-DNA II) or plasmid vector backbone sequences.

The *dmo* expression cassette contains the following genetic elements: promoter for the full-length transcript (FLt) of peanut chlorotic streak caulimovirus (PClSV), 5' UTR leader sequence from the RNA of tobacco etch virus (TEV), chloroplast-targeting sequence of the *RbcS* gene family from *Pisum sativum* (pea), coding sequence for the dicamba monooxygenase (DMO) protein from *Stenotrophomonas maltophilia*, and the 3' UTR sequence from an expressed gene of *Medicago truncatula* of unknown function (Genbank Accession MH931406).

The *aadA* expression cassette, which encodes an aminoglycoside-modifying enzyme that confers spectinomycin and streptomycin resistance (Fling *et al.*, 1985) and allows selection of transformed tissue, contains the following genetic elements: enhancer from the 35S RNA of figwort mosaic virus (FMV), promoter, leader, and intron sequences of the *EF-1*α gene from *Arabidopsis thaliana*, chloroplast-targeting sequence of the *ShkG* gene from *Arabidopsis thaliana,* 3' UTR sequence from *Pisum sativum* (pea) *rbcS* gene family. The *splA* expression cassette, encodes the sucrose phosphorylase enzyme (Piper *et al.*, 1999) which, when expressed during embryo development, interferes with sucrose metabolism, leading to a recognizable seed phenotype to provide a visual demonstration that T-DNA II is present or absent. The *splA* expression cassette contains the following genetic elements: 5' UTR leader, promoter, and enhancer sequence of an unknown seed protein gene from *Vicia faba* (broad bean), and 3' UTR sequence of the *nopaline synthase (nos)* gene from *Agrobacterium tumefaciens* pTi. Although both *aadA* and *splA* selectable marker expression cassettes were present in PV-BNHT508701, selection for transformants was based on spectinomycin resistance conferred by *aadA* and *splA* was not used.

The backbone region of PV-BNHT508701 contains two origins of replication (*ori-pBR322 and ori-pRi*) for maintenance of the plasmid vector in bacteria, a coding sequence for repressor of primer (ROP) protein for the maintenance of the plasmid vector copy number in *Escherichia coli* (*E. coli*), and a bacterial selectable marker gene (*nptII*) driven by the promoter of the ribosomal RNA operon from *Agrobacterium tumefaciens.*

The *dmo* Coding Sequence and DMO Protein

The *dmo* expression cassette contains the *dmo* gene encoding a precursor protein of 424 amino acids (340 amino acids encoded by the *dmo* gene; 81 amino acids encoded by *rbc*S gene (RbcS), which contains the 57 amino acids of chloroplast targeting sequence (CTP) and the first 24 amino acids of the small subunit ribulose 1,5–bisphosphate carboxylase; and three amino acids from an intervening sequence (IS). MON 94100 expresses two forms of DMO protein. Processing of the polypeptide in the chloroplast removes the RbcS, IS, and the N-terminal methionine resulting in a MON 94100 DMO protein with 339 amino acids. Alternative processing occurs when only the CTP is cleaved to produce a MON 94100 DMO protein with 367 amino acids (Figure 2). The *dmo* open reading frame in the expression cassette encodes the DMO protein from *S. maltophilia* (Herman *et al.*, 2005; Wang *et al.*, 1997). The expression of the DMO protein confers tolerance to dicamba herbicide.

For details, please refer to Appendix 1 ([redacted] 2020, (TRR0000306)).

```
1   MASMISSSAV TTVSRASRGQ SAAMAPFGGL KSMTGFPVRK VNTDITSITS NGGRVKCMQV

61  WPPIGKKKFE TLSYLPPLTR DSRAMATFVR NAWYVAALPE ELSEKPLGRT ILDTPLALYR

121 QPDGVVAALL DICPHRFAPL SDGILVNGHL QCPYHGLEFD GGGQCVHNPH GNGARPASLN

181 VRSFPVVERD ALIWICPGDP ALADPGAIPD FGCRVDPAYR TVGGYGHVDC NYKLLVDNLM

241 DLGHAQYVHR ANAQTDAFDR LEREVIVGDG EIQALMKIPG GTPSVLMAKF LRGANTPVDA

301 WNDIRWNKVS AMLNFIAVAP EGTPKEQSIH SRGTHILTPE TEASCHYFFG SSRNFGIDDP

361 EMDGVLRSWQ AQALVKEDKV VVEAIERRRA YVEANGIRPA MLSCDEAAVR VSREIEKLEQ

421 LEAA
```

Figure 2. Deduced Amino Acid Sequence of the MON 94100 DMO Precursor Protein

The amino acid sequence of the MON 94100 DMO precursor protein was deduced from the full-length coding nucleotide sequence present in PV-BNHT508701 (See Table 1 for more detail). The RbcS and IS (single- and double-underlined), and the N-terminal methionine (boxed with dash line) were cleaved in the chloroplast, resulting in a MON 94100 DMO protein with 339 amino acids that begins at the position 86. Alternative processing occurs when only the CTP (single-underlined) is cleaved to produce another MON 94100 DMO protein with 367 amino acids that begins at the position 58.

Regulatory Sequences

The *dmo* coding sequence in T-DNA I is under the regulation of the *PClSV* promoter, the *TEV* leader sequence, the *RbcS(Ps)* chloroplast targeting sequence and the *guf-Mt1* 3' untranslated region. The *PClSV* promoter is the promoter for the full-length transcript (FLt) of peanut chlorotic streak caulimovirus (PClSV) that directs transcription in plant cells (Maiti and Shepperd, 1998). The *TEV* leader is the 5' untranslated region from the RNA of tobacco etch virus (TEV) and is involved in regulating gene expression (Niepel and Gallie, 1999). The *RbcS(Ps)* targeting sequence encodes the chloroplast transit peptide and the first 24 amino acids of the protein from the ribulose-1,5-bisphosphate carboxylase oxygenase gene from pea (*Pisum sativum*) (Fluhr *et al.*, 1986) that directs transport of the DMO protein to the chloroplast. The *guf-Mt1* 3' untranslated region is from an expressed gene of *Medicago truncatula* of unknown function (Genbank Accession MH931406) that directs polyadenylation of mRNA (Hunt, 1994).

The *aadA* coding sequence in T-DNA II is under the regulation of the *FMV* enhancer, *EF-1α* promoter, the *CTP2* targeting sequence, and the *E9* untranslated region. The *EF-1α* promoter consists of the promoter, leader, and intron sequences from *Arabidopsis thaliana* encoding elongation factor EF-1α (Axelos *et al.*, 1989) that directs transcription in plant cells. The *FMV* enhancer is the enhancer sequence of the 35S RNA of figwort mosaic virus (FMV) (Richins *et al.*, 1987) that enhances transcription in most plant cells (Rogers, 2000). The *CTP2* targeting sequence of the *ShkG* gene from *Arabidopsis thaliana* encodes the EPSPS transit peptide region (Klee *et al.*, 1987; Herrmann, 1995) that directs transport of the protein to the chloroplast. The *E9* 3' untranslated region from *Pisum sativum* (pea) *rbcS* gene family encodes the small subunit of ribulose bisphosphate carboxylase protein (Coruzzi *et al.*, 1984) that directs polyadenylation of the mRNA.

The *splA* coding sequence in T-DNA II is under the regulation of the *Usp* promoter and the *nos* 3' untranslated region. The *Usp* promoter consists of the leader, promoter, and enhancer sequences from *Vicia faba* (broad bean) encoding an unknown seed protein that is involved in regulating gene expression in plant cells (Bäumlein *et al.*, 1991). The *nos* 3' untranslated region from *Arabidopsis tumefaciens* pTi nopaline synthase (*nos*) gene encodes NOS that directs polyadenylation of the mRNA (Bevan *et al.*, 1983; Fraley *et al.*, 1983).

T-DNA Border Regions

PV-BNHT508701 contains Left and Right Border regions (Figure 3 and Table 1) that were derived from *Agrobacterium tumefaciens* plasmids. The border regions each contains a nick site that is the site of DNA exchange during transformation (Barker *et al.*, 1983; Depicker *et al.*, 1982; Zambryski *et al.*, 1982). The border regions separate the T-DNAs from the plasmid backbone region and are involved in the efficient transfer of T-DNAs into the canola genome. PV-BNHT508701 contains two Left Border regions and two Right Border regions, where one Left Border and Right Border region set flanks T-DNA I and another set flanks T-DNA II. T-DNA II was inserted and then segregated out of the canola genome through traditional breeding. The absence of the T-DNA II sequence in MON 94100 was confirmed by sequencing and bioinformatic analyses (Section A.3).

Genetic Elements Outside of the T-DNA Border Regions

Genetic elements that exist outside of the T-DNA border regions are those that are essential for the maintenance or selection of PV-BNHT508701 in bacteria and are referred to as plasmid backbone. The selectable marker, *nptII* is the coding sequence for an enzyme from transposon Tn5 that confers neomycin and kanamycin resistance (Fraley *et al.*, 1983) in *E. coli* and *Agrobacterium* for use in molecular cloning. The *rrn* promoter used to drive *nptII* is the promoter for the ribosomal RNA operon from *Agrobacterium tumefacien*s (Bautista-Zapanta *et al.*, 2002). The origin of replication, *ori-pBR322*, is required for the maintenance of the plasmid in *E. coli* and is derived from the plasmid vector pBR322 (Sutcliffe, 1979). The origin of replication, *ori-pRi*, is required for the maintenance of the plasmid in *Agrobacterium* and is derived from the broad host plasmid *pRi* (Ye *et al.*, 2011). Coding sequence *rop* encodes the repressor of primer (ROP) protein which is necessary for the maintenance of higher plasmid vector copy number in *E. coli* (Giza and Huang, 1989). Because these elements are outside the border regions, they are not expected to be transferred into the canola genome. The absence of the backbone and other unintended plasmid sequence in MON 94100 was confirmed by sequencing and bioinformatic analyses (Section A.3).

Table 1. Summary of Genetic Elements in PV-BNHT508701

Genetic Element	Location in Plasmid Vector	Function (Reference)
B[1]-Right Border Region	1-285	DNA region from *Agrobacterium tumefaciens* containing the right border sequence used for transfer of the T–DNA (Depicker *et al.*, 1982; Zambryski *et al.*, 1982)
Intervening Sequence	286-319	Sequence used in DNA cloning
P[2]-*PClSV*	320-752	Promoter for the full-length transcript (FLt) of peanut chlorotic streak caulimovirus (PClSV) that directs transcription in plant cells (Maiti and Shepperd, 1998)
Intervening Sequence	753-772	Sequence used in DNA cloning
L[3]-*TEV*	773-904	5' UTR leader sequence from the RNA of tobacco etch virus (TEV) that is involved in regulating gene expression (Niepel and Gallie, 1999)
Intervening Sequence (IS)	905-905	Sequence used in DNA cloning
TS[4]-*RbcS (Ps)*	906-1148	Targeting sequence and the first 24 amino acids from *Pisum sativum* (pea) *rbcS* gene family encoding the small subunit ribulose 1,5–bisphosphate carboxylase protein that is expressed in the chloroplast (Fluhr *et al.*, 1986)
Intervening Sequence	1149-1157	Sequence used in DNA cloning
CS[5]-*dmo*	1158-2180	Coding sequence for the dicamba monooxygenase (DMO) protein from *Stenotrophomonas maltophilia* (Herman *et al.*, 2005; Wang *et al.*, 1997)
Intervening Sequence	2181-2249	Sequence used in DNA cloning
T[6]-*guf-Mt1*	2250-2749	3' UTR from an expressed gene of *Medicago truncatula* of unknown function (Genbank Accession MH931406) that directs polyadenylation of mRNA
Intervening Sequence	2750-2847	Sequence used in DNA cloning

Table 1. Summary of Genetic Elements in PV-BNHT508701 (Continued)

B-Left Border Region	2848-3289	DNA region from *Agrobacterium tumefaciens* containing the left border sequence used for transfer of the T–DNA (Barker *et al.*, 1983)
Intervening Sequence	3290-3498	Sequence used in DNA cloning
CS-*nptII*	3499-4293	Coding sequence of the *neo* gene from transposon Tn*5* of *E. coli* encoding neomycin phosphotransferase II (NPT II) (Beck *et al.*, 1982) that confers neomycin and kanamycin resistance (Fraley *et al.*, 1983)
P-*rrn*	4294-4518	Promoter of the ribosomal RNA operon from *Agrobacterium tumefaciens* (Bautista-Zapanta *et al.*, 2002) that drives transcription in bacteria
Intervening Sequence	4519-4594	Sequence used in DNA cloning
OR[7]-*ori-pBR322*	4595-5183	Origin of replication from plasmid pBR322 for maintenance of plasmid in *E. coli* (Sutcliffe, 1979)
Intervening sequence	5184-5610	Sequence used in DNA cloning
CS-*rop*	5611-5802	Coding sequence for repressor of primer protein from the ColE1 plasmid for maintenance of plasmid copy number in *E. coli* (Giza and Huang, 1989)
Intervening sequence	5803-5990	Sequence used in DNA cloning
OR-*ori-pRi*	5991-10104	Origin of replication from plasmid pRi for maintenance of plasmid in *Agrobacterium* (Ye *et al.*, 2011)
Intervening Sequence	10105-10111	Sequence used in DNA cloning
B-Left Border Region	10112-10430	DNA region from *Agrobacterium tumefaciens* containing the left border sequence used for transfer of the T-DNA (Barker *et al.*, 1983)
Intervening Sequence	10431-10462	Sequence used in DNA cloning

Table 1. Summary of Genetic Elements in PV-BNHT508701 (Continued)

T-*nos*	10463-10715	3' UTR sequence of the *nopaline synthase (nos)* gene from *Agrobacterium tumefaciens* pTi encoding NOS that directs polyadenylation (Bevan *et al.*, 1983; Fraley *et al.*, 1983)
Intervening Sequence	10716-10731	Sequence used in DNA cloning
CS-*splA*	10732-12189	Coding sequence of the *splA* gene from *Agrobacterium tumefaciens* strain C58 encoding the sucrose phosphorylase protein that catalyzes the conversion of sucrose to fructose and glucose–1–phosphate (Piper *et al.*, 1999)
Intervening Sequence	12190-12201	Sequence used in DNA cloning
P-*Usp*	12202-13380	5' UTR leader, promoter, and enhancer sequence of an unknown seed protein gene from *Vicia faba* (broad bean) encoding an unknown seed protein gene that is involved in regulating gene expression (Bäumlein *et al.*, 1991)
Intervening Sequence	13381-13431	Sequence used in DNA cloning
T-*E9*	13432-14074	3' UTR sequence from *Pisum sativum* (pea) rbcS gene family encoding the small subunit of ribulose bisphosphate carboxylase protein (Coruzzi *et al.*, 1984) that directs polyadenylation of the mRNA
Intervening Sequence	14075-14089	Sequence used in DNA cloning
aadA	14090-14881	Bacterial coding sequence for an aminoglycoside-modifying enzyme, 3"(9) -*O*-nucleotidyltransferase, from the transposon Tn7 (Fling *et al.*, 1985) that confers spectinomycin and streptomycin resistance

Table 1. Summary of Genetic Elements in PV-BNHT508701 (Continued)

TS-*CTP2*	14882-15109	Targeting sequence of the *ShkG* gene from *Arabidopsis thaliana* encoding the EPSPS transit peptide region that directs transport of the protein to the chloroplast (Klee *et al.*, 1987; Herrmann, 1995)
Intervening Sequence	15110-15118	Sequence used in DNA cloning
P-*EF-1α*	15119-16266	Promoter, leader , and intron sequences of the *EF–1*α gene from *Arabidopsis thaliana* encoding elongation factor EF–1α (Axelos *et al.*, 1989) that directs transcription in plant cells
Intervening Sequence	16267-16289	Sequence used in DNA cloning
E*[8]*-FMV	16290-16826	Enhancer from the 35S RNA of figwort mosaic virus (FMV) (Richins *et al.*, 1987)that enhances transcription in most plant cells (Rogers, 2000)
Intervening Sequence	16827-16876	Sequence used in DNA cloning
B-Right Border Region	16877-17233	DNA region from *Agrobacterium tumefaciens* containing the right border sequence used for transfer of the T-DNA (Depicker *et al.*, 1982; Zambryski *et al.*, 1982)
Intervening Sequence	17234-17248	Sequence used in DNA cloning

[1] B, Border
[2] P, Promoter
[3] L, Leader
[4] TS, Targeting Sequence
[5] CS, Coding Sequence
[6] T, Transcription Termination Sequence
[7] OR, Origin of Replication
[8] E, Enhancer

A.3(c)(ii) Detailed map of the location and orientation of all genetic elements

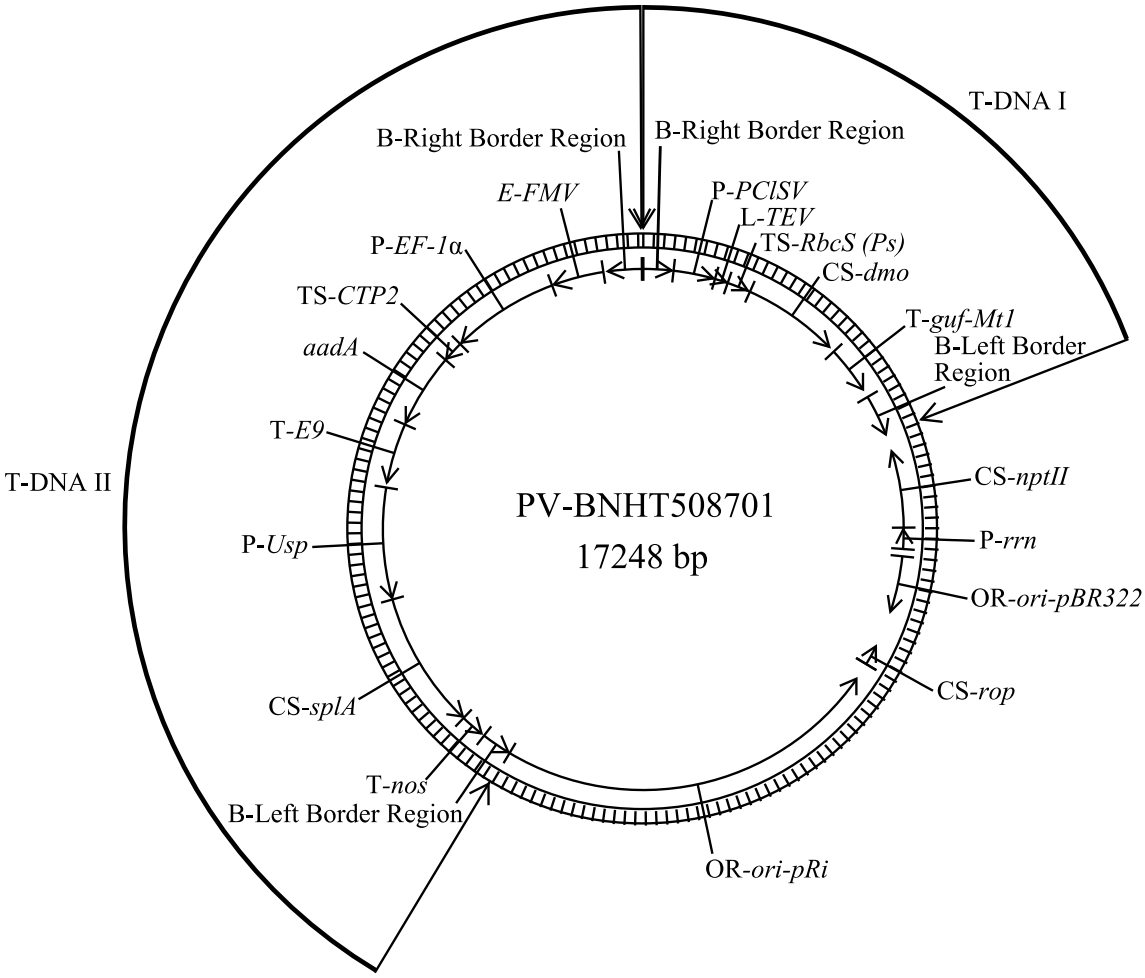

Figure 3. Circular Map of PV-BNHT508701

A circular map of PV-BNHT508701 used to develop MON 94100 is shown. PV-BNHT508701 contains two T–DNAs. Genetic elements are shown on the exterior of the map.

A.3(d) Full characterisation of the genetic modification in the new organism, including:

A.3(d)(i) Identification of all transferred genetic material and whether it has undergone any rearrangements

This section contains a comprehensive molecular characterization of the genetic modification present in MON 94100. It provides information on the DNA insertion(s) into the plant genome of MON 94100, and additional information relative to the arrangement and stability of the introduced genetic material. The information provided in this section addresses the relevant factors in Codex Plant Guidelines, Section 4, paragraphs 30, 31, 32, and 33 (Codex Alimentarius, 2009).

A schematic representation of the Next Generation Sequencing (NGS) methodology and the basis of the characterization using NGS and PCR sequencing are illustrated in Figure 4 below. Appendix 1 ([redacted] 2020, (TRR0000306)) defines the test, control and reference substances, and provides an additional overview of these techniques, their use in DNA characterization in canola plants and the materials and methods.

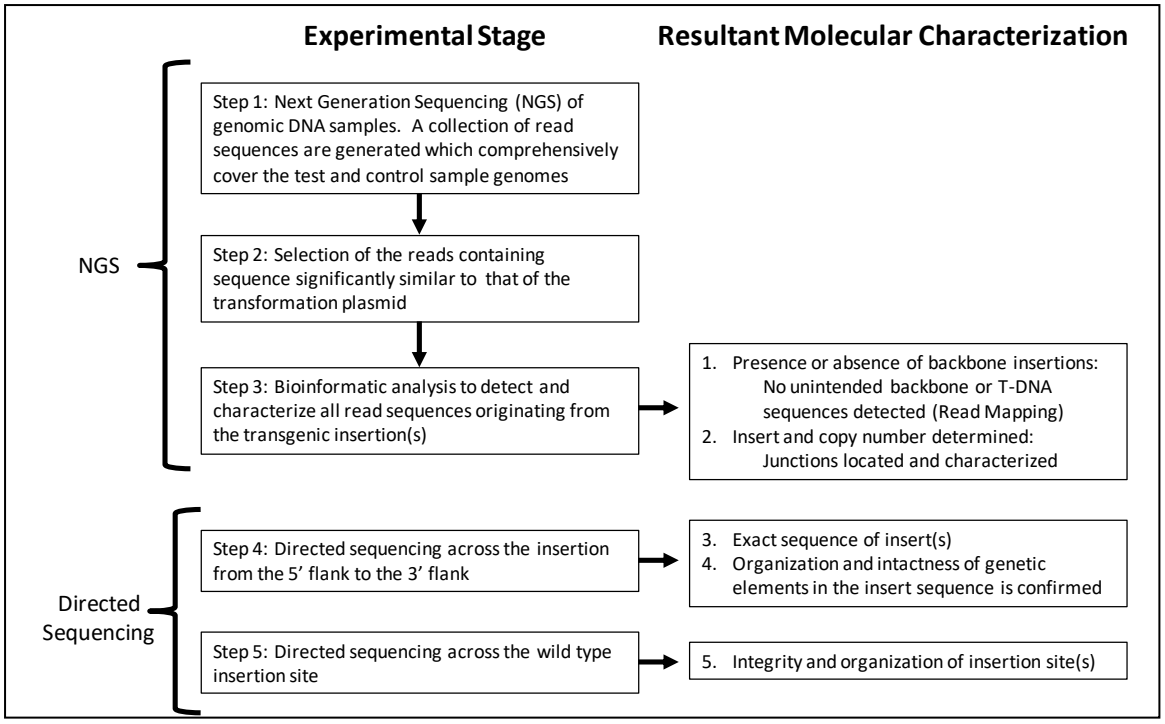

Figure 4. Molecular Characterization using Sequencing and Bioinformatics

Genomic DNA from MON 94100 (Test) and the conventional control was sequenced using technology that produces a set of short, randomly distributed sequence reads that comprehensively cover test and control genomes (Step 1). Utilizing these genomic sequence reads, bioinformatics searches are conducted to identify all sequence reads that are significantly similar to the transformation plasmid (Step 2). These identified captured reads are then mapped and analyzed to determine the presence/absence of transformation plasmid backbone sequences, identify the insert and junctions, and to determine the insert and copy number (Step 3). Using directed sequencing, overlapping PCR products were also produced which span any insert and the wild type insertion locus (Step 4 and Step 5 respectively); these overlapping PCR products are sequenced to allow for detailed characterization of the inserted DNA and insertion site.

The NGS method was used to characterize the genomic DNA from MON 94100 and the conventional control by generating short (~150 bp) randomly distributed sequence fragments (sequencing reads) in sufficient number to ensure comprehensive coverage of the sample genomes. It has previously been reported that 75× coverage of the genome is adequate to provide comprehensive coverage and detection of all inserted DNA (Kovalic *et al.*, 2012). A comprehensive analysis of NGS as a characterization method demonstrated that coverage depth as low as 11x is sufficient to detect both intended transgenes as well as unintended inserted vector-derived fragments as small as 25 base pairs (Cade *et al.*, 2018). Therefore, a targeted level of 75x coverage is a robust level of sequencing for the complete characterization of both homozygous and hemizygous transgenes, and well in excess of the levels which have been demonstrated as sufficient for identifying unintended inserted fragments. To confirm sufficient sequence coverage of the genome, the ~150 bp sequence reads are analyzed to determine the coverage of a known single-copy endogenous canola locus. This establishes the depth of coverage (the median number of times each base of the genome is independently sequenced). Furthermore, a transformation plasmid spike was sequenced to >75× to assess method sensitivity through modeling of 1/10th and one full genome equivalent plasmid spike. This confirms the method's ability to detect any sequences derived from the transformation plasmid. Bioinformatic analyses were used to select sequencing reads that contained sequences similar to the transformation plasmid, and these were analysed to determine the number of DNA inserts. NGS was run on five breeding generations of MON 94100 and the appropriate conventional controls. Results of NGS are shown in Sections A.3(d) and A.3(f).

The DNA inserts of MON 94100 were characterized by mapping of sequencing reads to the transformation plasmid and identifying junctions. Examples of five types of NGS reads are shown in Figure 5. The junctions of the DNA insert and the flanking DNA are unique for each insertion (Kovalic *et al.*, 2012). Therefore, insertion sites can be recognized by analyzing for sequence reads containing such junctions.

Directed sequencing (locus-specific PCR and DNA sequencing analyses, Figure 4, Step 4) complements the NGS method. It assesses the sequence identity of the insert relative to the corresponding sequence from the T-DNA I in PV-BNHT508701 and demonstrates that each genetic element in the insert was intact without rearrangement. It also characterizes the flank sequence beyond the insert corresponding to the genomic DNA of MON 94100. Directed sequencing results are described in Sections A.3(d)(i) and A.3(d)(ii).

The stability of the T-DNA present in MON 94100 across multiple breeding generations was evaluated by NGS as described above by determining the number and identity of the DNA inserts in each generation. For a single copy T-DNA I insert, two junction sequence classes are expected. In the case of an event where a single insertion locus is stably inherited over multiple breeding generations, two identical junction sequence classes would be detected in all the breeding generations tested. Results are described in Section A. 3 (f)(i).

Segregation analysis of T-DNA I was conducted to determine the inheritance and generational stability of the insert in canola. Segregation analysis corroborates the insert stability demonstrated by NGS and independently establishes the genetic behavior of T-DNA I. Results are described in Section A.3(f)(i).

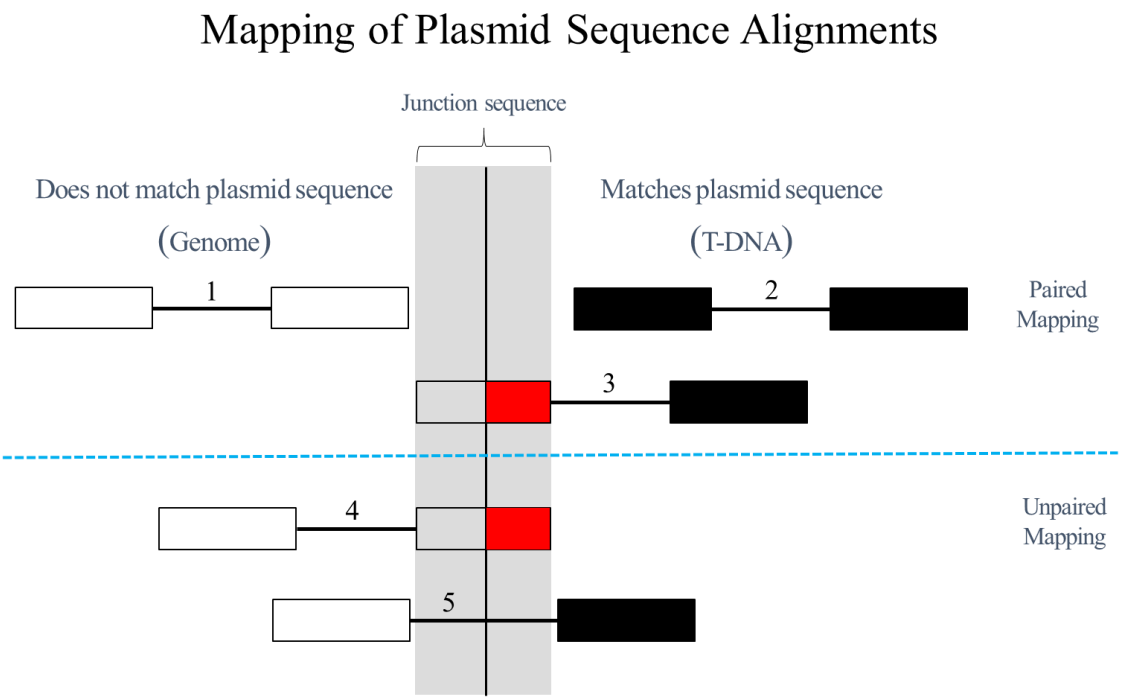

Figure 5. Five Types of NGS Reads

NGS yields data in the form of read pairs where sequence from each end of a size selected DNA fragment is returned. Depicted above are five types of sequencing reads/read pairs generated by NGS sequencing which can be found spanning or outside of junction points. Sequence boxes are color-filled if it matches with plasmid sequence, and empty if it matches with genomic sequence. Grey highlighting indicates sequence reads spanning the junction. Junctions are detected by examining the NGS data for reads having portions of plasmid sequences that span less than the full read, as well as reads mapping adjacent to the junction points where their mate pair does not map to the plasmid sequence. The five types of sequencing reads/read pairs being (1) Paired and unpaired reads mapping to genomic sequence outside of the insert, greater than 99.999% of collected reads fall into this category and are not evaluated in this analysis, (2) Paired reads mapping entirely to the transformation plasmid sequence, such reads reveal the presence of transformation sequence in planta, (3) Paired reads where one read maps entirely within the inserted DNA and the other read maps partially to the insert (indicating a junction point), (4) Single read mapping partially to the transformation plasmid DNA sequence (indicating a junction point) where its mate maps entirely to the genomic flanking sequence and (5) Single read mapping entirely to the transformation plasmid DNA sequence where its mate maps entirely to genomic flanking sequence, such reads are part of the junction signature.

A.3(d)(ii) Determination of number and identity of DNA inserts in MON 94100

The number of inserted DNA sequences from PV-BNHT508701 in MON 94100 was assessed by generating a comprehensive collection of reads via NGS of MON 94100 genomic DNA using the R3 generation. A plasmid map of PV-BNHT508701 is shown in Figure 3. Table 2 provides descriptions of the genetic elements present in MON 94100. A schematic representation of the insert and flanking sequences in MON 94100 is shown in Figure 6**.**

Next Generation Sequencing for MON 94100 and Conventional Control Genomic DNA

Genomic DNA from five breeding generations of MON 94100 (Figure 7) and conventional controls were isolated from seed and prepared for sequencing. These genomic DNA libraries were used to generate short (~150 bp) randomly distributed sequencing reads of the canola genome (Figure 4, Step 1).

To demonstrate sufficient sequence coverage the ~150 bp sequence reads were analyzed by mapping all reads to a known single copy endogenous locus (*Brassica napus*, GSBRNA2T00089284001) in each of the five breeding generations. The analysis of sequence coverage plots showed that the depth of coverage (i.e., the median number of times any base of the genome is expected to be independently sequenced) was 75× or greater for the five generations of MON 94100 (R3, R3F1, R4, R5, and R6) and the conventional control. It has been previously demonstrated 75× depth of coverage provides comprehensive coverage and ensures detection of inserted DNA (Kovalic *et al.*, 2012).

To produce the positive control sample for sequencing, a plasmid DNA library was created as described in Appendix 1 and spiked into a conventional control library at approximately 0.07%. The collected data were sampled to represent a single genome equivalent dataset and a 1/10th genome equivalent dataset. This result demonstrates that all nucleotides of PV-BNHT508701 are observed by the sequencing and bioinformatic assessments performed and that a detection level of at least 1/10th genome equivalent was achieved for the plasmid DNA sequence assessment.

For details, please refer to Appendix 1 ([redacted] 2020, (TRR0000306)).

Table 2. Summary of Genetic Elements in MON 94100

Genetic Element[1]	Location in Sequence[2]	Function (Reference)
5' Flanking DNA	1-1000	DNA sequence flanking the 5' end of the insert
B[3]-Right Border Region[r1]	1001-1070	DNA region from *Agrobacterium tumefaciens* containing the right border sequence used for transfer of the T–DNA (Depicker *et al.*, 1982; Zambryski *et al.*, 1982)
Intervening Sequence	1071-1104	Sequence used in DNA cloning
P[4]-*PClSV*	1105-1537	Promoter for the full length transcript (FLt) of peanut chlorotic streak caulimovirus (PClSV) that directs transcription in plant cells (Maiti and Shepperd, 1998)
Intervening Sequence	1538-1557	Sequence used in DNA cloning
L[5]-*TEV*	1558-1689	5' UTR leader sequence from the RNA of tobacco etch virus (TEV) that is involved in regulating gene expression (Niepel and Gallie, 1999)
Intervening Sequence (IS)	1690	Sequence used in DNA cloning
TS[6]-*RbcS (Ps)*	1691-1933	Targeting sequence and the first 24 amino acids from *Pisum sativum* (pea) rbcS gene family encoding the small subunit ribulose 1,5–bisphosphate carboxylase protein that is expressed in the chloroplast (Fluhr *et al.*, 1986)
Intervening Sequence	1934-1942	Sequence used in DNA cloning
CS[7]-*dmo*	1943-2965	Coding sequence for the dicamba monooxygenase (DMO) protein from *Stenotrophomonas maltophilia* (Herman *et al.*, 2005; Wang *et al.*, 1997)
Intervening Sequence	2966-3034	Sequence used in DNA cloning
T[8]-*guf-Mt1*	3035-3534	3' UTR from an expressed gene of *Medicago truncatula* of unknown function (GenBank Accession MH931406) that directs polyadenylation of mRNA
Intervening Sequence	3535-3632	Sequence used in DNA cloning
B-Left Border Region[r1]	3633-3913	DNA region from *Agrobacterium tumefaciens* containing the left border sequence used for transfer of the T–DNA (Barker *et al.*, 1983)
3' Flanking DNA	3914-4913	DNA sequence flanking the 3' end of the insert

[1] Although flanking sequences and intervening sequences are not functional genetic elements, they comprise a portion of the sequence.
[2] Numbering refers to the sequence of the insert in MON 94100 and adjacent DNA
[3] B, Border
[4] P, Promoter
[5] L, Leader
[6] TS, Targeting Sequence
[7] CS, Coding Sequence
[8] T, Transcription Termination Sequence
[r1] Superscript in Left and Right Border Regions indicate that the sequence in MON 94100 were truncated compared to the sequences in PV-BNHT508701

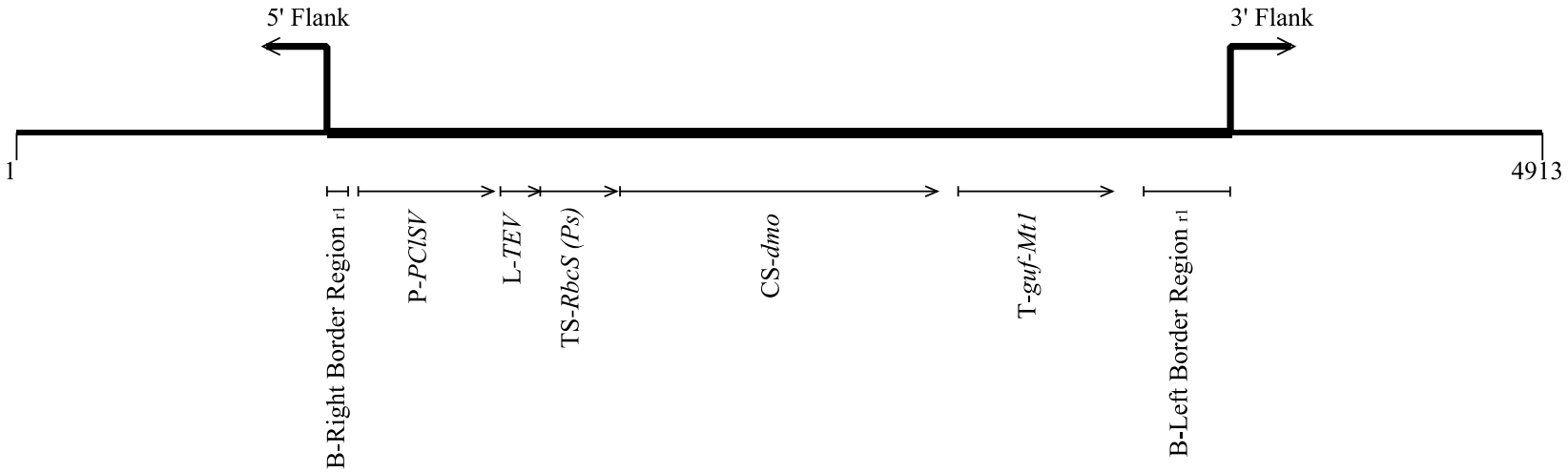

Figure 6. Schematic Representation of the Insert and Flanking Sequences in MON 94100

DNA derived from T-DNA I of PV-BNHT508701 integrated in MON 94100. Right-angled arrows indicate the ends of the integrated T-DNA and the beginning of the flanking sequence. Identified on the map are genetic elements within the insert. This schematic diagram may not be drawn to scale.

r1 Superscript in Left and Right Border Regions indicate that the sequence in MON 94100 was truncated compared to the sequences in PV-BNHT508701

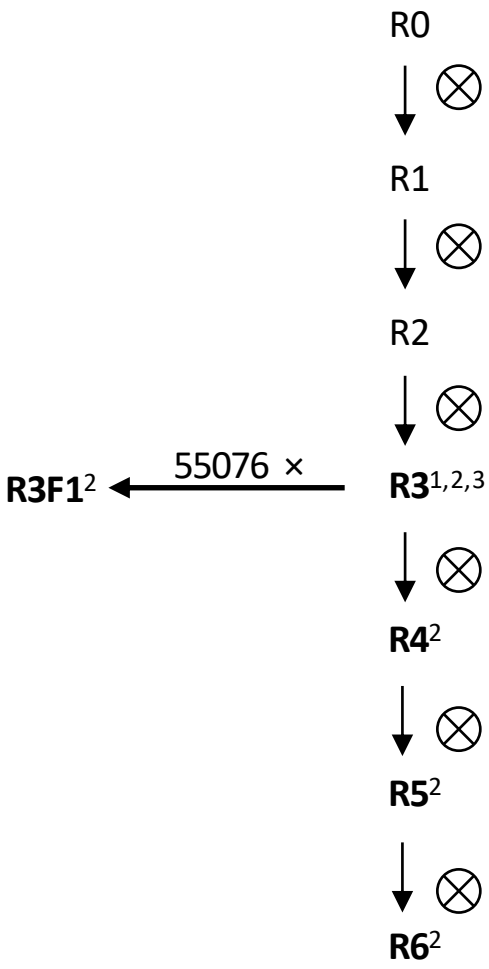

Figure 7. Breeding History of MON 94100

The generations used for molecular characterization and insert stability analyses are indicated in bold text. R0 corresponds to the transformed plant, ⊗ designates self-pollination.
[1] Generation used for molecular characterization
[2] Generations used to confirm insert stability
[3] Generation used for commercial development of MON 94100

Selection of Sequence Reads Containing Sequence of the PV-BNHT508701

The transformation plasmid, PV-BNHT508701 was transformed into the parental variety 65037 to produce MON 94100. Consequently, any DNA inserted into MON 94100 will consist of sequences that are similar to the PV-BNHT508701 DNA sequence. Therefore, to fully characterize the DNA from PV-BNHT508701 inserted in MON 94100, it is sufficient to completely analyze only the sequence reads that have similarity to PV-BNHT508701 (Figure 4, Step 2).

Using established criteria (described in Appendix 1), sequence reads similar to PV-BNHT508701 were selected from MON 94100 sequence datasets and were then used as input data for bioinformatic junction sequence analysis. PV-BNHT508701 sequences were also compared against the conventional control sequence dataset.

Determination of T-DNA Copy Number and Presence or Absence of Plasmid Vector Backbone

By mapping sequence reads to the transformation plasmid sequence and identifying junction signatures, the presence or absence of backbone sequence and the number of T-DNA insertions can be determined. For a single copy T-DNA insert sequence at a single genomic locus, a single junction signature pair and few, if any, reads aligning with the transformation plasmid backbone sequences are expected.

When reads from the conventional canola data set were aligned with the transformation plasmid sequence, a very small number of reads mapped sporadically across the plasmid sequence (Figure 8, see Panels 1 and 2; Panel 3 illustrates the read depth). An additional conventional control hybrid with conventional female parent line 55076 (55076 × 65037) for R3F1 was evaluated in the generational stability analysis (see **Error! Reference source not found.**) and produced comparable read maps.

When reads from the MON 94100 (R3) dataset were aligned with the transformation plasmid sequence, large numbers of reads mapped to T DNA I, and a few unpaired reads mapped to the T-DNA II element P-EF1α (Figure 9).

Low level detection of plasmid sequences is common and has previously been observed and reported on in similar studies (Zastrow-Hayes *et al.*, 2015; Yang *et al.*, 2013). Such observations are typically due to the presence of bacterial contamination in samples used in the preparation of DNA, or the result of the host plants genome having regions of low-level identity to elements within the transformation construct. Notably, these low coverage reads are observed across all generations as well as all control lines sequenced and upon manual review, were determined to not be unexpected DNA insertions.

The mapping of a large number of sequencing reads from the MON 94100 (R3) dataset to the T-DNA I was expected and fully consistent with the presence of the inserted DNA in MON 94100. Also, no reads in the MON 94100 (R3) generation dataset were identified that align with the plasmid backbone. As a result, it is concluded that MON 94100 (R3) does not contain inserted sequence from the transformation plasmid backbone.

To determine the insert number in MON 94100 (R3), selected reads mapping to T-DNA I as described above were analyzed to identify junctions. This bioinformatic analysis is used to find and classify partially matched reads characteristic of the ends of insertions. The number of unique junctions determined by this analysis are shown in

Table 3.

Table 3. Unique Junction Sequence Results

Sample	Junctions Detected
MON 94100 (R3)	2
Conventional canola	0

Detailed mapping information of the junction sequences is shown in Figure 9. The location and orientation of the junction sequences relative to T-DNA I insert determined for MON 94100 are illustrated in Figure 9, panels 1 and 2. As shown in the figure, there are two junctions identified in MON 94100. Both junctions contain the T-DNA I border sequence joined to flanking genomic sequence, indicating that they represent the sequences at the junctions of the intended T-DNA I insert and the canola genome. As described earlier, no junctions were detected in any of the conventional canola control samples.

Considered together, the absence of plasmid backbone and the presence of two junctions (joining T-DNA borders and flanking sequences) indicate a single intended T-DNA I at a single locus in the genome of MON 94100. Both of these junctions originate from the same locus of the MON 94100 genome and are linked by contiguous, known and expected DNA sequence. This is demonstrated by complete coverage of the sequenced reads spanning the interval between the junctions and the directed sequencing of overlapping PCR products described in Section A.3.

Based on the comprehensive NGS and junction identification, it is concluded that MON 94100 contains one copy of the T-DNA I inserted into a single locus. This conclusion is confirmed by the sequencing and analysis of overlapping PCR products from this locus as described below.

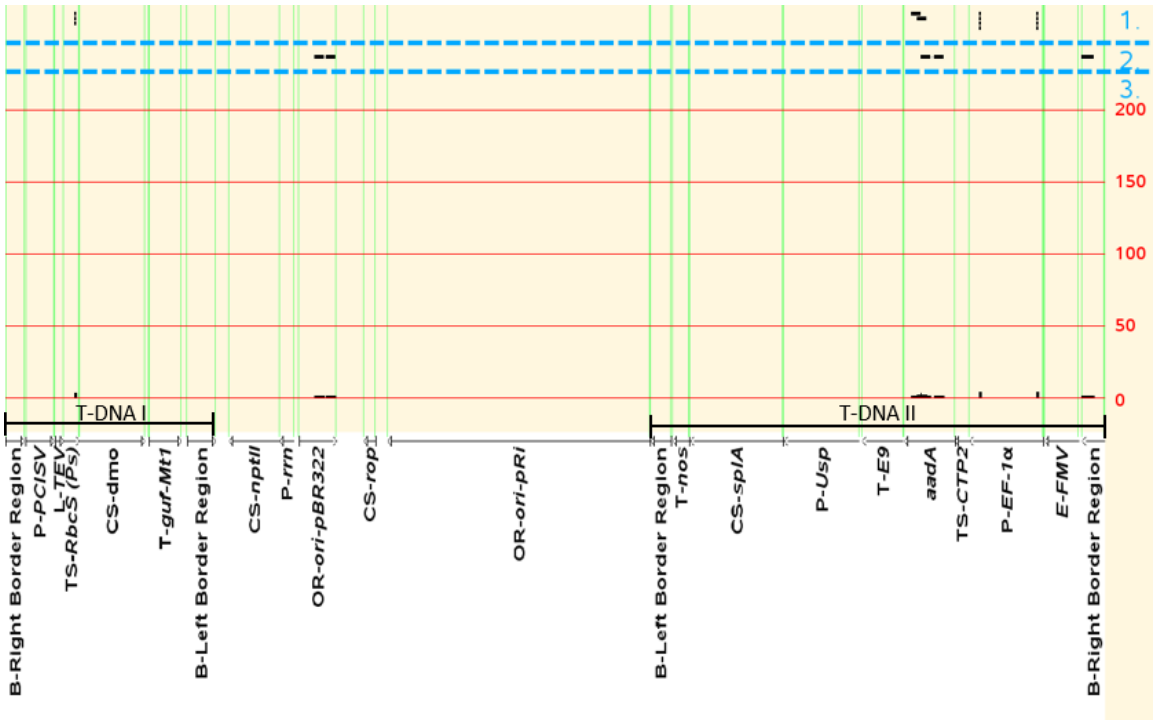

Figure 8. Read Mapping of Conventional Canola Versus PV-BNHT508701

Panel 1 shows the location of unpaired mapped reads, Panel 2 shows paired mapped reads, and Panel 3 shows a representation of combined raw read depth for unpaired and paired reads across the reference sequence. Vertical lines, in green, show genetic element boundaries. Comparable results were observed when read mapping 55076 × 65037 versus PV-BNHT508701. The additional conventional control was used for the generational stability analysis (see Table 4).

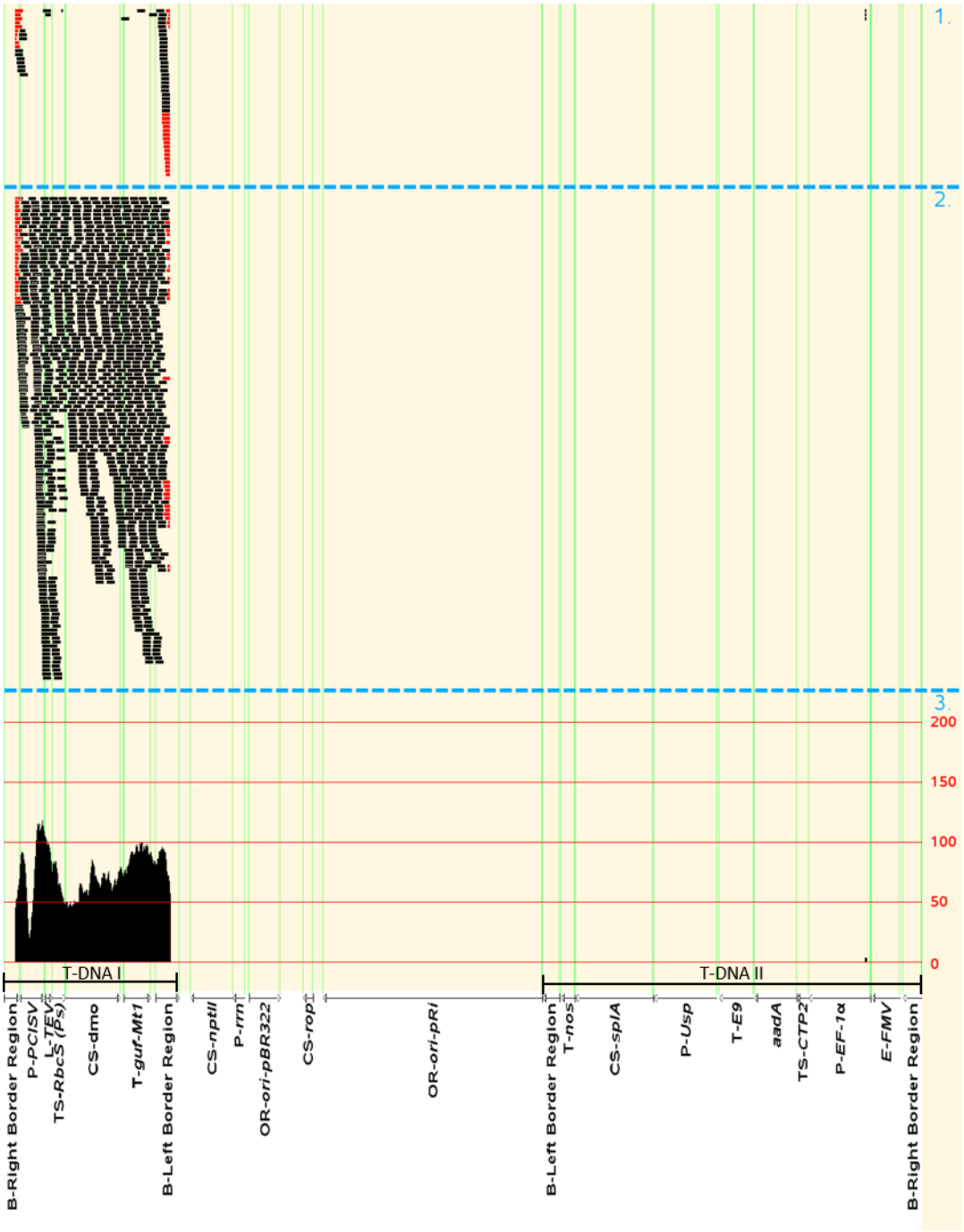

Figure 9. Read Mapping of MON 94100 (R3) Versus PV-BNHT508701

Panel 1 shows the location of unpaired mapped reads. Panel 2 shows paired mapped reads and Panel 3 shows a representation of combined raw read depth for unpaired and paired reads across the reference sequence. Vertical lines, in green, show genetic element boundaries. The region of flank junction sequences that align with the transformation plasmid are shown in red. Comparable results were observed when read mapping the R3F1, R4, R5, and R6 generations of MON 94100 versus PV-BNHT508701 (see Table 4 for the generational stability analysis).

A.3(d)(iii) Full DNA sequence, including junction regions

The organization of the elements within the DNA insert and the adjacent genomic DNA was assessed using directed DNA sequence analysis (refer to Figure 4, Step 4). PCR primers were designed to amplify two overlapping regions of the MON 94100 genomic DNA that span the entire length of the insert and the adjacent DNA flanking the insert (Figure 10). The amplified PCR products were subjected to DNA sequencing analyses. The results of this analysis confirm that the MON 94100 insert is 2,913 bp and that each genetic element within T-DNA I is intact compared to PV-BNHT508701. The border regions both contain small terminal deletions with the remainder of the inserted border regions being identical to the sequence in PV-BNHT508701. The sequence and organization of the insert was also shown to be identical to the corresponding T-DNA I of PV-ZBNHT508701 as intended. This analysis also shows that only T-DNA I elements (described in Table 2) were present within the inserted DNA. In addition, 1,000 base pairs flanking the 5′ end of the MON 94100 insert (Table 2**,** bases 1-1000) and 1000 base pairs flanking the 3′ end of the MON 94100 insert (Table 2**,** bases 3914-4913) were determined.

For details, please refer to Appendix 1 ([redacted] 2020, (TRR0000306)).

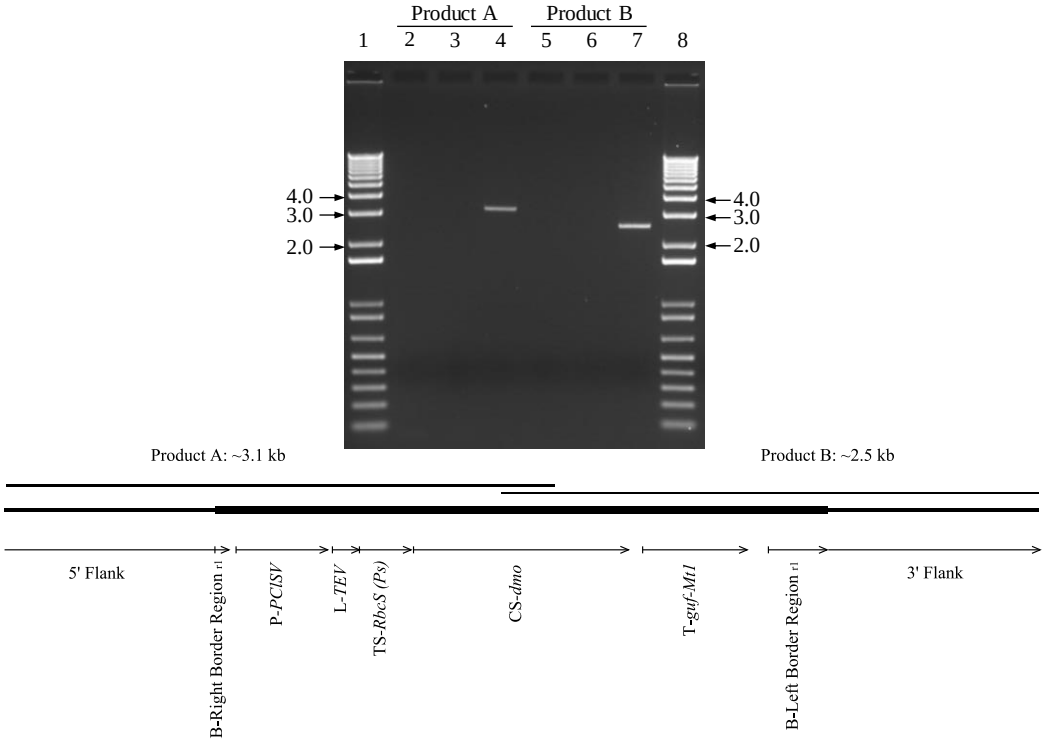

Figure 10. Overlapping PCR Analysis across the Insert in MON 94100

PCR was performed on both conventional control genomic DNA and genomic DNA of the R3 generation of MON 94100 using two pairs of primers to generate overlapping PCR fragments from MON 94100 for sequencing analysis. To verify size and specificity of the PCR products, 1 µl of each of the PCR reactions was loaded on the gel. The expected product size for each amplicon is provided in the illustration of the insert in MON 94100 that appears at the bottom of the figure. This figure is a representative of the data generated in the study. Lane designations are as follows:

Lane	
1	1 Kb Plus DNA Ladder
2	No template control
3	Conventional Control
4	MON 94100
5	No template control
6	Conventional Control
7	MON 94100
8	1 Kb Plus DNA Ladder

Arrows on the agarose gel photograph denote the size of the DNA, in kilobase pairs, obtained from the 1 Kb Plus DNA Ladder (Invitrogen) on the ethidium bromide stained gel.

r1 Superscript in Left and Right Border Regions indicate that the sequence in MON 94100 was truncated compared to the sequences in PV-BNHT508701

Sequencing of the MON 94100 Insertion Site

PCR and sequence analysis were performed on genomic DNA extracted from the conventional control to examine the insertion site in conventional canola (see Figure 4, Step 5). The PCR was performed with one primer specific to the genomic DNA sequence flanking the 5' end of the MON 94100 insert paired with a second primer specific to the genomic DNA sequence flanking the 3' end of the insert (Figure 11). A sequence comparison between the PCR product generated from the conventional control and the sequence generated from the 5' and 3' flanking sequences of MON 94100 indicates that 8 basepairs (bp) of canola genomic DNA were deleted during integration of the T-DNA I. Such changes are common during plant transformation (Anderson *et al.*, 2016) and these changes presumably resulted from double stranded break repair mechanisms in the plant during *Agrobacterium*-mediated transformation process (Salomon and Puchta, 1998).

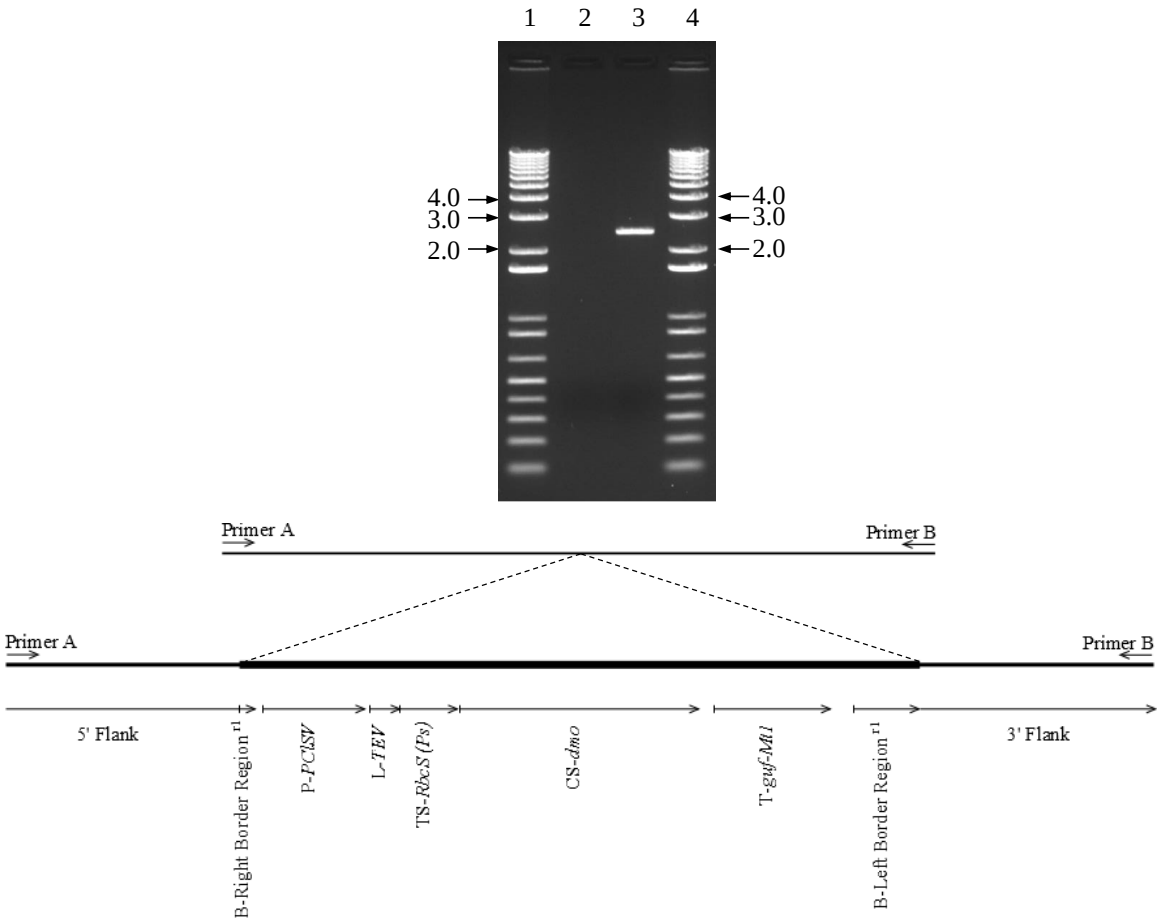

Figure 11. PCR Amplification of the MON 94100 Insertion Site

PCR analysis was performed to evaluate the insertion site. PCR was performed on conventional control genomic DNA using Primer A, specific to the 5′ flanking sequence, and Primer B, specific to the 3′ flanking sequence of the insert in MON 94100. The DNA generated from the conventional control PCR was used for sequencing analysis. This illustration depicts the MON 94100 insertion site in the conventional control (upper panel) and the MON 94100 insert (lower panel). Approximately 1 µl of each of the PCR reactions was loaded on the gel. This figure is representative of the data generated in the study. Lane designations are as follows:

Lane	
1	1 Kb Plus DNA Ladder
2	No template control
3	Conventional Control
4	1 Kb Plus DNA Ladder

Arrows on the agarose gel photograph denote the size of the DNA, in kilobase pairs, obtained from the 1 Kb Plus DNA Ladder (Invitrogen) on the ethidium bromide stained gel.
[r1] Superscript in Left and Right Border Regions indicate that the sequence in MON 94100 was truncated compared to the sequences in PV-BNHT508701.

A.3(d)(iv) Map of the organisation of the inserted DNA (each site)

PCR and DNA sequence analyses performed on MON 94100 and the conventional control determined the organisation of the genetic elements within the insert as given in Figure 11.

A.3(d)(v) Identification and characterisation of unexpected ORFs

Each unique transformation (MON 94100) must be assessed with bioinformatic assessment of potential allergenicity, toxicity and adverse biological activity for putative polypeptides derived from different reading frames of the entire T-DNA I insert or that span the 5' and 3' insert junctions due to the specific location in which the transformation occurred.

The 2009 Codex Alimentarius Commission guidelines for the safety assessment of food derived from biotechnology crops (Codex Alimentarius, 2009) includes an assessment element on the identification and evaluation of "*open reading frames within the inserted DNA or created by the insertion with contiguous plant genomic DNA*." These assessments examine the potential homology of any putative polypeptides or proteins that could be produced from open reading frames (ORFs) in the insert or at the plant-insert junction to known toxins or allergens. These analyses are conducted even if there is no evidence that such alternative reading frames in the insert or such ORFs at the plant-insert junction are capable of being transcribed or translated into a protein. Bioinformatic analyses were performed on the MON 94100 insert and flanking genomic DNA sequences to assess the potential for allergenicity, toxicity, or biological activity of putative polypeptides encoded by all six reading frames present in the MON 94100 insert DNA, as well as ORFs spanning the 5' and 3' insert DNA-flanking sequence junctions (Figure 12). Results from these bioinformatics analyses demonstrate that any putative polypeptides encoded by the MON 94100 event sequence are unlikely to exhibit allergenic, toxic or otherwise biologically adverse properties.

In addition to the bioinformatic analysis conducted on MON 94100 DMO protein (see Sections B.2(d) and B.2(f)), insert and flanking bioinformatic evaluations are depicted in Figure 12. ORFs spanning the 5' flanking sequence DNA-inserted DNA junctions, and 3' flanking sequence DNA-inserted DNA junctions were translated from stop codon to stop codon in all six reading frames (three forward reading frames and three reading frames in reverse complement orientation). Putative polypeptides of eight amino acids or greater from each reading frame that span the junction sites were then compared to toxin, allergen, and all protein databases using bioinformatic tools. The data generated from these analyses confirm that even in the highly unlikely occurrence that a translation product other than MON 94100 DMO protein were derived from frames one to six of the insert DNA or the ORFs spanning the insert junctions, they would not share a sufficient degree of sequence similarity with other proteins to indicate they would be potentially allergenic, toxic, or have other safety implications. Therefore, there is no evidence for concern regarding the relatedness of putative polypeptides from MON 94100 to known toxins and allergens, or biologically active putative peptides.

For details, please refer to Appendix 2 ([redacted] 2019, (MSL0030274)) and Appendix 3 ([redacted] 2019, (MSL0030273)).

Bioinformatics Evaluation of the T-DNA Insert in MON 94100

Bioinformatic analyses were performed to assess the potential of toxicity, allergenicity or biological activity of any putative peptides encoded by translation of reading frames 1 through 6 of the inserted DNA in MON 94100 (Figure 12).

The FASTA sequence alignment tool was used to assess structural relatedness between the query sequences and any protein sequences in the AD_2019, TOX_2019, and PRT_2019 databases. Structural similarities shared between each putative polypeptide with each sequence in the database were examined. The extent of structural relatedness was evaluated by detailed visual inspection of the alignment, the calculated percent identity and alignment length to ascertain if alignments exceeded Codex (Codex Alimentarius, 2009) thresholds for FASTA searches of the AD_2019 database, and the *E*-score. Alignments having an *E*score- less than 1×10^{-5} are deemed significant because they may reflect shared structure and function among sequences. In addition to structural similarity, each putative polypeptide was screened for short polypeptide matches using a pair-wise comparison algorithm. In these analyses, eight contiguous and identical amino acids were defined as immunologically relevant, where eight represents the typical minimum sequence length likely to represent an immunological epitope ([redacted] 2006) and evaluated against the AD_2019 database.

The results of the search comparisons showed that no relevant structural similarity to known allergens and toxins were observed for any of the putative polypeptides when compared to proteins in the allergen (AD_2019) or toxin (TOX_2019) databases. Furthermore, no short (eight amino acid) polypeptide matches were shared between any of the putative polypeptides and proteins in the allergen database.

When the frames were used to query the PRT_2019 database, the results of these analyses positively identified the following genetic elements within the MON 94100 T-DNA I: (1) frame 1 was observed to contain DMO protein and associated element *TS-RbcS* (*Ps*) which is composed of the chloroplast transit peptide and the first 24 amino acids of the fully processed protein derived from *Pisum sativum* (pea) *RbcS* gene (Rubisco small subunit); (2) frame 2-6 were not observed to define genetic elements within the MON 94100 T-DNA I. Each of the genetic elements are described and expected based on the known sequence of the MON 94100 T-DNA I. The frame 1 results do not indicate potential for adverse biological activity. No other relevant sequence similarities between the six reading frames translated from the MON 94100 T-DNA I were observed with allergens, toxins, or other biologically active proteins of concern.

Taken together, these data demonstrate the lack of relevant similarities between known allergens or toxins for putative peptides derived from all six reading frames from the inserted DNA sequence of MON 94100. As a result, in the unlikely event that a translation product other than DMO was derived from reading frames 1 to 6, these putative polypeptides are not expected to be cross-reactive allergens, toxins, or display adverse biological activity.

Bioinformatics Evaluation of the DNA Sequences Flanking the 5′ and 3′ Junctions of the MON 94100 Insert: Assessment of Putative Peptides

Analyses of putative polypeptides encoded by DNA spanning the 5' and 3' genomic junctions of the MON 94100 inserted DNA were performed using a bioinformatic comparison strategy. The purpose of the assessment is to evaluate the potential for novel open reading frames (ORFs) that may have homology to known allergens, toxins, or proteins that display adverse biological activity. Sequences spanning the 5' and 3' genomic DNA-insert DNA junctions, (Figure 12) were translated from stop codon (TGA, TAG, TAA) to stop codon in all six reading frames. Putative polypeptides from each reading frame, that spanned the insert junctions and were eight amino acids or greater in length, were compared to AD_2019, TOX_2019, and PRT_2019 databases using FASTA and to the AD_2019 database using an eight amino acid sliding window search.

The FASTA sequence alignment tool was used to assess structural relatedness between the query sequences and any protein sequences in the AD_2019, TOX_2019, and PRT_2019 databases. Similarities shared between each putative polypeptide with each sequence in the database were examined. The extent of structural relatedness was evaluated by detailed visual inspection of the alignment, the calculated percent identity, and the *E*-score. Alignments having *E*-scores less than 1×10^{-5} are deemed significant because they may reflect shared structure and function among sequences. In addition to sequence similarity, sequences were screened for short polypeptide matches using a pair-wise comparison algorithm. In these analyses, eight contiguous and identical amino acids were defined as immunologically relevant, where eight represents the typical minimum sequence length likely to represent an immunological epitope ([redacted] 2006).

The bioinformatic analysis performed using the putative peptide sequences translated from junctions is theoretical as there is no reason to suspect, or evidence to indicate, the presence of transcripts spanning the flank junctions. The results of these bioinformatic analyses indicate that no structurally relevant sequence similarities were observed between the putative flank junction derived sequences and allergens, toxins, or biologically active proteins. As a result, in the unlikely occurrence that any of the peptides analyzed herein is found *in planta*, none would share significant similarity or identity to known allergens, toxins, or other biologically active proteins that could affect human or animal health.

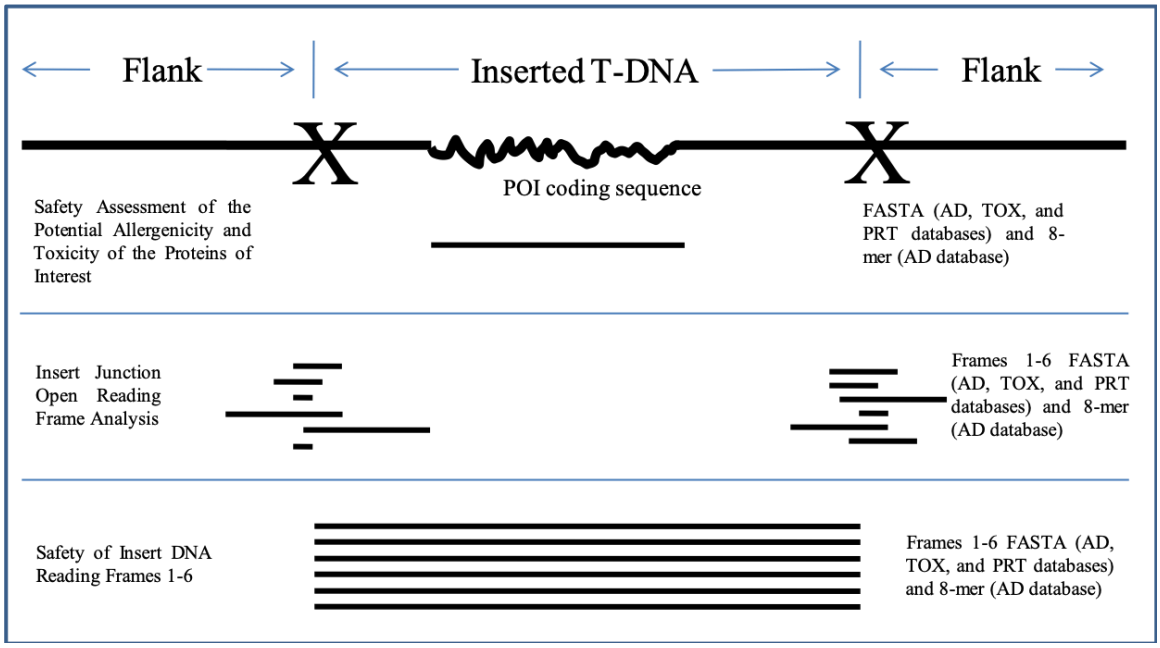

Figure 12. Schematic Summary of MON 94100 Bioinformatic Analyses

AD: AD_2019, TOX: TOX_2019, PRT: PRT_2019; 8-mer represents the eight amino acid sliding window search

Bioinformatic Assessment of Putative Open Reading Frames of MON 94100 Insert and Flanking Sequences Summary and Conclusions

A conservative bioinformatic assessment of potential allergenicity, toxicity and adverse biological activity for putative polypeptides derived from different reading frames of the entire T-DNA I insert or that span the 5' and 3' insert junctions was conducted for MON 94100. There are no analytical data that indicate any putative polypeptides subjected to bioinformatic evaluation are produced by MON 94100. Moreover, the data generated from these analyses confirm that even in the highly unlikely occurrence that a translation product other than MON 94100-produced DMO protein was derived from frames 1 to 6 of the insert DNA, or the insert junctions, it would not share a sufficient degree of sequence similarity with other proteins to indicate they would be potentially allergenic, toxic, or have other safety implications. Therefore, there is no evidence for concern regarding the putative polypeptides for MON 94100 relatedness to known toxins, allergens, or biologically active putative peptides.

A.3(e) Family tree or breeding process

MON 94100 canola was derived from a single plant transformant of canola variety 65037. Variety 65037 (CFIA, 2019) was used as the conventional canola comparator to support the safety assessment of MON 94100 canola. MON 94100 and the conventional control 65037 have similar genetic backgrounds with the exception of the *dmo* expression cassette, thus, the effect of the *dmo* expression cassette and the expressed DMO protein can be assessed in an unbiased manner in comparative safety assessments.

For more details, see MON 94100 breeding history, Figure 7.

Please also refer to Section A.3(f)(i).

A.3(f) Evidence of the stability of the genetic changes

A.3(f)(i) Pattern of inheritance of insert and number of generations monitored

In order to demonstrate the genetic stability of the T-DNA I present in MON 94100 through multiple breeding generations, NGS reads from five breeding generations of MON 94100 were mapped to the transformation plasmid for junction identification. The breeding history of MON 94100 is presented in Figure 7, and the specific generations tested are indicated in the figure legend. The MON 94100 R3 generation was used for the molecular characterization analyses discussed in Sections A.3(c) to A.3(d). To assess stability, four additional generations were evaluated by NGS as previously described in Section A.3(c) and compared to the fully characterized MON 94100 R3 generation. The conventional controls used for the generational stability analysis included 65037, and 55076 × 65037 which represent similar background genetics to each of the analyzed MON 94100 breeding generations. Genomic DNA isolated from each of the selected generations of MON 94100 and conventional controls were used for mapping and subsequent junction identification (Table 4).

To determine the insert number in the MON 94100 samples, the sequences generated and selected as described above in Section A.3(d)(ii) were analyzed to identify junctions. The number of any resultant unique junctions containing the PV-BNHT508701 DNA sequence determined by this analysis is shown in the table below.

Table 4. Junction Sequences Detected

Sample	Junctions Detected
MON 94100 (R3)	2
MON 94100 (R3F1)	2
MON 94100 (R4)	2
MON 94100 (R5)	2
MON 94100 (R6)	2
65037	0
55076 × 65037	0

As shown by alignment to the full flank/insert sequence obtained from directed sequencing, a single conserved pair of junctions linked by contiguous known and expected DNA sequence is present in MON 94100 (R3). Two identical junctions are found in each of the breeding generations (R3, R3F1, R4, R5, and R6), confirming the insertion of a single copy of T-DNA I from PV-BNHT508701 at a single locus in the genome of MON 94100, and the consistency of these junctions in the mapping data across all generations tested demonstrates that this single locus is stably maintained throughout the MON 94100 breeding process.

These results demonstrate that the single locus of integration characterized in the R3 generation of MON 94100 is found in five breeding generations of MON 94100, confirming the stability of the insert. This comprehensive NGS and bioinformatic analysis of NGS data from multiple generations supports the conclusion that MON 94100 contains a single, stable, inserted T-DNA I.

Please also refer to Appendix 4 ([redacted] (MSL0030193)).

The MON 94100 T-DNA I resides at a single locus within the canola genome and therefore should be inherited according to Mendelian principles of inheritance. During development of lines containing MON 94100, phenotypic and genotypic segregation data were recorded to assess the inheritance and stability of the MON 94100 T-DNA I using Chi square (χ^2) analysis over several generations. The χ^2 analysis is based on comparing the observed segregation ratio to the expected segregation ratio according to Mendelian principles.

The MON 94100 breeding path for generating segregation data is described in Figure 13. The transformed R0 plant was self-pollinated to generate R1 seed. An individual plant homozygous for the presence of the MON 94100 T-DNA I was identified in the R1 segregating population via a Real-Time TaqMan® PCR assay.

The homozygous positive R1 plant was self-pollinated to give rise to R2 seed. The R2 plants were self-pollinated to produce R3 seed. R3 plants homozygous for the MON 94100 T-DNA I were crossed via traditional breeding techniques to a Bayer CropScience's elite inbred parent (CP 3878) that did not contain the *dmo* coding sequence to produce hemizygous R3F1 seed. The R3F1 plants were crossed again with CP 3878 to produce BC1F1 seed. The BC1F1 generation was tested for the presence of the MON 94100 T-DNA I by end-point TaqMan® PCR assay to select for hemizygous MON 94100 plants. At the BC1F1 generation, the MON 94100 T-DNA I was predicted to segregate at a 1:1 ratio (hemizygous positive: homozygous negative) according to Mendelian inheritance principles.

Selection of hemizygous backcross plants, followed by crossing with CP 3878 and testing for the presence of the T-DNA I was repeated for two additional generations, to produce hemizygous BC2F1 seed and hemizygous BC3F1 seed, each at a predicted 1:1 (hemizygous positive: homozygous negative) segregation ratio according to Mendelian inheritance principles.

A Pearson's chi-square (χ^2) analysis was used to compare the observed segregation ratios of the MON 94100 T-DNA I to the expected ratios. The χ^2 analysis was performed using the statistical program R Version 3.3.2 (2016-10-31).

The Chi-square was calculated as:

$$\chi^2 = \sum [(| o - e |)^2 / e]$$

where o = observed frequency of the genotype or phenotype and e = expected frequency of the genotype or phenotype. The level of statistical significance was predetermined to be 5% ($\alpha = 0.05$).

The results of the χ^2 analysis of the segregating progeny of MON 94100 are presented in Table 5 The χ^2 value in the BC1F1, BC2F1, and BC3F1 generations indicated no statistically-significant difference between the observed and expected segregation ratios of MON 94100 T-DNA I. These results support the conclusion that the MON 94100 T-DNA I resides at a single locus within the canola genome and is inherited according to Mendelian principles. These results are also consistent with the molecular characterization data indicating that MON 94100 contains a single intact copy of the T-DNA I inserted at a single locus in the canola genome (Sections A.3(d) to A.3(f)).

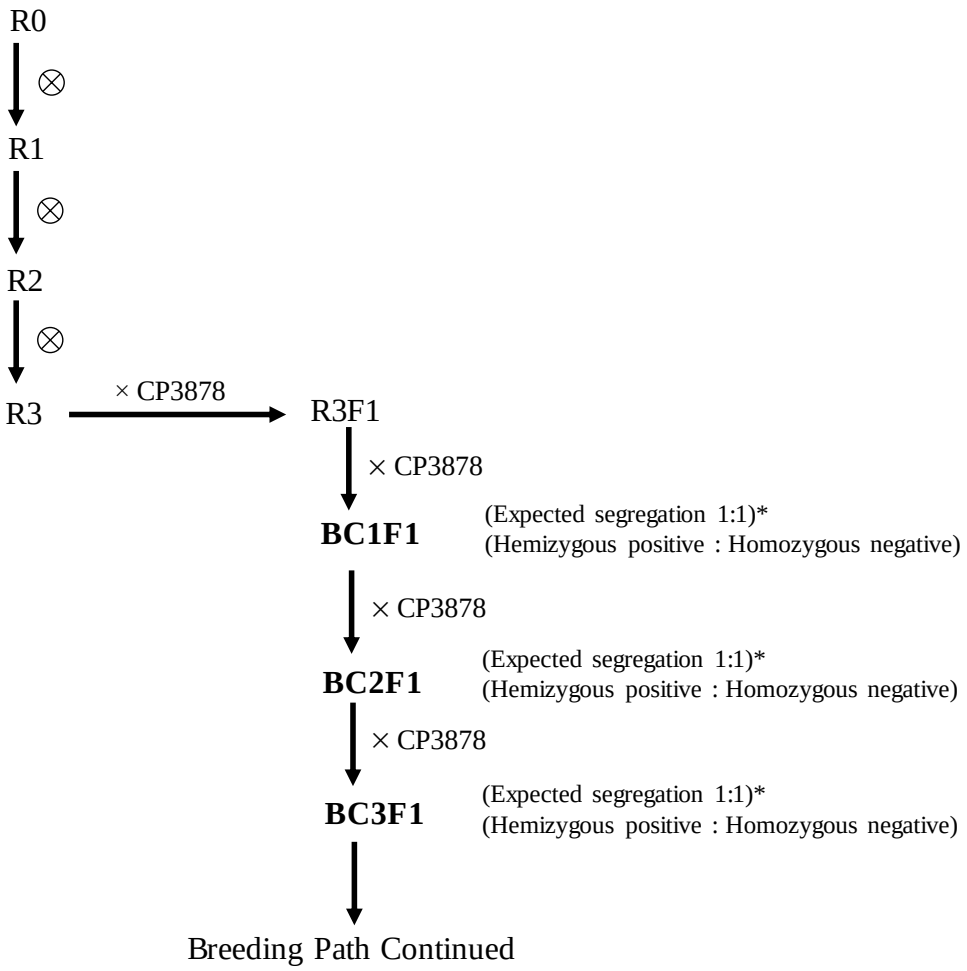

Figure 13. Breeding Path for Generating Segregation Data for MON 94100

*Chi-square analysis was conducted on segregation data from BC1F1, BC2F1, and BC3F1 generations (bolded text).
⊗: Self-Pollinated
×: Cross-Pollinated
BC: Back Cross

Table 5. Segregation of the Expression Cassette During the Development of MON 94100

				1:1 Segregation			
Generation	**Total Plants**	**Observed # Plant Positive**	**Observed # Plant Negative**	**Expected # Plant Positive**	**Expected # Plant Negative**	**χ^2**	**Probability**
BC1F1	347	167	180	173.50	173.50	0.49	0.485
BC2F1	484	237	247	242.00	242.00	0.21	0.649
BC3F1	435	211	224	217.50	217.50	0.39	0.533

Characterization of the Genetic Modification Summary and Conclusion

As described above, characterization of the genetic modification in MON 94100 was conducted using a combination of sequencing, PCR, and bioinformatics. The results of this characterization demonstrate that MON 94100 contains a single copy of the intended T-DNA I containing the *dmo* expression cassette that is stably integrated at a single locus and is inherited according to Mendelian principles over multiple generations. These conclusions are based on the following:

- Molecular characterization of MON 94100 by NGS demonstrated that MON 94100 contained a single DNA insert. These whole-genome sequence analyses provided a comprehensive assessment of MON 94100 to determine the presence of sequences derived from PV-BNHT508701 and demonstrated that MON 94100 contained a single DNA insert with no detectable T-DNA II or backbone sequences.
- Directed sequencing (locus-specific PCR, DNA sequencing and analyses) of MON 94100, which characterized the complete sequence of the single DNA insert from PV-BNHT508701, the adjacent flanking DNA, and the 5' and 3' insert-to-flank junctions. This analysis confirmed that the sequence and organization of the DNA is identical to the corresponding region in the PV-BNHT508701 T-DNA I. Furthermore, the genomic organization at the insertion site was assessed by comparing the sequences flanking the T-DNA I insert in MON 94100 to the sequence of the insertion site in conventional canola. This analysis determined that no major DNA rearrangement occurred at the insertion site in MON 94100 upon DNA integration.
- Generational stability analysis by NGS demonstrated that the single PV-BNHT508701 T-DNA I insert in MON 94100 has been maintained through five breeding generations, thereby confirming the stability of the T-DNA in MON 94100.
- Segregation data confirm that the inserted T-DNA I segregated following Mendelian inheritance patterns, which corroborates the insert stability demonstrated by NGS and independently establishes the nature of the T-DNA I at a single chromosomal locus.

Taken together, the characterization of the genetic modification in MON 94100 demonstrates that a single copy of the intended T-DNA I was stably integrated at a single locus of the canola genome and that no T-DNA II or plasmid backbone sequences were present in MON 94100.

A.3(f)(ii) Pattern of expression of phenotype over several generations

In order to assess the presence of the DMO protein in MON 94100 across multiple breeding generations, Western blot analysis of MON 94100 was conducted on seed tissue collected from generations R3, R3F1, R4, R5, and R6 of MON 94100, using seed tissue of the conventional control (55076+65037) as negative control.

The presence of the DMO protein was demonstrated in five breeding generations of MON 94100 using Western blot analysis. The *E. coli*-produced DMO+27 protein reference standard (1 ng) was used as a reference for the positive identification of the DMO protein (Figure 14, lane 3). The presence of the DMO protein in seed tissue samples of MON 94100 was determined by visual comparison of the bands detected in five breeding generations (Figure 14, lanes 5-9) to the *E. coli*-produced DMO+27 protein reference standard. The MON 94100-produced DMO protein migrated indistinguishably from that of the *E. coli*-produced DMO+27 protein standard analyzed on the same Western blot. As expected, the DMO protein was not detected in the conventional control grain extract (Figure 14, lane 10).

For details, please also refer to Appendix 5 ([redacted] (MSL0030222)).

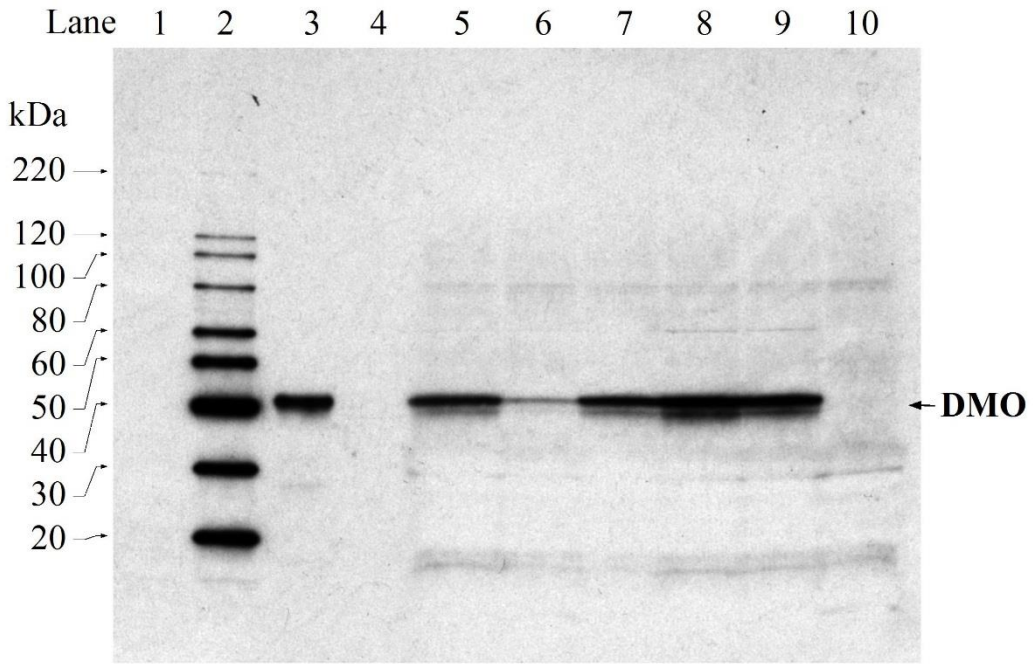

Figure 14. Presence of DMO Protein in Multiple Generations of MON 94100

Western blot probed with a polyclonal anti-DMO primary antibody and an HRP-conjugated anti-goat IgG secondary antibody. The 12-second exposure image is shown. The approximate MWs (kDa) of the MagicMark™ Protein Standards were shown on the left. Lane designations are as follows:

Lane	Sample	Amount
1	Precision Plus™ Protein Standards	5 µl
2	MagicMark™ Protein Standards	2 µl
3	*E. coli*-produced DMO+27 protein	1 ng
4	Empty	-
5	Test Substance, R3, 11485840	10 µl
6	Test Substance, R3F1, 11479261	10 µl
7	Test Substance, R4, 11492723	10 µl
8	Test Substance, R5, 11492724	10 µl
9	Test Substance, R6, 11492725	10 µl
10	Conventional Control, 11479580	10 µl

B. INFORMATION RELATED TO THE SAFETY OF THE GM FOOD

B.1 Characterisation and Safety Assessment

B.1(a) Characterisation and equivalence of MON 94100 DMO protein from

Identity of Function of the DMO Protein

DMO protein has been isolated from the bacterium *S. maltophilia* strain DI-6 (Krueger *et al.*, 1989; Herman *et al.*, 2005; Palleroni and Bradbury, 1993). MON 94100 expresses the DMO protein to confer tolerance to dicamba herbicide. DMO is an enzyme that catalyzes the demethylation of dicamba to the non-herbicidal compounds 3,6-dichlorosalicylic acid (DCSA) and formaldehyde (Chakraborty *et al.*, 2005). DCSA is a known metabolite of dicamba in cotton, soybean, soil, and livestock, whose safety has been evaluated by the FAO-WHO and EPA (FAO-WHO, 2011b; U.S. EPA, 2009b). The other reaction product, formaldehyde, is found naturally in many plants at levels up to several hundred ppm (Adrian-Romero *et al.*, 1999).

MON 94100 DMO protein is targeted to chloroplasts by a chloroplast transit peptide (CTP) to allow co-localization with the endogenous reductase and ferredoxin enzymes that supply electrons for the DMO demethylation reaction as described by Behrens *et al.* (2007). In the construction of the plasmid vector used in the development of MON 94100, PV-BNHT508701, a transit peptide coding sequence from Rubisco gene (*RbcS*) was joined to the *dmo* coding sequence to transport the produced protein to the canola chloroplast; this coding sequence results in the production of a precursor protein consisting of the DMO protein, a transit peptide, and an intervening sequence (IS), and is referred to as the MON 94100 DMO precursor protein. Typically, transit peptides are precisely removed from the precursor protein following delivery to the targeted plastid (della-Cioppa *et al.*, 1986) resulting in the fully processed protein. However, there are examples in the literature of alternatively processed forms of a protein targeted to a plant's chloroplast (Behrens *et al.*, 2007; Clark and Lamppa, 1992). Such alternative processing is observed with the DMO precursor protein produced in MON 94100. Data from N-terminal sequencing analysis of the MON 94100-produced DMO indicate that processing of the DMO precursor protein expressed in MON 94100 produced the same two isoforms of the fully processed MON87708 soybean DMO protein, DMO+27 and DMO. The determined amino acid sequence of DMO+27 is identical to wild-type DMO, except for a methionine at position 1 and 27 additional amino acids on its N-terminus derived from RbcS and IS. Therefore, the term "MON 94100 DMO protein" will be used to refer to both forms of the protein collectively and distinctions will only be made, where necessary.

The determined amino acid sequence of MON 94100 DMO is identical sequence to the wild-type DMO protein sequence derived from the DI-6 strain of *S. maltophilia* (Herman *et al.*, 2005), except for the insertion of an alanine at position 2, a single amino acid change at position 112 (tryptophan to cysteine) and an additional 27 amino acids encoded by the *RbcS* gene at the N-terminus for MON 94100 DMO+27 (Figure 15). The differences in the amino acid sequence among the wild-type DMO, and DMO proteins in MON 88701, MON 87708, MON 87419, MON 87429 and MON 94100 are not anticipated to have an effect on the structure of the catalytic site, functional activity, immunoreactivity or specificity because the N-terminus and position two are sterically distant from the catalytic site (D'Ordine *et al.*, 2009; Dumitru *et al.*, 2009).

For details, please also refer to Appendix 6 ([redacted] 2019, (MSL0030875)).

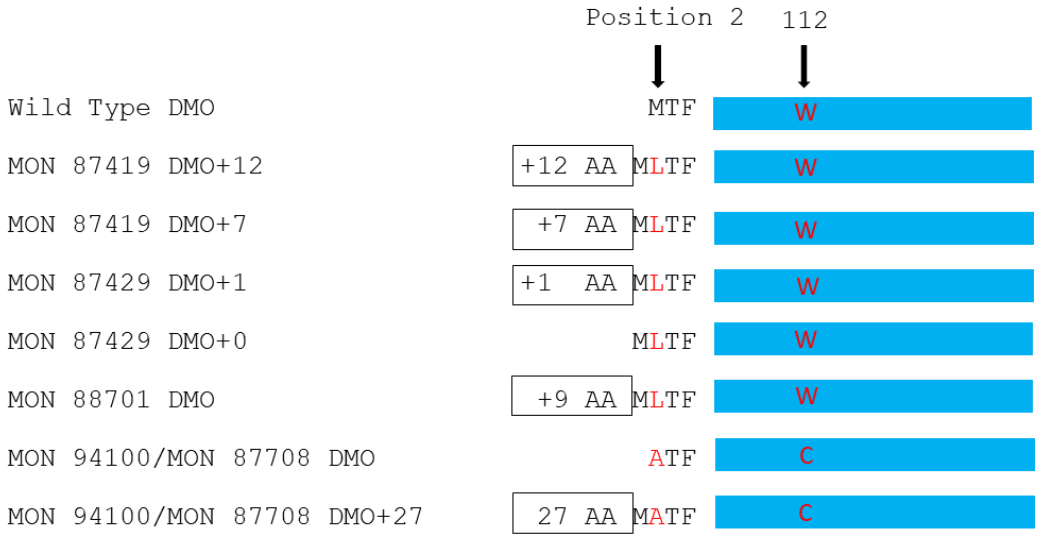

Figure 15. Forms of DMO Protein and Their Relation to the Wild-Type DMO Protein

The diagram represents the various DMO forms discussed in this section. Position refers to amino acid residues as wild-type DMO and the N-terminal boxed region indicates residues from CTPs. The blue regions indicate regions of 100% amino acid identity. The wild-type DMO form isolated from *S. maltophilia* was the first form sequenced (Herman *et al.*, 2005). The determined amino acid sequences of MON 94100 DMO and MON 87708 DMO are identical. The MON 94100 and MON 87708 DMO proteins have an identical sequence to the wild-type DMO protein, except for the insertion of an alanine at position 2, a single amino acid change at position 112 (tryptophan to cysteine) and an additional 27 amino acids encoded by the *RbcS* gene and IS at the N-terminus for MON 94100/MON 87708 DMO+27. The MON 94100/MON 87708 DMO (fully processed) protein additionally lacks a lead methionine residue.

Equivalence Studies of the DMO Protein

The safety assessment of crops derived through biotechnology includes characterization of the physicochemical and functional properties of and confirmation of the safety of the introduced protein(s). For the safety data generated using plant-produced MON 87708 DMO to be applied to plant-produced MON 94100 DMO protein, the equivalence of the plant-produced proteins must first be demonstrated. To assess the equivalence between plant-produced MON 94100 DMO and plant-produced MON 87708 DMO proteins, a small quantity of the MON 94100 DMO protein was purified from grain of MON 94100 canola. The MON 94100-produced DMO protein was characterized and the equivalence of the physicochemical characteristics and functional activity between the MON 94100-produced DMO and the MON 87708-produced DMO proteins was assessed using a panel of six analytical tests as shown in Table 6. Taken together, these data provide a detailed characterization of the MON 94100-produced DMO protein and establish the equivalence of MON 94100- and MON 87708-produced DMO proteins.

Table 6. Summary of MON 94100 DMO Protein Identity and Equivalence

Analytical Test Assessment	Section Cross Reference	Analytical Test Outcome
1. N-terminal sequence	B.1 (a)(i)	• The N-terminal sequences of two forms of DMO proteins were identified, referred to as MON 94100 DMO+27 and MON 94100 DMO • The N-terminal sequences of MON 94100-produced DMO+27 and DMO were consistent with the N-terminal sequences of the MON 87708-produced DMO+27 and DMO proteins observed by MALDI-TOF MS
2. LC-MS/MS[1]	B.1 (a)(ii)	• The peptide masses yielded by LC-MS/MS[1] analysis were consistent with the peptide masses from the theoretical trypsin digest of the MON 94100-produced DMO sequence
3. Western blot analysis	B.1 (a)(iii)	• MON 94100-produced DMO protein identity was confirmed using a Western blot probed with an antibody specific for DMO proteins • Immunoreactive properties of the MON 94100-produced DMO and the MON 87708-produced DMO proteins were shown to be equivalent
4. Apparent molecular weight (MW)	B.1 (a)(iv)	• Electrophoretic mobility and apparent molecular weight of the MON 94100-produced DMO and the MON 87708-produced DMO proteins were shown to be equivalent
5. Glycosylation analysis	B.1 (a)(v)	• MON 94100-produced DMO and MON 87708-produced DMO proteins were both shown to not be glycosylated
6. Functional activity	B.1 (a)(vi)	• Functional activity of the MON 94100-produced DMO and the MON 87708-produced DMO proteins were shown to be equivalent

[1] LC-MS/MS = Liquid chromatography coupled to tandem mass spectrometry

A summary of the data obtained to support the characterization of the MON 94100-produced DMO and a conclusion of protein equivalence is below.

B.1(a)(i) Results of the N-terminal sequencing analysis

The expected N-terminal sequence for the MON 94100 DMO protein deduced from the *dmo* gene present in MON 94100 canola, was determined by LC-MS/MS, except that the N-terminal methionine was cleaved *in vivo* by methionine aminopeptidase and other aminopeptidases (see Figure 16). The cleavage of the N-terminal methionine from proteins *in vivo* by methionine aminopeptidase is common in many organisms (Bradshaw *et al.*, 1998; Wang *et al.*, 2016). The N-terminal sequence for the DMO protein of MON 94100 was consistent with the N-terminal sequence for the DMO protein from MON 87708 soybean observed by MALDI-TOF MS (Figure 16). Hence, the sequence information confirms the identity of the DMO protein isolated from the grain of MON 94100 and its equivalence to the MON 87708 DMO protein.

The expected N-terminal sequence for the DMO+27 protein deduced from the additional 27 amino acids at the N-terminus encoded by the target gene was observed by LC-MS/MS analysis. The N-terminal sequence for the DMO+27 protein isolated from MON 94100 was consistent with the N-terminal sequence for the DMO+27 protein from MON 87708 observed by MALDI-TOF MS (Figure 17 and Appendix 6). Hence, the sequence information confirms the identity of the DMO+27 protein isolated from the grain of MON 94100 and its equivalence to the MON 87708 DMO+27 protein.

For details, pleases refer to Appendix 6 ([redacted] 2019, (MSL0030875)).

Amino acid residue # from N-terminus	→1	2	3	4	5	6	7	8	9	10	11	12	13	14	15	16
MON 87708 DMO sequence	→	A	T	F	V	R	N	A	W	Y	V	A	A	L	P	E
		|	|	|	|	|	|	|	|	|	|	|	|	|	|	|	|
Expected DMO sequence	→M	A	T	F	V	R	N	A	W	Y	V	A	A	L	P	E
		|	|	|	|	|	|	|	|	|	|	|	|	|	|	|	|
Experimental MON 94100 DMO sequence	→	A	T	F	V	R	N	A	W	Y	V	A	A	L	P	E

Figure 16. N-Terminal Sequence of the DMO Protein of MON 94100

The experimental sequence obtained from the DMO from MON 94100 was compared to the expected sequence deduced from the *dmo* gene present in MON 94100. The DMO protein from MON 87708 sequence above was derived from the reference substance COA (lot 7546, see Appendix 6). The single letter International Union of Pure and Applied Chemistry - International Union of Biochemistry (IUPAC-IUB) amino acid code is M, methionine; A, Alanine; T, Threonine: F, Phennylalanine; V, Valine; R, Arginine; N, Asparagine; W, Tryptophan; Y, Tyrosine; V, Valine; L, leucine; P, proline; E, Glutamic acid.

Amino acid residue # from N-terminus	→	1	2	3	4	5	6	7	8	9	10	11	12	13	14	15
MON 87708 DMO+27 sequence	→	M	Q	V	W	P	P	I	G	K	K	K	F	E	T	L
		|	|	|	|	|	|	|	|	|	|	|	|	|	|	|	|
Expected DMO+27 sequence	→	M	Q	V	W	P	P	I	G	K	K	K	F	E	T	L
		|	|	|	|	|	|	|	|	|	|	|	|	|	|	|	|
Experimental MON 94100 DMO+27 sequence	→	M	Q	V	W	P	P	I	G	K	K	K	F	E	T	L

Figure 17. N-Terminal Sequence of the DMO+27 Protein of MON 94100

The experimental sequence obtained from the DMO+27 of MON 94100 was compared to the expected N-terminal sequence from the additional 27 amino acids at the N-terminus encoded by the *RbcS* gene that resulted from incomplete processing of the chloroplast transit peptide in MON 94100. The DMO+27 protein of MON 87708 sequence above was derived from the reference substance COA (lot 7546, see Appendix 6).

B.1(a)(ii) Results of nano LC-MS/MS mass fingerprint analysis

Peptide mass fingerprint analysis is a standard technique used for confirming the identity of proteins. The ability to identify a protein using this method is dependent upon matching a sufficient number of observed tryptic peptide fragment masses with predicted tryptic peptide fragment masses. In general, protein identification made by peptide mapping is considered to be reliable if >40% of the protein sequence was identified by matching experimental masses observed for the tryptic peptide fragments to the expected masses for the fragments (Biron *et al.*, 2006; Krause *et al.*, 1999). The identity of the MON 94100-produced DMO protein was confirmed by LC-MS/MS analysis of peptide fragments produced by the trypsin digestion of the MON 94100-produced DMO protein.

There were 43 unique peptides identified that corresponded to the masses expected to be produced by trypsin digestion of the DMO from MON 94100 (Table 7). The identified masses with the highest score were listed in the Table 7 and used to assemble a coverage map of the entire DMO protein from MON 94100 Figure 18A). The experimentally determined coverage of the DMO from MON 94100 was 100 % (Figure 18A, 339 out of 339 amino acids). This analysis further confirms the identity of DMO from MON 94100.

There were 16 unique peptides identified that corresponded to the masses expected to be produced by trypsin digestion of the DMO from MON 87708 (Table 8) by MALDI-TOF MS analysis during the protein characterization. The identified masses were used to assemble a coverage map of the entire DMO protein from MON 87708 (Figure 18B). The experimentally determined coverage of the DMO from MON 87708 was 62%, 211 out of 339 amino acids of the expected protein sequence was covered by the identified peptides (Figure 18B).

There were 50 unique peptides identified that corresponded to the masses expected to be produced by trypsin digestion of the DMO+27 of MON 94100 (Table 9). The identified masses with the highest score were listed in the Table 9 and used to assemble a coverage map of the entire DMO+27 protein (Figure 19A). The experimentally determined coverage of the DMO+27 of MON 94100 was 98% (Figure 19A, 361 out of 367 amino acids). This analysis further confirms the identity of DMO+27 of MON 94100.

There were 16 unique peptides identified that corresponded to the masses expected to be produced by trypsin digestion of the DMO+27 of MON 87708 (Table 10) by MALDI-TOF MS analysis during the protein characterization. The identified masses were used to assemble a coverage map of the entire DMO+27 of MON 87708 (Figure 19B). The experimentally determined coverage of the DMO+27 of MON 87708 was 61%, 223 out of 367 amino acids of the expected protein sequence was covered by the identified peptides (Figure 19B).

Table 7. Summary of the Tryptic Masses Identified for the DMO from MON 94100 Canola Using LC-MS/MS

Experimental Mass[1]	Calculated Mass[2]	Difference[3]	Fragment[4]	Sequence[5]
592.3332	592.3333	-0.0001	1 - 5	ATFVR
1718.8526	1718.8515	0.0011	6 - 20	NAWY...LSEK
2142.1131	2142.1109	0.0022	6 - 24	NAWY...PLGR
441.2698	441.27	-0.0002	21 - 24	PLGR
1274.7239	1274.7234	0.0005	25 - 35	TILD...ALYR
1759.9026	1759.9039	-0.0013	36 - 51	QPDG...CPHR
4196.9465	4196.9446	0.0019	52 - 90	FAPL...NGAR
755.4292	755.429	0.0002	91 - 97	PASLNVR
832.4441	832.4443	-0.0002	98 - 104	SFPVVER
2696.2712	2696.2727	-0.0015	105 - 129	DALI...FGCR
719.3604	719.3602	0.0002	130 - 135	VDPAYR
1468.6407	1468.6405	0.0002	136 - 148	TVGG...CNYK
1993.0149	1993.0204	-0.0055	149 - 165	LLVD...YVHR
1107.4951	1107.4945	0.0006	166 - 175	ANAQ...AFDR
1505.7229	1505.7222	0.0007	166 - 178	ANAQ...RLER
1500.786	1500.7858	0.0002	179 - 192	EVIV...ALMK
2684.4144	2684.4129	0.0015	179 -204	EVIV…LMAK
1169.6494	1169.6478	0.0016	193 - 204	IPGG...LMAK
1585.9017	1585.9014	0.0003	193 - 207	IPGG...KFLR
1427.6805	1427.6793	0.0012	208 - 220	GANT...NDIR
1855.8957	1855.8965	-0.0008	208 - 223	GANT...RWNK
2188.1374	2188.1350	0.0024	221 - 240	WNKV…GTPK
1743.9227	1743.9229	-0.0002	224 - 240	VSAM...GTPK
2581.3298	2581.3322	-0.0024	224 - 247	VSAM...IHSR
855.4198	855.4199	-0.0001	241 - 247	EQSIHSR
2396.0897	2396.0856	0.0041	248 - 268	GTHI...GSSR
1576.7199	1576.7192	0.0007	269 - 282	NFGI...GVLR
2604.2638	2604.2642	-0.0004	269 -291	NFGI…ALVK
1029.5611	1029.5607	0.0004	283 - 291	SWQA...ALVK
1401.725	1401.7252	-0.0002	283 - 294	SWQA...KEDK
2297.2404	2297.2379	0.0025	283 - 302	SWQA...AIER
1285.6878	1285.6878	0.0000	292 - 302	EDKV...AIER
913.5229	913.5233	-0.0004	295 - 302	VVVEAIER
1069.6251	1069.6244	0.0007	295 - 303	VVVE...IERR
1147.6111	1147.6098	0.0013	304 - 313	RAYV...NGIR
2448.2003	2448.2002	0.0001	304 - 325	RAYV...AAVR
991.5089	991.5087	0.0002	305 - 313	AYVE...NGIR
2292.0976	2292.099	-0.0014	305 - 325	AYVE...AAVR

Experimental Mass[1]	Calculated Mass[2]	Difference[3]	Fragment[4]	Sequence[5]
1318.6013	1318.6009	0.0004	314 - 325	PAML...AAVR
1613.8626	1613.8624	0.0002	326 - 339	VSRE...LEAA
517.2746	517.2748	-0.0002	329 - 332	EIEK
1271.6611	1271.6608	0.0003	329 - 339	EIEK...LEAA
772.3962	772.3967	-0.0005	333 - 339	LEQLEAA

[1] Only experimental masses that matched calculated masses with the highest scores are listed in the table.
[2] The calculated mass is the exact molecular mass calculated from the matched peptide sequence.
[3] The calculated difference = experimental mass – calculated mass.
[4] Fragment numbering is based on the expected N-terminal sequence from the pMON116516 plasmid.
[5] For peptide matches greater than nine amino acids in length the first 4 residues and last 4 residues are shown separated by dots (…).

Table 8. Summary of the Tryptic Masses Identified for the DMO from MON 87708 Soybean Using MALDI-TOF MS

Experimental Mass[1]	Calculated Mass[2]	Difference[3]	Fragment[4]	Sequence[5]
2142.1851	2142.1109	0.0742	6 - 24	NAWY…PLGR
1274.7619	1274.7234	0.0385	25 - 35	TILDT…ALYR
1760.9473	1760.8880	0.0594	36 - 51	QPDG…CPHR
832.4699	832.4443	0.0256	98 - 104	SFPVVER
2698.3572	2698.2407	0.1165	105 -129	DALI…FGCR
719.3803	719.3602	0.0201	130 - 135	VDPAYR
1993.0902	1993.0204	0.0699	149 - 165	LLVD…YVHR
1107.5277	1107.4945	0.0332	166 - 175	ANAQ…AFDR
1505.7699	1505.7222	0.0477	166 - 178	ANAQ…RLER
1427.7268	1427.6793	0.0475	208 - 220	GANT…NDIR
1743.9728	1743.9229	0.0049	224 - 240	VSAM…GTPK
2397.1575	2397.0696	0.0880	248 - 268	GTHI…GSSR
1576.7708	1576.7192	0.0517	269 - 282	NFGI…GVLR
1285.7243	1285.6878	0.0336	292 -302	EDKV…AIER
913.5499	913.5233	0.0267	295 - 302	VVVEAIER
2293.1851	2293.0831	0.1021	305 - 325	AYVE…AAVR

[1] Only experimental masses that matched calculated masses are listed in the table.
[2] The calculated mass is the exact molecular mass calculated from the matched peptide sequence.
[3] The calculated difference = experimental mass – calculated mass.
[4] Fragment numbering is based on the expected N-terminal sequence from the pMON58498 plasmid.
[5] For peptide matches greater than nine amino acids in length the first 4 residues and last 4 residues are shown separated by dots (…).

Table 9. Summary of the Tryptic Masses Identified for the DMO+27 from MON 94100 Canola Using LC-MS/MS

Experimental Mass[1]	Calculated Mass[2]	Difference[3]	Fragment[4]	Sequence[5]
1068.5793	1068.5790	0.0003	1 - 9	MQVW...PIGK
1196.6752	1196.6740	0.0012	1 - 10	MQVW...IGKK
923.5229	923.5229	0.0000	2 - 9	QVWPPIGK
1691.9613	1691.9610	0.0003	10 - 23	KKFE...PLTR
1563.8664	1563.8661	0.0003	11 - 23	KFET...PLTR
1435.7721	1435.7711	0.0010	12 - 23	FETL...PLTR
794.4112	794.4109	0.0003	27 - 33	AMATFVR
1718.8524	1718.8515	0.0009	34 - 48	NAWY...LSEK
2142.1126	2142.1109	0.0017	34 - 52	NAWY...PLGR
441.2699	441.2700	-0.0001	49 - 52	PLGR
1274.7239	1274.7234	0.0005	53 - 63	TILD...ALYR
1759.9056	1759.9039	0.0017	64 - 79	QPDG...CPHR
4196.9479	4196.9446	0.0033	80 - 118	FAPL...NGAR
755.4289	755.4290	-0.0001	119 - 125	PASLNVR
1569.8631	1569.8627	0.0004	119 - 132	PASL...VVER
832.4448	832.4443	0.0005	126 - 132	SFPVVER
2696.2639	2696.2727	-0.0088	133 - 157	DALI...FGCR
3397.6151	3397.6224	-0.0073	133 - 163	DALI...PAYR
719.3589	719.3602	-0.0013	158 - 163	VDPAYR
1468.6416	1468.6405	0.0011	164 - 176	TVGG...CNYK
1993.0184	1993.0204	-0.0020	177 - 193	LLVD...YVHR
1107.4945	1107.4945	0.0000	194 - 203	ANAQ...AFDR
1505.7228	1505.7222	0.0006	194 - 206	ANAQ...RLER
1500.7857	1500.7858	-0.0001	207 - 220	EVIV...ALMK
2684.4138	2684.4129	0.0009	207 - 232	EVIV…LMAK
1169.6498	1169.6478	0.0020	221 - 232	IPGG...LMAK
1585.9026	1585.9014	0.0012	221 - 235	IPGG...KFLR
1427.6837	1427.6793	0.0044	236 - 248	GANT...NDIR
2188.1363	2188.1350	0.0013	249 -268	WNKV…GTPK
1743.9229	1743.9229	0.0000	252 - 268	VSAM...GTPK
2581.3359	2581.3322	0.0037	252 - 275	VSAM...IHSR
855.4197	855.4199	-0.0002	269 - 275	EQSIHSR
2396.0841	2396.0856	-0.0015	276 - 296	GTHI...GSSR
1576.7223	1576.7192	0.0031	297 - 310	NFGI...GVLR
2604.2656	2606.2642	-0.0014	297 -319	NFGI…ALVK
1029.5609	1029.5607	0.0002	311 - 319	SWQA...ALVK
1401.7260	1401.7252	0.0008	311 - 322	SWQA...KEDK

Experimental Mass[1]	Calculated Mass[2]	Difference[3]	Fragment[4]	Sequence[5]
2297.2395	2297.2379	0.0016	311 - 330	SWQA...AIER
1285.6888	1285.6878	0.0010	320 - 330	EDKV...AIER
1441.7903	1441.7889	0.0014	320 - 331	EDKV...IERR
913.5234	913.5233	0.0001	323 - 330	VVVEAIER
1069.6244	1069.6244	0.0000	323 - 331	VVVE...IERR
1147.6107	1147.6098	0.0009	332 - 341	RAYV...NGIR
2448.2003	2448.2002	0.0001	332 - 353	RAYV...AAVR
991.5086	991.5087	-0.0001	333 - 341	AYVE...NGIR
2292.1030	2292.0990	0.0040	333 - 353	AYVE...AAVR
1318.6007	1318.6009	-0.0002	342 - 353	PAML...AAVR
517.2746	517.2748	-0.0002	357 - 360	EIEK
1271.6612	1271.6608	0.0004	357 - 367	EIEK...LEAA
772.3963	772.3967	-0.0004	361 - 367	LEQLEAA

[1] Only experimental masses that matched calculated masses with the highest scores are listed in the table.
[2] The calculated mass is the exact molecular mass calculated from the matched peptide sequence.
[3] The calculated difference = experimental mass – calculated mass.
[4] Fragment numbering is based on the expected N-terminal sequence from the pMON116516 plasmid.
[5] For peptide matches greater than nine amino acids in length the first 4 residues and last 4 residues are shown separated by dots (…).

Table 10. Summary of the Tryptic Masses Identified for the DMO+27 from MON 87708 Soybean Using MALDI-TOF MS

Experimental Mass[1]	Calculated Mass[2]	Difference[3]	Fragment[4]	Sequence[5]
1793.8598	1793.9312	-0.0714	12 - 26	FETL…RDSR
2142.1748	2142.1109	0.0639	34 - 52	NAWY…PLGR
1274.7615	1274.7234	0.0381	53 - 63	TILD…ALYR
1760.9400	1760.888	0.0521	64 - 79	QPDG…CPHR
832.4707	832.4443	0.0264	126 - 132	SFPVVER
2698.3148	2698.2407	0.1011	133 -157	DALI…FGCR
719.3816	719.3602	0.0214	158 - 163	VDPAYR
1993.0806	1993.0204	0.0603	177- 193	LLVD…YVHR
1107.5259	1107.4945	0.0314	194 -203	ANAQ…AFDR
1505.7641	1505.7222	0.0419	194 - 206	ANAQ…RLER
1427.7226	1427.6793	0.0433	236 - 248	GANT…NDIR
1743.9218	1743.9229	-0.0011	252 - 268	VSAM…GTPK
2397.1426	2397.0696	0.0731	276 - 296	GTHI…GSSR
1576.7667	1576.7192	0.0476	297 - 310	NFGI…GVLR
913.5501	913.5233	0.0269	323 - 330	VVVEAIER
2293.1704	2293.0831	0.0874	333 - 353	AYVE…AAVR

[1] Only experimental masses that matched calculated masses are listed in the table.
[2] The calculated mass is the exact molecular mass calculated from the matched peptide sequence.
[3] The calculated difference = experimental mass – calculated mass.
[4] Fragment numbering is based on the expected N-terminal sequence from the pMON58498 plasmid.
[5] For peptide matches greater than nine amino acids in length the first 4 residues and last 4 residues are shown separated by dots (…).

(A)

```
  1 ATFVRNAWYV AALPEELSEK PLGRTILDTP LALYRQPDGV VAALLDICPH
 51 RFAPLSDGIL VNGHLQCPYH GLEFDGGGQC VHNPHGNGAR PASLNVRSFP
101 VVERDALIWI CPGDPALADP GAIPDFGCRV DPAYRTVGGY GHVDCNYKLL
151 VDNLMDLGHA QYVHRANAQT DAFDRLEREV IVGDGEIQAL MKIPGGTPSV
201 LMAKFLRGAN TPVDAWNDIR WNKVSAMLNF IAVAPEGTPK EQSIHSRGTH
251 ILTPETEASC HYFFGSSRNF GIDDPEMDGV LRSWQAQALV KEDKVVVEAI
301 ERRRAYVEAN GIRPAMLSCD EAAVRVSREI EKLEQLEAA
```

(B)

```
  1 ATFVRNAWYV AALPEELSEK PLGRTILDTP LALYRQPDGV VAALLDICPH
 51 RFAPLSDGIL VNGHLQCPYH GLEFDGGGQC VHNPHGNGAR PASLNVRSFP
101 VVERDALIWI CPGDPALADP GAIPDFGCRV DPAYRTVGGY GHVDCNYKLL
151 VDNLMDLGHA QYVHRANAQT DAFDRLEREV IVGDGEIQAL MKIPGGTPSV
201 LMAKFLRGAN TPVDAWNDIR WNKVSAMLNF IAVAPEGTPK EQSIHSRGTH
251 ILTPETEASC HYFFGSSRNF GIDDPEMDGV LRSWQAQALV KEDKVVVEAI
301 ERRRAYVEAN GIRPAMLSCD EAAVRVSREI EKLEQLEAA
```

Figure 18. Peptide Map of the DMO from MON 94100 Canola and DMO from MON 87708 Soybean

(A). The amino acid sequence of the DMO from MON 94100 was deduced from the *dmo* gene present in MON 94100. Boxed regions correspond to peptides that were identified from the DMO from MON 94100 sample using LC-MS/MS. In total, 100% coverage (339 out of 339 amino acids) of the expected protein sequence was covered by the identified peptides.

(B). The amino acid sequence of the DMO from MON 87708 was deduced from the *dmo* gene present in MON 87708. Boxed regions correspond to peptides that were identified from the DMO from MON 87708 sample using MALDI-TOF MS. In total, 62% coverage (211 out of 339 amino acids) of the expected protein sequence was covered by the identified peptides.

(A)

```
  1 MQVWPPIGKK KFETLSYLPP LTRDSRAMAT FVRNAWYVAA LPEELSEKPL
 51 GRTILDTPLA LYRQPDGVVA ALLDICPHRF APLSDGILVN GHLQCPYHGL
101 EFDGGGQCVH NPHGNGARPA SLNVRSFPVV ERDALIWICP GDPALADPGA
151 IPDFGCRVDP AYRTVGGYGH VDCNYKLLVD NLMDLGHAQY VHRANAQTDA
201 FDRLEREVIV GDGEIQALMK IPGGTPSVLM AKFLRGANTP VDAWNDIRWN
251 KVSAMLNFIA VAPEGTPKEQ SIHSRGTHIL TPETEASCHY FFGSSRNFGI
301 DDPEMDGVLR SWQAQALVKE DKVVVEAIER RRAYVEANGI RPAMLSCDEA
351 AVRVSREIEK LEQLEAA
```

(B)

```
  1 MQVWPPIGKK KFETLSYLPP LTRDSRAMAT FVRNAWYVAA LPEELSEKPL
 51 GRTILDTPLA LYRQPDGVVA ALLDICPHRF APLSDGILVN GHLQCPYHGL
101 EFDGGGQCVH NPHGNGARPA SLNVRSFPVV ERDALIWICP GDPALADPGA
151 IPDFGCRVDP AYRTVGGYGH VDCNYKLLVD NLMDLGHAQY VHRANAQTDA
201 FDRLEREVIV GDGEIQALMK IPGGTPSVLM AKFLRGANTP VDAWNDIRWN
251 KVSAMLNFIA VAPEGTPKEQ SIHSRGTHIL TPETEASCHY FFGSSRNFGI
301 DDPEMDGVLR SWQAQALVKE DKVVVEAIER RRAYVEANGI RPAMLSCDEA
351 AVRVSREIEK LEQLEAA
```

Figure 19. Peptide Map of the DMO+27 from MON 94100 Canola and MON 87708 Soybean

(A). The amino acid sequence of the canola DMO+27 from MON 94100 was deduced from the *dmo* and *rbcS* gene present in MON 94100. Boxed regions correspond to peptides that were identified from the canola DMO+27 from MON 94100 sample using LC-MS/MS. In total, 98% coverage (361 out of 367 amino acids) of the expected protein sequence was covered by the identified peptides.
(B). The amino acid sequence of the soy DMO+27 from MON 87708 was deduced from the *dmo* and *rbcS* gene present in MON 87708. Boxed regions correspond to peptides that were identified from the soy DMO+27 from MON 87708 sample using MALDI-TOF MS. In total, 61% (Or 60.8%. 60% coverage was listed on COA, which might be an omitting the decimal point by the software) coverage (223 out of 367 amino acids) of the expected protein sequence was covered by the identified peptides.

B.1(a)(iii) Results of Western blot analysis of the MON 94100 DMO protein isolated from the grain of MON 94100 and immunoreactivity comparison to MON 87708 DMO protein isolated from the grain of MON 87708

Western blot analysis was conducted using goat anti-DMO polyclonal antibody as additional means to confirm the identity of the MON 94100-produced DMO protein isolated from the MON 94100 grain to assess the equivalence of the immunoreactivity of the MON 94100-produced and MON 87708-produced DMO proteins.

The results showed that immunoreactive bands with the same electrophoretic mobility were present in all lanes loaded with the MON 94100-produced and MON 87708-produced DMO proteins (Figure 20). As expected, the signal intensity increased with increasing load amounts of the MON 94100-produced and MON 87708-produced DMO proteins, thus, supporting identification of MON 94100-produced DMO protein.

To compare the immunoreactivity of the MON 94100-produced and MON 87708-produced DMO proteins, densitometric analysis was conducted on the bands that migrated at the expected apparent MW for DMO proteins (use single area that contain both ~38 to ~41 kDa bands). The signal intensity (reported in OD) of the bands of interest in lanes loaded with MON 94100-produced and MON 87708-produced DMO proteins were measured (Table 11). Although the expression ratio between DMO+27 and DMO bands in MON 94100-produced DMO and the MON 87708-produced DMO proteins are different, the mean signal intensity of the MON 94100-produced DMO proteins was within the acceptance limits for equivalence, ± 35% of the mean signal intensity of the MON 87708-produced DMO proteins. It has been reported that a variability in Western blotting up to 35% is common since higher variability was observed with this technology (Anthony *et al.*, 2014) hence, the MON 94100-produced DMO and MON 87708-produced DMO proteins were determined to have equivalent immunoreactivity.

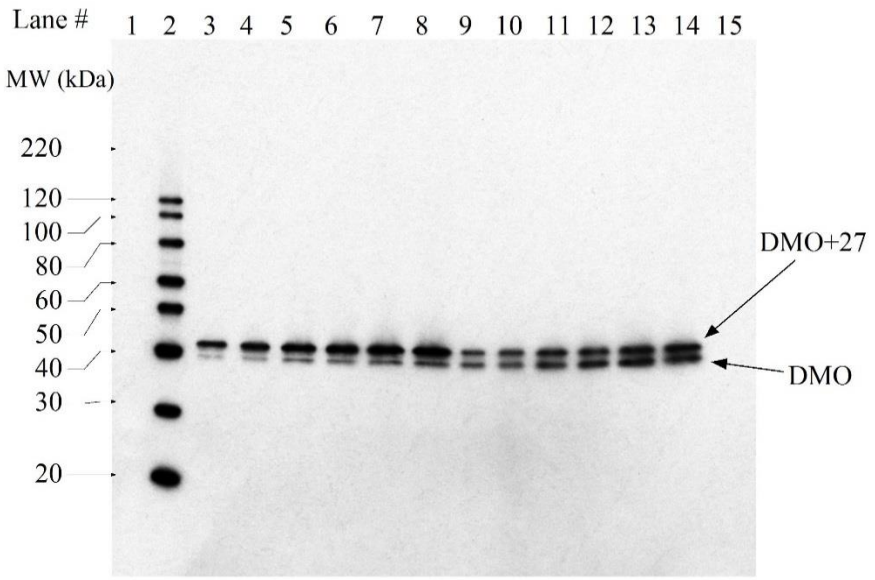

Figure 20. Immunoreactivity Analysis of MON 94100-produced and MON 87708-produced DMO Proteins by Western Blot

Aliquots of the MON 94100-produced and MON 87708-produced DMO proteins were subjected to SDS-PAGE and electrotransferred to a nitrocellulose membrane. Proteins were detected using goat anti-DMO polyclonal antibody as the primary antibody. Immunoreactive bands were visualized using HRP-conjugated secondary antibody and an ECL system. The 10-second exposure is shown. The approximate MW (kDa) of the MagicMark XP standards are shown on the left. The DMO+27 and DMO proteins were indicated with arrows in the image. Lane designations are as follows:

Lane	Sample	Amount (ng)
1	Precision Plus Protein™ Standards	-
2	MagicMark XP	-
3	MON 94100-produced DMO	3
4	MON 94100-produced DMO	3
5	MON 94100-produced DMO	6
6	MON 94100-produced DMO	6
7	MON 94100-produced DMO	9
8	MON 94100-produced DMO	9
9	MON 87708-produced DMO	3
10	MON 87708-produced DMO	3
11	MON 87708-produced DMO	6
12	MON 87708-produced DMO	6
13	MON 87708-produced DMO	9
14	MON 87708-produced DMO	9
15	Empty	-

Table 11. Immunoreactivity of the MON 94100 and MON 87708-produced DMO Proteins

Mean Signal Intensity from MON 94100-produced DMO [1] (OD)	Mean Signal Intensity from MON 87708-produced DMO [1] (OD)	Acceptance Limits[2] (OD)
2108	1994	1296 – 2692

[1] Each value represents the mean of six values (n = 6) for the area that contain both DMO and DMO+27 bands, rounded to a whole number.

[2] The acceptance limits are for the MON 94100-produced DMO protein and are based on the interval between -35% (1994 x 0.65 = 1296) and +35 % (1994 x 1.35 = 2692) of the mean of the MON 87708-produced DMO signal intensity across all loads.

B.1(a)(iv) Results of the MON 94100 DMO protein molecular weight and purity analysis

For apparent molecular weight (MW) and purity determination, the MON 94100-produced DMO and the MON 87708-produced DMO proteins were subjected to SDS-PAGE. Following electrophoresis, the gel was stained with Brilliant Blue G-Colloidal stain and analyzed by densitometry. The MON 94100-produced DMO proteins (Figure 21, lanes 3-8) migrated to the same position on the gel as the MON 87708-produced DMO proteins (Figure 21, lane 2) and the apparent MW of DMO+27 and DMO was calculated to be 39.4 and 38.0 kDa respectively (Table 12). Because the experimentally determined apparent MW of the MON 94100-produced DMO protein was within the acceptance limits for equivalence (Table 13), the MON 94100-produced DMO and MON 87708-produced DMO proteins were determined to have equivalent apparent MWs.

The purity of the MON 94100-produced DMO protein including, both DMO+27 and DMO bands was calculated based on the six lanes loaded on the gel (Figure 21, lanes 3-8). The average purity was determined to be 92% (Table 12).

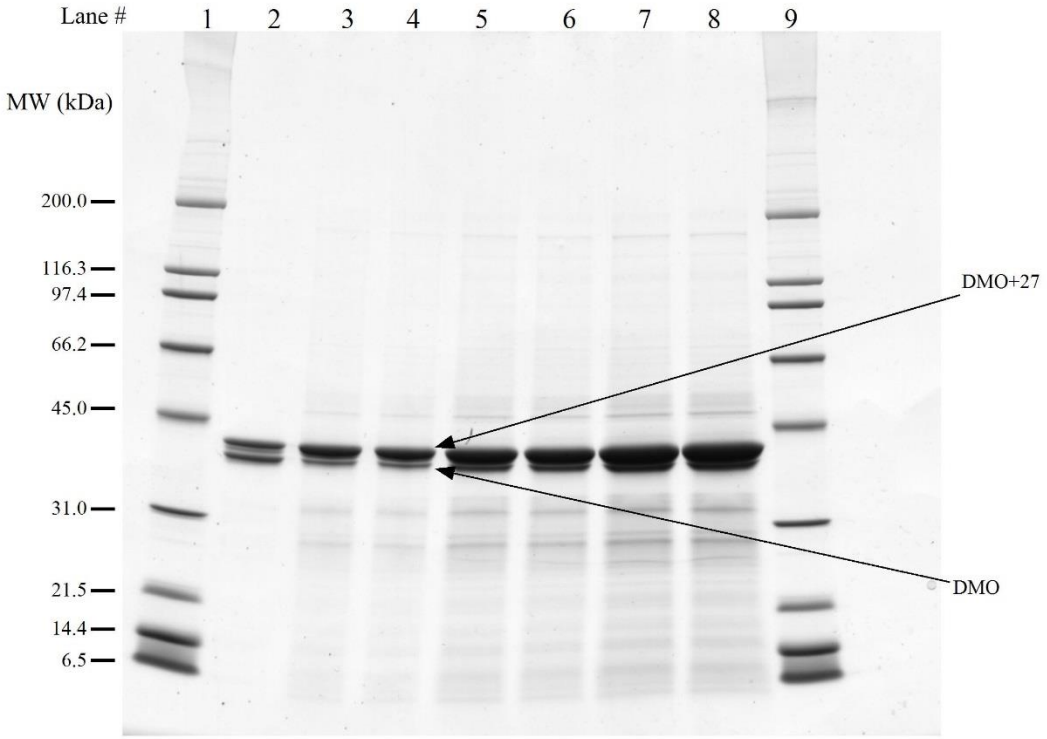

Figure 21. Purity and Apparent Molecular Weight Analysis of the MON 94100-produced DMO Protein

Aliquots of the MON 94100-produced and the MON 87708-produced DMO proteins were subjected to SDS-PAGE and the gel was stained with Brilliant Blue G-Colloidal stain. The MWs (kDa) are shown on the left and correspond to the standards loaded in lanes 1 and 9. Lane 10 was empty and was not labeled. The DMO+27 and DMO proteins were indicated with arrows in the image. Lane designations are as follows:

Lane	Sample	Amount (µg)
1	Broad Range MW Standard	5.0
2	MON 87708-produced DMO	1.0
3	MON 94100-produced DMO	1.0
4	MON 94100-produced DMO	1.0
5	MON 94100-produced DMO	2.0
6	MON 94100-produced DMO	2.0
7	MON 94100-produced DMO	3.0
8	MON 94100-produced DMO	3.0
9	Broad Range MW Standard	5.0
10	Empty	

Table 12. Apparent Molecular Weight and Purity Analysis of the MON 94100-produced DMO Protein

	Apparent MW[1] (kDa)	Purity[2] (%)
Average (n=6)		
DMO+27	39.4	92
DMO	38.0	

[1]Final MW was rounded to one decimal place.
[2]Average % purity was rounded to the nearest whole number and included both DMO+27 and DMO bands.

Table 13. Apparent Molecular Weight Comparison Between the MON 94100-produced DMO and MON 87708-produced DMO Proteins

Proteins	Apparent MW of MON 94100-Produced DMO Protein (kDa)	Apparent MW MON 87708-Produced DMO Protein[1] (kDa)	Acceptance Limits[2] (kDa)
DMO+27	39.4	41.3	39.2 - 42.9
DMO	38.0	38.9	36.5 - 40.6

[1] From the COA for the apparent MW of the MON 87708-produced DMO protein.
[2] Data obtained for the MON 87708-produced DMO protein were used to generate the prediction interval (Appendix 6).

B.1(a)(v) MON 94100-produced DMO and MON 87708-produced DMO glycosylation analysis

Some eukaryotic proteins are post-translationally modified by the addition of carbohydrate moieties (Rademacher *et al.*, 1988). To test whether the DMO protein was glycosylated when expressed in the MON 94100 canola grain, the MON 94100-produced DMO protein was analyzed using an ECL™ glycoprotein detection method. Transferrin, a glycosylated protein, was used as a positive control in the assy. To assess equivalence of the MON 94100-produced and MON 87708-produced DMO proteins, the MON 87708-produced DMO protein was also analyzed.

A clear glycosylation signal was observed at the expected molecular weight (~80 kDa) in the lanes containing the positive control (transferrin) and the band intensity increased with increasing concentration (Figure 22A). In contrast, no glycosylation signal was observed in the lanes containing the MON 87708-produced DMO protein or MON 94100-produced DMO protein (Figure 22A).

To confirm that MON 94100-produced and MON 87708-produced DMO proteins were appropriately loaded for glycosylation analysis, a second membrane with identical loadings and transfer time was stained with Coomassie Blue R250 for protein detection. Both the MON 94100-produced and MON 87708-produced DMO proteins were detected (Figure 22B). These data indicate that the glycosylation status of MON 94100-produced DMO protein is equivalent to that of the MON 87708-produced DMO protein and that neither is glycosylated.

A. B.

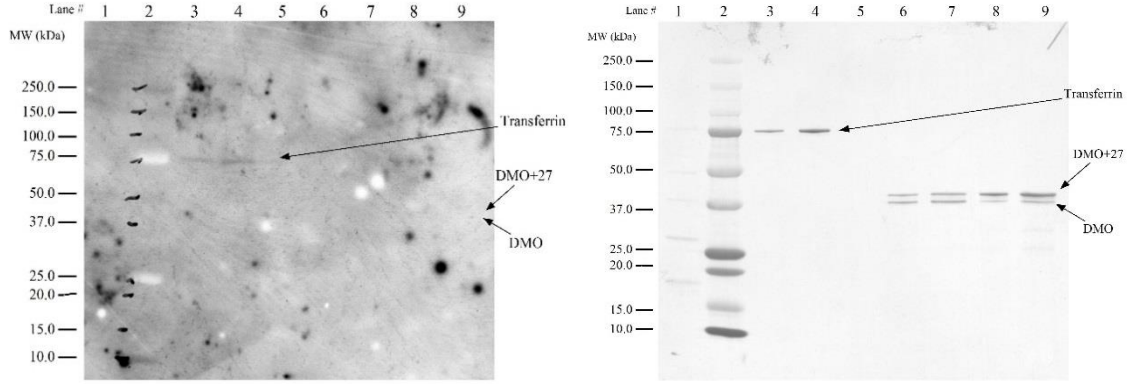

Figure 22. Glycosylation Analysis of the MON 94100-produced DMO Protein and MON 87708-produced DMO Protein

Aliquots of the transferrin (positive control), MON 87708-produced and MON 94100-produced DMO proteins were subjected to SDS-PAGE and electrotransferred to a PVDF membrane. The MWs (kDa) correspond to the Precision Plus Protein™ Standards. The arrows show the expected migration of the MON 94100-produced and MON 87708-produced DMO proteins and transferrin. Lanes 5 and 10 were empty, and lane 10 was cropped from both images. The DMO+27 and DMO proteins were indicated with arrows in the image. (A) Where present, the labeled carbohydrate moieties were detected by addition of streptavidin conjugated to HRP followed by ECL reagents and exposure to Hyperfilm®. The 5-second exposure is shown. (B) An equivalent blot was stained with Coomassie Blue R250 to confirm the presence of proteins. Lane designations are as follows, (the MagicMark XP in lane 1 did not show signal with ECL due to oxidation during the glycosylation detection process).

Lane	Sample	Amount (ng)
1	MagicMark XP	-
2	Precision Plus Protein™ Standards	-
3	Transferrin (positive control)	100
4	Transferrin (positive control)	200
5	Empty	-
6	MON 87708-produced DMO	100
7	MON 87708-produced DMO	200
8	MON 94100-produced DMO	100
9	MON 94100-produced DMO	200
10	Empty	-

B.1(a)(vi) MON 94100-produced DMO and MON 87708-produced DMO functional activity

The functional activity of the MON 94100-produced and MON 87708-produced DMO proteins were determined by measuring the amount of dicamba that was converted to DCSA by the DMO enzyme via HPLC separation and fluorescence detection. In this assay, the enzyme activity is expressed as specific activity (nmol × minute^{-1} × mg^{-1}).

The specific activity of the MON 94100 and MON 87708-produced DMO proteins were determined to be 566 and 217 nmol × minute^{-1} × mg^{-1}, respectively (Table 14). Because both specific activity of MON 94100-produced and MON 87708-produced DMO proteins were within the acceptance limits (Table 14), the proteins were determined to have equivalent functional activity.

Table 14. Functional Activity of MON 94100-produced DMO Protein and MON 87708-produced DMO Protein

MON 94100-Produced DMO[1] (nmol × minute^{-1} × mg^{-1})	MON 87708-Produced DMO[1] (nmol × minute^{-1} × mg^{-1})	Acceptance Limits[2] (nmol × minute^{-1} × mg^{-1})
566	217	26 - 859

[1] Value refers to mean calculated based on n = 5 and rounded to a whole number.
[2] Data obtained for the MON 87708-produced DMO was used to generate a prediction interval for setting the acceptance limits rounded to a whole number.

B.1(a)(vii) MON 94100 DMO protein identity and equivalence to MON 87708 DMO - Conclusion

The MON 94100-produced DMO protein purified from MON 94100 grain was characterized, and a comparison of the physicochemical and functional properties between the MON 94100-produced and the MON 87708-produced DMO proteins was conducted following a panel of analytical tests: 1) the N-terminal sequence of the MON 94100-produced DMO protein was confirmed by LC-MS/MS analysis to be equivalent to that of MON 87708 DMO; 2) LC-MS/MS analysis yielded peptide masses consistent with the expected peptide masses from the theoretical trypsin digest of the *dmo* gene product present in MON 94100; 3) the MON 94100-produced and the MON 87708-produced DMO proteins were both detected on a Western blot probed with antibodies specific for DMO protein and the immunoreactive properties of both proteins was shown to be equivalent; 4) the electrophoretic mobility and apparent molecular weight of the MON 94100-produced and the MON 87708-produced DMO proteins were shown to be equivalent; 5) the glycosylation status of the MON 94100-produced and the MON 87708-produced DMO proteins was determined to be equivalent and neither to be glycosylated; and 6) the functional activity of the MON 94100-produced and the MON 87708-produced DMO proteins was demonstrated to be equivalent. These results demonstrate that the MON 94100-produced DMO and the MON 87708-produced DMO proteins are equivalent. This demonstration of protein equivalence confirms that the MON 87708-produced DMO protein is appropriate for use as a surrogate in the evaluation of the safety of the MON 94100-produced DMO protein.

B.1(b) Antibiotic Resistance Marker Genes

MON 94100 does not contain genes that encode resistance to antibiotic markers. Molecular characterisation data presented in Section A.3(d) demonstrate the absence of antibiotic resistance marker gene in MON 94100.

B.2 New Proteins

B.2(a) Description of DMO protein expressed in MON 94100

B.2(a)(i) Description of DMO Protein Expressed in MON 94100

Wild type DMO was initially purified from *Stenotrophomonas maltophilia* (*S. maltophilia*) strain DI-6 (Palleroni and Bradbury, 1993; Herman *et al.*, 2005), isolated from soil at a dicamba manufacturing plant (Krueger *et al.*, 1989). DMO protein is targeted to chloroplasts by a chloroplast transit peptide (CTP) to allow co-localization with the endogenous reductase and ferredoxin enzymes that supply electrons for the DMO demethylation reaction as described by Behrens *et al.* (2007). In the construction of the plasmid vector used in the development of MON 94100, PV-BNHT508701, a transit peptide coding sequence from Rubisco gene (*rbcS*) was joined to the *dmo* coding sequence to transport the produced protein to the canola chloroplast; this coding sequence results in the production of a precursor protein consisting of the DMO protein, a transit peptide, and an intervening sequence (IS), and is referred to as the MON 94100 DMO precursor protein. Typically, transit peptides are precisely removed from the precursor protein following delivery to the targeted plastid (della-Cioppa *et al.*, 1986) resulting in the fully processed protein. However, there are examples in the literature of alternatively processed forms of a protein targeted to a plant's chloroplast (Behrens *et al.*, 2007; Clark and Lamppa, 1992). Such alternative processing is observed with the DMO precursor protein produced in MON 94100 similar to earlier products (listed below) containing DMO proteins that are globally approved. Data from N-terminal sequencing analysis of the MON 94100-produced DMO indicate that processing of the DMO precursor protein expressed in MON 94100 produced the same two isoforms of the MON 87708 soybean DMO protein, DMO+27 and DMO. The determined amino acid sequence of DMO+27 is identical to wild-type DMO, except for a methionine at position 1 and 27 additional amino acids on its N-terminus derived from RbcS and IS. Therefore, the term "MON 94100 DMO protein" will be used to refer to both forms of the protein collectively and distinctions will only be made, where necessary.

There are no differences between the DMO protein produced in MON 94100 and the DMO protein present in MON 87708 soybean which was approved by FSANZ in 2012 (A1063). MON 88701 cotton and MON 87419 maize were approved by FSANZ in 2014 (A1080) and 2016 (A1118), respectively, also contain DMO proteins. The MON 87708, MON 88701 and MON 87419 DMO proteins were assessed following the multiple approaches to the safety assessment of DMO protein, leading to the conclusion that food and feed products derived from DMO-containing MON 87708 soybean, MON 88701 cotton and MON 87419 maize and their progeny are as safe and nutritious as food and feed derived from conventional soybean and cotton, respectively. The determined amino acid sequence of the two forms of the MON 94100 DMO protein is identical to the two forms of DMO protein expressed in MON 87708 (Figure 23). Except for minor amino acid differences at the N-terminus of MON 94100 expressed DMO protein, position 2 and position 112 of the amino acid sequence, the MON 94100 DMO protein is identical to the DMO proteins expressed in MON 88701 cotton (A1080), MON 87419 maize (A1118) and MON 87429 maize (under FSANZ's review) (Figure 23). These minor amino acid differences among the DMO proteins expressed in MON 94100, MON 88701, MON 87419, and MON 87429 are not anticipated to have an effect on the structure of the catalytic site, functional activity, immunoreactivity or specificity of the protein (D'Ordine *et al.*, 2009; Dumitru *et al.*, 2009). Therefore, all appropriate digestibility and heat susceptibility studies reported on DMO proteins in MON 87708 soybean (A1063) and MON 88701 cotton (A1080) apply to the

MON 94100 DMO protein. These studies concluded the DMO protein was readily digested and lost substantial activity following heat treatment. The safety of these DMO proteins has also been reviewed and approved in numerous other countries (*e.g.*, Australia/New Zealand, Canada, Colombia, Japan, Korea, Mexico and Taiwan for MON 88701 cotton; Australia/New Zealand, Brazil, Canada, China, European Union, Indonesia, Japan, Korea, Mexico, Philippines, Taiwan and Vietnam for MON 87708 soybean)[4].

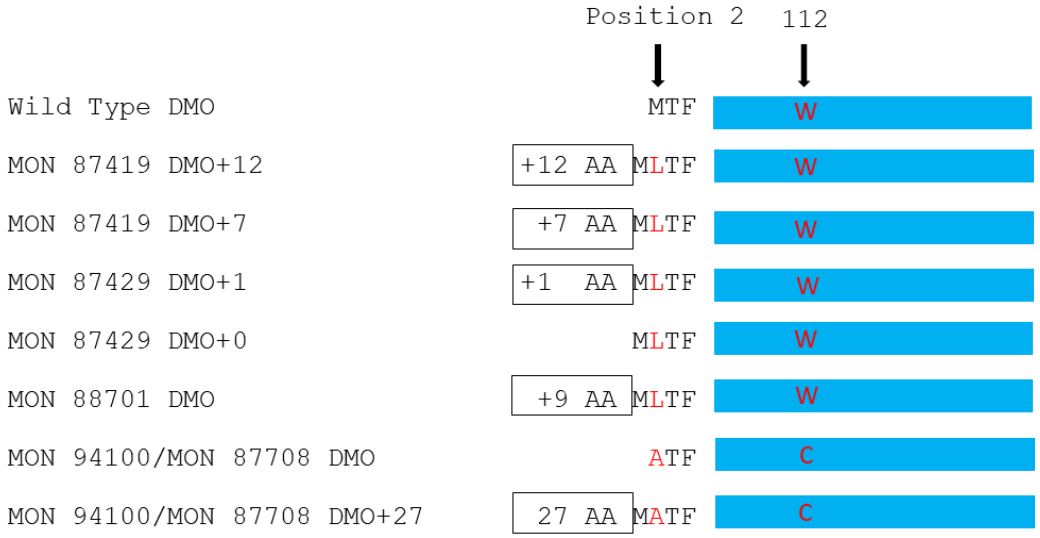

Figure 23. Forms of DMO Protein and Their Relation to the Wild-Type DMO Protein

The diagram represents the various DMO forms discussed in this section. Position refers to amino acid residues as wild-type DMO and the N-terminal boxed region indicates residues from CTPs. The blue regions indicate regions of 100% amino acid identity except as noted for position 112. The wild-type DMO form isolated from *S. maltophilia* was the first form sequenced (Herman *et al.*, 2005). The determined amino acid sequences of MON 94100 DMO and MON 87708 DMO are identical. The MON 94100 and MON 87708 DMO proteins have an identical sequence to the wild-type DMO protein, except for the insertion of an alanine at position 2, a single amino acid change at position 112 (tryptophan to cysteine) and an additional 27 amino acids encoded by the *rbcS* gene and IS at the N-terminus for MON 94100/MON 87708 DMO+27. The MON 94100/MON 87708 DMO (fully processed) protein additionally lacks a lead methionine residue.

[4] Source Biotechnology Industry Organization BIOTradeStatus database (http://www.biotradestatus.com/).

B.2(a)(ii) Mode-of-action of DMO Expressed in MON 94100

MON 94100 contains a demethylase gene from *S. maltophilia* that expresses a DMO protein. As a mono-oxygenase protein, the DMO protein is part of a larger oxygenase family of enzymes that incorporate one or two oxygen atoms into substrates and are widely distributed in many universal metabolic pathways (Harayama *et al.*, 1992). DMO is a Rieske-type non-heme iron oxygenase and is part of a three component system comprised of a reductase, a ferredoxin, and a terminal oxygenase, which in this case is the DMO protein. In MON 94100 canola, these three proteins work together to catalyze the demethylation of the broadleaf herbicide dicamba to the non-herbicidal compound 3,6-dichlorosalicylic acid (DCSA) and formaldehyde, thus conferring dicamba tolerance (Chakraborty *et al.*, 2005). This three-component redox system is presented in Figure 24.

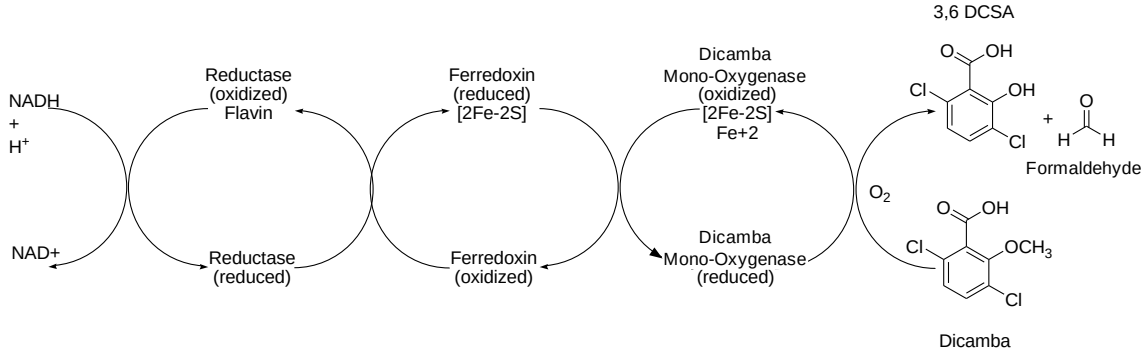

Figure 24. Three Components of the DMO Oxygenase System

Depicted is the electron transport chain that starts with NADH and ends with DMO resulting in the demethylation of dicamba to form DCSA.

The crystal structure of a C-terminal histidine tagged DMO protein, which is identical to wild-type DMO except for an additional alanine at position two and a C-terminal polyhistidine tag, has been solved (D'Ordine *et al.*, 2009; Dumitru *et al.*, 2009). The addition of a polyhistidine tag fused to the N- or C-terminus of a protein of interest is commonly used as a tool to aid in protein purification (Hochuli *et al.*, 1988). The crystal structure of active DMO was determined to be a trimer comprised of three identical DMO monomers (D'Ordine *et al.*, 2009; Dumitru *et al.*, 2009). Each DMO monomer contains a Rieske [2Fe-2S] cluster domain and a non-heme iron center domain (D'Ordine *et al.*, 2009; Dumitru *et al.*, 2009) that are typical of all Rieske-type mono-oxygenases (Ferraro *et al.*, 2005). To catalyze the demethylation of dicamba, electrons transferred from NADH are shuttled through endogenous reductase and ferredoxin to the terminal DMO protein. The electrons are received by the Rieske [2Fe-2S] cluster of one DMO protein molecule in the trimer and transferred to the non-heme iron center at the catalytic site of an adjacent DMO protein molecule in the trimer (D'Ordine *et al.*, 2009; Dumitru *et al.*, 2009), where it reductively activates oxygen to catalyze the final demethylation of dicamba. Electron transport from the Rieske [2Fe-2S] cluster domain to the non-heme iron center domain cannot occur within a monomer since the distance is too great (D'Ordine *et al.*, 2009; Dumitru *et al.*, 2009). As a result of the demethylation reaction, the non-herbicidal compound DCSA and formaldehyde are formed from dicamba. DCSA is a known cotton, soybean, soil, and livestock metabolite whose safety has been evaluated by the FAO-WHO and EPA (FAO-WHO, 2011a; FAO-WHO, 2011b; U.S. EPA, 2009b). The other reaction product, formaldehyde, is found naturally in many plants and edible fungi (Tashkov, 1996;

Adrian-Romero *et al.*, 1999). Thus, neither DCSA nor formaldehyde generated by the action of DMO on dicamba pose a significant food or feed safety risk.

B.2(a)(iii) Specificity of DMO Expressed in MON 94100

The substrate specificity of DMO expressed in MON 94100 was evaluated to understand potential interactions DMO may have with endogenous compounds structurally similar to dicamba that are found in plants. It is known that DMO protein has high specificity to dicamba. Based on the interactions noted in crystallography studies with DMO (D'Ordine *et al.*, 2009; Dumitru *et al.*, 2009), only compounds structurally similar to dicamba (phenyl carboxylic acids containing methoxy moieties and chlorine moieties) were considered to be potential substrates of DMO. In order to evaluate the selectivity of DMO for dicamba herbicide as compared to potential endogenous substrates, a series of *in vitro* studies were previously performed and reported for MON 87708. Endogenous compounds evaluated in those studies included ferulic acid, o-anisic acid, sinapic acid, syringic acid, and vanillic acid. These substrates were chosen because they are structurally similar to dicamba and are found in plants. The results demonstrated that DMO did not catabolize the potential endogenous substrates tested and supported the conclusion that DMO has a high specificity for dicamba.

Similar results were obtained for the DMO produced in MON 87429. Evaluations for potential catabolism of o-anisic acid by *E. coli*-produced MON 87429 DMO used the same qualitative assay reported for MON 87708. Although o-anisic acid is not known to be present in corn, this substance was chosen for this confirmatory experiment since, among the five substrates used in the original study for MON 87708, this is the substrate that is most structurally similar to dicamba. For o-anisic acid, similarly to the previously reported results for MON 87708, no new peaks that would be indicative of the predicted demethylated product were observed, confirming that the MON 87429 DMO does not catabolize o-anisic acid. These results taken together with the previously reported results demonstrate that DMO has a high specificity for dicamba as a substrate.

A literature survey was conducted to search for endogenous compounds in canola that are structurally similar to dicamba (phenyl carboxylic acids containing methoxy moieties and chlorine moieties). The search was done using SciFinder with the key words as follows: canola, phenolic compounds, *Brassica* oilseeds. In the literature, no phenyl compounds with chlorine moieties were identified in canola. As discussed above, plant-endogenous compounds containing methoxy and phenyl carboxylic acid moieties and structurally similar to dicamba have been ruled out as potential substrates of DMO produced by MON 87429 corn and MON 87708 soybean, as has o-anisic acid, the plant-endogenous compound that has the greatest structural similarity to dicamba. The lack of endogenous substrate compounds in canola together with the previously reported results, demonstrate that MON 94100 DMO has a high specificity for dicamba as a substrate.

B.2(b) Expression levels of DMO protein in MON 94100

DMO protein levels in various tissues of MON 94100 were determined using an Enzyme-linked Immunosorbent Assay (ELISA) as part of the characterization of MON 94100 (Appendix 7 ([redacted] (MSL0030937)). Levels of the introduced proteins were determined in relevant tissues and can be used to assess potential human and animal dietary exposure to MON 94100 DMO protein. Tissues of MON 94100 were collected from four replicate plots planted in a randomized complete block design during the 2018 growing season from a total of five field sites in the United States and Canada. The field sites were representative of canola-producing regions suitable for commercial production. Forage, leaf, grain, and root tissue samples were collected from each replicated plot at all field sites treated with Dicamba herbicide.

The ELISA results obtained for each sample were averaged across the five sites and are summarized in Table 15. The mean DMO protein level in MON 94100 across all sites was highest in root at 5.0 µg/g dry weight (dw) and lowest in grain at 0.64 µg/g dw.

For details, please refer to Appendix 7 ([redacted] (MSL0030937)).

Table 15. Summary of DMO Protein Levels in Canola Tissues Collected from MON 94100 Produced in the United States and Canadian Field Trials in 2018, Treated with Intended Herbicide

Tissue Type	Development Stage[1]	Mean (SE) Range (µg/g dw)[2]	LOQ/LOD[3] (µg/g dw)
Forage	BBCH 19-59	2.5 (0.35) 0.42 - 6.7	0.094/0.040
Leaf	BBCH 13-16	2.5 (0.19) 0.95 - 3.6	0.094/0.008
Grain	BBCH 99	0.64 (0.068) 0.38 - 1.8	0.094/0.006
Root	BBCH 19-59	5.0 (0.37) 1.8 - 8.3	0.094/0.004

[1]BBCH scale used to identify plant phenological development stages developed by the Biologische Bundesanstalt, Bundessortenamt und Chemische Industrie

[2]Protein levels are expressed as the arithmetic mean and standard error (SE) as microgram (µg) of protein per gram (g) of tissue on a dry weight basis (dw). The means, SE, and ranges (minimum and maximum values) were calculated for each tissue across all sites (n=20 replicates).

[3]LOQ=limit of quantitation, LOD=limit of detection.

B.2(c) History of human consumption of novel substances or similarity to substances previously consumed in food

As described below, MON 94100 DMO is homologous to proteins that are common in the environment and in the diets of animals and humans. Given the extensive exposure of humans and animals to these homologous oxygenase proteins, it can be concluded that the oxygenase proteins have a history of safe use.

When determining the homology among proteins, both the linear amino acid sequence of the protein as well as the higher order structure of the proteins should be taken into account. Higher order structures are a relevant measure of homology since structure is more conserved than amino acid sequence (Caetano-Anollés *et al.*, 2009). In general, changes in the amino acid sequence of proteins largely occur through evolutionary mechanisms and are mostly conservative, meaning that such changes do not alter the high order structure of the protein and consequently do not alter the functional activity of the protein (Caetano-Anollés *et al.*, 2009; Illergård *et al.*, 2009). The conservation of high order structure is predominant within important functional and structural domains of proteins in similar classes (Illergård *et al.*, 2009). Therefore, it is necessary to understand the structural similarity shared between DMO and other proteins in order to properly assess their homology and determine if homologues of MON 94100 DMO are widely distributed in nature and/or present in foods or feeds consumed by humans or animals.

As described in Section B.2(a), DMO is classified as an oxygenase. Oxygenases are enzymes that incorporate one or two oxygen atoms into their substrates and are widely distributed in many universal metabolic pathways (Harayama *et al.*, 1992). Within this large enzymatic class are mono-oxygenases, which incorporate a single oxygen atom as a hydroxyl group with the concomitant production of water and oxidation of NADH (Harayama *et al.*, 1992). Non-heme iron oxygenases, where iron is involved in the catalytic site, are an important class of oxygenases. Within this class are Rieske non-heme iron oxygenases, which contain a Rieske iron-sulfur [2Fe-2S] cluster. All Rieske non-heme iron oxygenases contain two catalytic domains, a non-heme iron domain (nh-Fe) that is a site of oxygen activation, and a Rieske [2Fe-2S] domain which functions by transporting electrons from ferredoxin to the non-heme iron domain (Ferraro *et al.*, 2005). MON 94100 DMO belongs to this class of oxygenases which are ubiquitous in diverse phyla ranging from bacteria to plants consumed by humans and animals (Ferraro *et al.*, 2005; Schmidt and Shaw, 2001).

The crystal structure of histidine-tagged DMO demonstrated that the quaternary structure of DMO is a trimer, where each individual monomer is in a precise orientation that allows for electron transport between two conserved domains; the Rieske and the non-heme iron domains. Similar to all Rieske non-heme iron oxygenases, DMO monomers contain these two catalytically important and highly conserved domains (D'Ordine *et al.*, 2009; Dumitru *et al.*, 2009; Ferraro *et al.*, 2005). Conservation of these domains ensures that the resulting secondary and tertiary structural domains are in the correct spatial orientation with regard to the non-heme iron and the Rieske [2Fe-2S] domains; which ensures electron transport from ferredoxin and between the monomers of DMO (D'Ordine *et al.*, 2009; Ferraro *et al.*, 2005).

Rieske domains are ubiquitous in numerous bacterial and plant proteins such as the iron-sulfur protein of the cytochrome bc_1 complex, chloroplast cytochrome b_6-f complex in spinach, and choline mono-oxygenases (Breyton, 2000; Darrouzet *et al.*, 2004; Gray *et al.*, 2004; Hibino *et al.*, 2002; Rathinasabapathi *et al.*, 1997; Russell *et al.*, 1998). The presence of two conserved domains, a Rieske [2Fe-2S] domain and a non-heme iron domain, suggests

that all Rieske type non-heme iron oxygenases share the same reaction mechanism, by which the Rieske domain transfers electrons from the ferredoxin to the non-heme iron to allow catalysis (Chakraborty *et al.*, 2005; Dumitru *et al.*, 2009; Ferraro *et al.*, 2005). The conservation of these important structural domains required for enzymatic activity is further evidence of the evolutionary relation of all Rieske non-heme iron oxygenases to each other (Nam *et al.*, 2001; Rosche *et al.*, 1997; Werlen *et al.*, 1996). Therefore, enzymes with structural homology and functional similarity to MON 94100 DMO have been described in plants and bacteria and have been extensively consumed by both humans and animals.

B.2(d) Assessment of Potential Toxicity

The assessment of the potential toxicity of an introduced protein takes into account several aspects of its biochemical characteristics (Delaney *et al.*, 2008). A protein introduced into canola is not likely to be associated with toxicity if: 1) the protein lacks any structural similarity to known toxins or other biologically-active proteins that could cause adverse effects in humans or animals; 2) the protein is structurally and functionally related to proteins with a history of safe consumption; and 3) the protein is readily inactivated or degraded in response to common food processing conditions (e.g., heating) and/or digestive enzymes. The lack of any effects in an acute oral mammalian toxicity study performed at dose levels substantially greater than anticipated human exposure levels can provide further confirmation that an introduced protein is unlikely to pose a significant risk to human or animal health.

Bioinformatic comparison (aa) of novel protein(s) to toxins

The assessment of the potential for protein toxicity includes bioinformatics analysis of the amino acid sequence of the introduced protein. The goal of the bioinformatic analysis is to ensure that the introduced protein does not share homology to known toxins or anti-nutritional proteins associated with adverse health effects.

Potential structural similarities shared between the MON 94100 DMO protein with sequences in a protein database were evaluated using the FASTA sequence alignment tool. The FASTA program directly compares amino acid sequences (*i.e.*, primary, linear protein structure) and the alignment data may be used to infer shared higher order structural similarities between two sequences (*i.e.*, secondary and tertiary protein structures). Proteins that share a high degree of similarity throughout the entire sequence are often homologous. Homologous proteins often have common secondary structures, common three-dimensional configuration, and, consequently, may share similar functions (Caetano-Anollés *et al.*, 2009; Illergård *et al.*, 2009).

FASTA bioinformatic alignment searches using the MON 94100 DMO amino acid sequence was performed with the toxin database to identify possible homology with proteins that may be harmful to human and animal health. Periodically, the databases used to evaluate proteins are updated. Since the most recent reports were completed, the toxin (TOX_2019) and protein (PRT_2019) databases have been revised and updated. In order to determine if proteins share significant sequence similarity to new sequences contained in the updated toxin database, they were used as queries for FASTA searches of the TOX_2019 database. The toxin protein database (TOX_2019) is a subset of sequences derived from the PRT_2019 database that was selected using a keyword search and filtered to remove likely non-toxin proteins. It is referred to herein as the TOX_2019 database and contains 34,642 sequences.

Using MON 94100 DMO as the query sequence, no alignments with an *E*-score of ≤1e-5 were obtained.

For details, please refer to Appendix 7 ([redacted](MSL0030937)).

B.2(e) Stability to heat or processing and/or degradation in gastric model

B.2(e)(i) Digestive fate of the MON 94100 DMO protein

Proteins introduced into crops using biotechnology are evaluated for their safety for human and animal consumption. The majority of ingested dietary proteins undergo hydrolytic degradation and/or proteolytic degradation to their constituent amino acids or small peptides, which are then absorbed and used for synthesis of proteins or other glucogenic or ketogenic metabolites by the body (Delaney *et al.*, 2008). Therefore, evaluating a protein's intrinsic sensitivity to proteolytic degradation with enzymes of the gastrointestinal tract is a key aspect to understanding the safety of any introduced proteins in GM crops. One characteristic of protein toxins and many allergens is their ability to withstand proteolytic degradation by enzymes present in the gastrointestinal tract (Astwood *et al.*, 1996; Moreno *et al.*, 2005; Vassilopoulou *et al.*, 2006; Vieths *et al.*, 1999). Allergenic proteins or their fragments, when presented to the intestinal immune system, can lead to a variety of gastrointestinal and systemic manifestations of immune-mediated allergy. The complete enzymatic degradation of an ingested protein by exposure to gastric pepsin and intestinal pancreatic proteases makes it highly unlikely that either the intact protein or protein fragment(s) will reach the absorptive epithelial cells of the small intestine where antigen processing cells reside (Moreno *et al.*, 2005). To reach these cells, protein or protein fragment(s) must first pass through the stomach where they are exposed to pepsin and then the duodenum where they are exposed to pancreatic fluid containing a mixture of enzymes called pancreatin. Therefore, the susceptibility of MON 94100 (using a surrogate DMO protein from MON 87708 DMO) protein to degradation by pepsin and pancreatin was assessed. Results presented in Section B.1(a) demonstrate that the MON 94100-produced DMO and the MON 87708-produced DMO proteins are equivalent. This demonstration of protein equivalence confirms that the MON 87708-produced DMO protein is appropriate for use as a surrogate in the evaluation of the safety of the MON 94100-produced DMO protein.

A correlation between the resistance to protein degradation by pepsin and the likelihood of the protein being an allergen has been previously assessed with a group of proteins consisting of both allergens and non-allergens (Astwood *et al.*, 1996; Codex Alimentarius, 2009), but this correlation is not absolute (Fu *et al.*, 2002). A standardized protocol to compare the relative resistance of proteins to degradation by pepsin has been established based on results obtained from an international, multi-laboratory study (Thomas *et al.*, 2004). The multi-laboratory study showed that the results of *in vitro* pepsin degradation assays were reproducible when a standard protocol was followed. Using this standardized *in vitro* pepsin degradation protocol, the susceptibility of DMO protein to pepsin degradation was assessed.

Incubation of test proteins with pancreatin is also used to assess the susceptibility of the protein to proteolytic degradation (Yagami *et al.*, 2000; Okunuki *et al.*, 2002). The relationship between protein allergenicity and susceptibility to pancreatin degradation is limited for several reasons. Namely, the protein has not been first exposed to the acidic, and proteolytic denaturing condition of the stomach, as would be the case *in vivo* (Helm, 2001).

Degradation of the MON 94100 DMO Protein by Pepsin

Degradation of the MON 87708-produced DMO protein by pepsin was evaluated over time by analyzing digestion mixtures incubated for targeted time intervals following a standardized protocol validated in an international, multi-laboratory ring study (Thomas *et al.*, 2004) collected at targeted incubation time points. The susceptibility of the DMO protein to pepsin degradation was assessed by visual analysis of a Brilliant Blue G-Colloidal stained SDS-PAGE gel and by visual analysis of a Western blot probed with an anti-DMO antibody. Both visualization methods were run concurrently with separate SDS-PAGE and Western blot analyses to estimate the limit of detection (LOD) of the DMO protein for each method.

For SDS-PAGE analysis of the digestibility of the DMO protein in pepsin, the gel was loaded with 1 µg of total test protein (based on pre-digestion protein concentrations) for each of the digestion samples (Figure 25A). After 0.5 min digestion (Pepsin Treated T1 sample), the intensity of the combined bands was reduced to approximately the same level as observed for pepsin alone (0 min No Test Protein Control; Figure 25, compare lanes 2 and 5) suggesting that most of the intact DMO protein was degraded.

No change in the DMO protein band intensity was observed in the absence of pepsin in the 0 min No Pepsin Control and 60 min No Pepsin Control samples (Figure 25A, lanes 3 and 12). This indicates that the degradation of the DMO protein was due to the proteolytic activity of pepsin and not due to instability of the protein while incubated in the pepsin test system over the course of the experiment.

The 0 min No Test Protein Control and 60 min No Test Protein Control (Figure 25A, lanes 2 and 13) demonstrated that the pepsin is stable throughout the experimental phase.

A separate SDS PAGE gel to estimate the LOD of the DMO protein was run concurrently with the SDS PAGE for the degradation assessment (Figure 25B). The LOD of the DMO protein was approximately 0.02 µg (Figure 25B, lane 6). The LOD was used to calculate the maximum relative amount of DMO protein that could remain visually undetected after digestion, which corresponded to approximately 2.0% (0.02µg/1µg × 100% = 2.0%) of the total protein loaded.

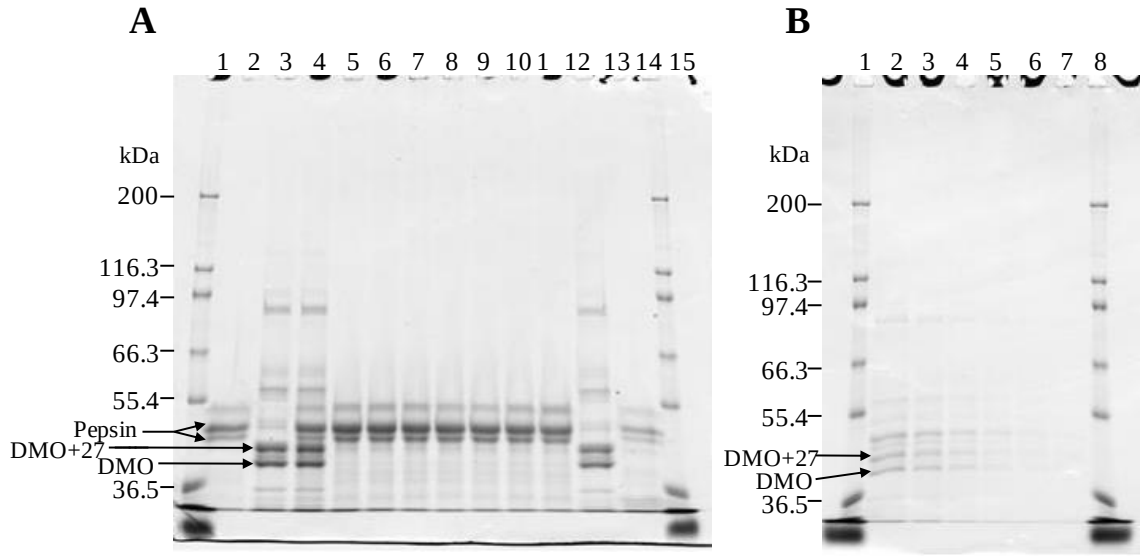

Figure 25. SDS-PAGE Analysis of the Digestion of DMO Protein by Pepsin

Colloidal Brilliant Blue G stained 8% Tris-glycine polyacrylamide gels were used to analyze the digestibility of the DMO proteins in Pepsin. **Panel A** corresponds to the DMO protein digestion in Pepsin. Based on pre-digestion protein concentrations, 1.0 µg of total protein was loaded in each lane containing the DMO proteins. **Panel B** corresponds to the limit of detection of the DMO proteins. Approximate molecular weights (kDa) are shown on the left and correspond to the markers loaded in each gel. N0 and N7 correspond to control samples that did not contain DMO. P0 and P7 correspond to controls that did not contain pepsin.

Lane	Sample	Incubation Time (min)	Lane	Sample	Amount (µg)
1	Mark 12 MWM	-	1	Mark 12 MWM	-
2	Pepsin N0	0	2	T0, protein+ Pepsin	0.25
3	Pepsin P0	0	3	T0, protein+ Pepsin	0.13
4	Pepsin T0	0	4	T0, protein+ Pepsin	0.06
5	Pepsin T1	0.5	5	T0, protein+ Pepsin	0.03
6	Pepsin T2	2	6	T0, protein+ Pepsin	0.02
7	Pepsin T3	5	7	T0, protein+ Pepsin	0.01
8	Pepsin T4	10	8	Mark 12 MWM	-
9	Pepsin T5	20			
10	Pepsin T6	30			
11	Pepsin T7	60			
12	Pepsin P7	60			
13	Pepsin N7	60			
14	Mark 12 MWM	-			
15	Blank	-			

For Western blot analysis of DMO Pepsin susceptibility, the DMO protein was loaded with approximately 20 ng per lane of total protein (based on pre-reaction total protein concentrations) for each reaction time point examined. The Western blot used to assess the resistance of the DMO protein to Pepsin digestion (Figure 26A) was run concurrently with a Western blot to estimate the LOD of the DMO protein (Figure 26B). The LOD of the DMO protein was approximately 0.30 ng (Figure 26B, lane 7). The LOD was used to calculate the maximum relative amount of DMO protein that could remain visually undetected after digestion, which corresponded to approximately 1.5% (0.3 ng /20 ng × 100% = 1.5%) of the total protein loaded.

Western blot analysis demonstrated that the DMO protein was degraded below the LOD within 0.5 min of incubation in the presence of Pepsin (Figure 26A, lane 5). Based on the Western blot LOD for the DMO protein, it can be concluded that more than 98% (100% - 1.5% = 98.5%) of the intact DMO protein was degraded within 0.5 min. No peptide fragments were detected at any timepoint in Pepsin by Western blot.

No apparent change in the DMO protein band intensity was observed in the absence of Pepsin in the 0 min No Pepsin Control and 60 min No Pepsin Control samples (Figure 26A, lanes 3 and 12). This indicates that the degradation of the DMO protein was due to the proteolytic activity of Pepsin and not due to instability of the protein while incubated in the assay buffer during the course of the experiment.

No immunoreactive bands were observed in the 0 min No Protein Control and 60 min No Protein Control samples (Figure 26A, lanes 2 and 13). This result indicates that there was no non-specific interaction between the Pepsin solution and the DMO-specific antibody under these experimental conditions.

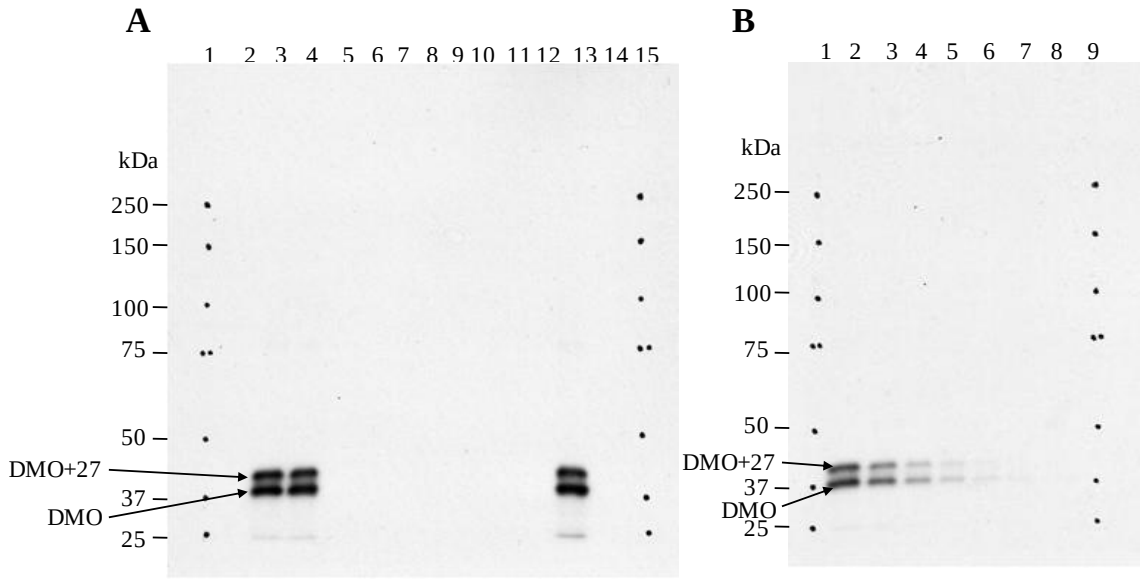

Figure 26. Western Blot Analysis of the Degradation of DMO Protein by Pepsin

Panel A corresponds to the DMO proteins digestion in SGF separated by SDS-PAGE using Tris-glycine 8% polyacrylamide gels. Based on pre-digestion protein concentrations, 20 ng (total protein) was loaded in the lanes containing the DMO proteins. **Panel B** corresponds to the limit of detection of the DMO proteins. The lanes have been cropped and re-numbered. Approximate molecular weights (kDa) are shown on the left, and correspond to the markers loaded in each gel. A 15 s exposure is shown. N0 and N7 correspond to control samples that did not contain DMO. P0 and P7 correspond to controls that did not contain pepsin.

Lane	Sample	Incubation Time (min)
1	Precision Plus MWM	-
2	Pepsin N0	0
3	Pepsin P0	0
4	Pepsin T0	0
5	Pepsin T1	0.5
6	Pepsin T2	2
7	Pepsin T3	5
8	Pepsin T4	10
9	Pepsin T5	20
10	Pepsin T6	30
11	Pepsin T7	60
12	Pepsin P7	60
13	Pepsin N7	60
14	Precision Plus MWM	-
15	Blank	-

Lane	Sample	Amount (ng)
1	Precision Plus MWM	-
2	T0, protein+ Pepsin	8.0
3	T0, protein+ Pepsin	4.0
4	T0, protein+ Pepsin	2.0
5	T0, protein+ Pepsin	1.0
6	T0, protein+ Pepsin	0.5
7	T0, protein+ Pepsin	0.3
8	T0, protein+ Pepsin	0.1
9	Precision Plus MWM	-

Degradation of the MON 94100 DMO by Pancreatin

The degradation of the MON 87708-produced DMO protein by pancreatin was assessed by Western blot analysis (Figure 27). The total loading of the DMO test protein for each timepoint examined was approximately 20 ng per lane (based on pre-reaction total protein concentrations). The Western blot used to assess the DMO protein degradation (Figure 27A) was run concurrently with the Western blot used to estimate the LOD Figure 27B) of the DMO protein. The LOD of the DMO protein was observed at approximately the 1.0 ng protein loading (Figure 27A, lane 6). The LOD was used to calculate the maximum relative amount of DMO protein that could remain visually undetected after digestion, which corresponded to approximately 5% (1.0 ng /20 ng × 100% = 5%) of the total protein loaded.

Western blot analysis demonstrated that a band corresponding to the DMO protein was degraded to a level below the LOD within 5 min of incubation in the presence of pancreatin (Figure 27A, lane 5), the first timepoint assessed. Therefore, based on the LOD, more than 95% (100% - 5%) of the DMO protein was degraded within 5 min. No peptide fragments were detected at any timepoint in Pepsin by Western blot.

No apparent change in the intact DMO band intensity was observed in the absence of pancreatin in the 0 h No Pancreatin Control and 24 h No Pancreatin Control samples (Figure 27A, lanes 3 and 13). This indicates that the degradation of all immunoreactive forms of the DMO protein was due to the proteolytic activity of pancreatin and not due to instability of the protein when incubated in 50 mM KH_2PO_4, pH 7.5 at 37.1ºC over the course of the experiment.

No immunoreactive bands were observed in the 0 h No Test Protein Control and 24 h No Test Protein Control samples (Figure 27A, lanes 2 and 14), demonstrating the absence of non-specific antibody interactions with the pancreatin solution.

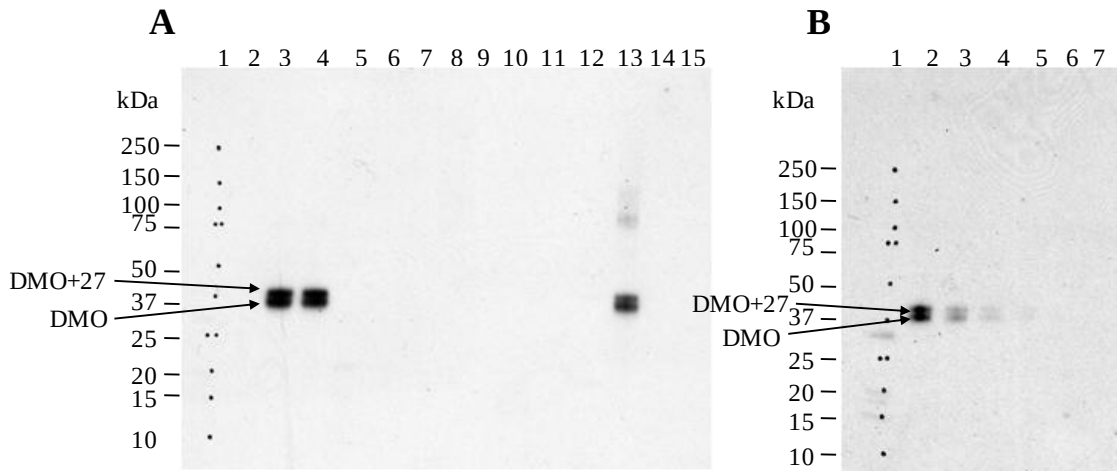

Figure 27. Western Blot Analysis of the Degradation of DMO Protein by Pancreatin

Panel A corresponds to the DMO proteins digestion in Pancreatin. Based on pre-digestion protein concentrations, 20 ng (total protein) was loaded in the lanes containing the DMO proteins. **Panel B** corresponds to the limit of detection of the DMO proteins, lanes were cropped. Approximate molecular weights (kDa) are shown on the left and correspond to the markers loaded in each gel. A 15 s exposure is shown. N0 and N8 correspond to control samples that did not contain DMO. P0 and P8 correspond to controls that did not contain pancreatin.

Lane	Sample	Incubation Time
1	Precision Plus MWM	-
2	Pancreatin N0	0
3	Pancreatin P0	0
4	Pancreatin T0	0
5	Pancreatin T1	5 min
6	Pancreatin T2	15 min
7	Pancreatin T3	30 min
8	Pancreatin T4	1 h
9	Pancreatin T5	2 h
10	Pancreatin T6	4 h
11	Pancreatin T7	8 h
12	Pancreatin T8	24 h
13	Pancreatin P8	24 h
14	Pancreatin N8	24 h
15	Mark 12 MWM	-

Lane	Sample	Amount (ng)
1	Precision Plus MWM	-
2	T0, protein+ Pancreatin	15
3	T0, protein+ Pancreatin	10
4	T0, protein+ Pancreatin	5
5	T0, protein+ Pancreatin	2.5
6	T0, protein+ Pancreatin	1
7	Mark 12 MWM	-

Digestive Fate of the MON 94100 DMO Protein – Conclusions

The ability of the DMO protein to be degraded by Pepsin and by pancreatin was evaluated in this study. The results of these evaluations demonstrate that at least 98% of the DMO proteins were digested within 30 s of incubation in Pepsin when analyzed using stained gel, and greater than 98% was digested when analyzed using Western blot with an anti-DMO antibody. On the stained gel, a fragment with a molecular weight of ~21 kDa was observed in SGF throughout the digest. This band was not observed on the Western blot and N-terminal sequencing data determined that it did not match any part of the DMO proteins. Most likely the fragment originated from one of the endogenous soybean proteins co-purified with the DMO protein.

Results of this study also demonstrated that greater than 95% of the DMO proteins were digested within 5 min of incubation in SIF with no proteolytic fragment(s) detected by Western blot using a DMO–specific antibody.

These results show that the intact DMO protein is readily degraded in either Pepsin or pancreatin. Rapid degradation of the DMO protein in Pepsin and pancreatin indicates that it is highly unlikely that the DMO protein will pose any safety concern to human health.

B.2(e)(ii) Heat susceptibility of the MON 94100 DMO protein

Temperature can have a profound effect on the structure and function of proteins. Heat treatment is widely used in the preparation of livestock meal derived from canola grain (Hammond and Jez, 2011). It is reasonable that such processing will have an effect on the functional activity and structure of DMO protein when consumed in different feed products derived from MON 94100, thus reducing any potential safety concerns posed by the protein. Therefore, an assessment of the effect of heating was conducted as a surrogate for the conditions encountered during the preparation of feeds from MON 94100 grain using a surrogate DMO protein from MON 87708 DMO. Results presented in Section B.1(a) demonstrate that the MON 94100-produced DMO and the MON 87708-produced DMO proteins are equivalent. This demonstration of protein equivalence confirms that the MON 87708-produced DMO protein is appropriate for use as a surrogate in the evaluation of the safety of the MON 94100-produced DMO protein.

The effect of heat treatment on the activity of the DMO protein was evaluated using DMO purified from MON 87708 grain. Heat treated samples and an unheated control sample of DMO protein were analyzed: 1) using a functional assay to assess the impact of temperature on the enzymatic activity of the DMO protein; and 2) using SDS-PAGE to assess the impact of temperature on protein integrity.

Aliquots of DMO protein were heated to 25, 37, 55, 75 and 95 ºC for either 15 or 30 minutes, while a separate aliquot of DMO protein was maintained on ice for the duration of the heat treatments to serve as a temperature control. The effect of heat treatment on the activity of DMO was evaluated using a functional activity assay. The effect of heat treatment on the integrity of the DMO protein was evaluated using SDS-PAGE analysis of the heated and temperature control DMO protein samples.

Results of the activity assay for DMO enzyme incubated for 15 and 30 minutes are listed in

Table 16 and Table 17, respectively. Activity of the reference standard was measured as 17.2 nmole DSCA/min/mg DMO enzyme. The control substance had activity of 16.6 nmole DSCA/min/mg of DMO enzyme, thus demonstrating that protein activity was maintained during incubation on ice. When heated at a temperature of 25 ºC with incubation times of 15 and 30 minutes and 37 ºC with an incubation time of 15 minutes, no effect on the activity of DMO enzyme was observed. The test substance heated to 37 ºC demonstrated a small reduction in DMO enzyme activity with 72 % activity remaining relative to the control substance after the 30 minute incubation. The level of DMO enzyme activity following incubation at temperatures of 55, 75 and 95 ºC was below the limit of quantification for incubations at both time points.

Analysis by SDS-PAGE stained with Brilliant Blue G-Colloidal (Figure 28 and Figure 29) demonstrated that the reference standard and control substance contain two major bands with an apparent molecular weight of approximately 39.8 and 42.0 kDa corresponding to the DMO enzyme (DMO and DMO+27). Results of the SDS-PAGE data for the heat treatment of the test substances incubated for 15 minutes and 30 minutes are illustrated in Figures 28 and 29, respectively. The control substance loaded on each respective gel (Figures 28 and 29, lane 7) showed equivalent band intensity at 39.8 and 42.0 kDa to the 100 % reference standard (Figures 28 and 2, lane 8); demonstrating that the DMO enzyme was stable on wet ice during the incubation period.

No apparent decrease in band intensity of the 39.8 and 42.0 kDa DMO enzyme bands were observed in the test substance when heated at temperatures of 25, 37 and 55 ºC for 15 minutes (Figure 28, lanes 2-4) or 30 minutes (Figure 29, lanes 2-4). The test substance heated to 75 ºC for 15 minutes show no visible change in band intensity at 39.8 and 42.0 kDa (Figure 28, lane 5). The test substance heated to 75 ºC for 30 minutes demonstrated a visible change in band intensity at 39.8 and 42.0 kDa (Figure 29, lane 5), greater than the DMO enzyme 10% reference equivalence. The test substance heated to 95 ºC for 15 minutes resulted in a visible change of band intensity at 39.8 kDa greater than the band intensity of the DMO enzyme 10% reference equivalence and a change in band intensity at 42.0 kDa similar to the DMO enzyme 10% reference equivalence (Figure 28, lane 6). The test substance heated to 95 ºC for 30 minutes resulted in a visible change in band intensity at 39.8 and 42.0 kDa less than the DMO enzyme 10% reference equivalence (Figure 29, lane 6).

These data demonstrate that the DMO protein behaves with a predictable tendency toward protein denaturation and loss of functional activity at elevated temperatures. Heat treatment is widely used in the preparation of feeds containing meal derived from canola grain. Therefore, it is reasonable to conclude that DMO protein would not be consumed as an active protein in feed products derived from MON 94100 due to standard processing practices that include heat treatment at or above 95 ºC for the majority of foods derived from processed canola (Hammond and Jez, 2011).

Table 16. DMO Activity Assay of Heat-Treated DMO Enzyme After 15 Minutes at Elevated Temperatures

Temperature	Specific Activity (nmole DSCA /min/mg DMO enzyme) [1]	% DMO Activity Remaining (% of control substance) [2]
0 ºC (control substance)	16.6	100 %
25 ºC	17.9	107 %
37 ºC	17.0	102 %
55 ºC	Below LOQ[3]	<25 %
75 ºC	Below LOQ[3]	<25 %
95 ºC	Below LOQ[3]	<25 %

[1] Mean specific activity determined from n=3.
[2]DMO enzyme activity of control substance was assigned 100 % active.
% DMO activity remaining = [specific activity of sample/specific activity of control substance] x 100
[3] The LOQ is 4.4 nmole DSCA /min/mg DMO enzyme.

Table 17. DMO Activity Assay of Heat-Treated DMO Enzyme After 30 Minutes at Elevated Temperatures

Temperature	Specific Activity (nmole DSCA /min/mg DMO enzyme) [1]	% DMO Activity Remaining (% of control substance) [2]
0 ºC (control substance)	16.6	100 %
25 ºC	17.8	107 %
37 ºC	12.0	72 %
55 ºC	Below LOQ[3]	<25 %
75 ºC	Below LOQ[3]	<25 %
95 ºC	Below LOQ[3]	<25 %

[1] Mean specific activity determined from n=3.
[2]DMO enzyme activity of control substance was assigned 100 % active.
% DMO activity remaining = [specific activity of sample/specific activity of control substance] x 100
[3] The LOQ is 4.4 nmole DSCA /min/mg DMO enzyme.

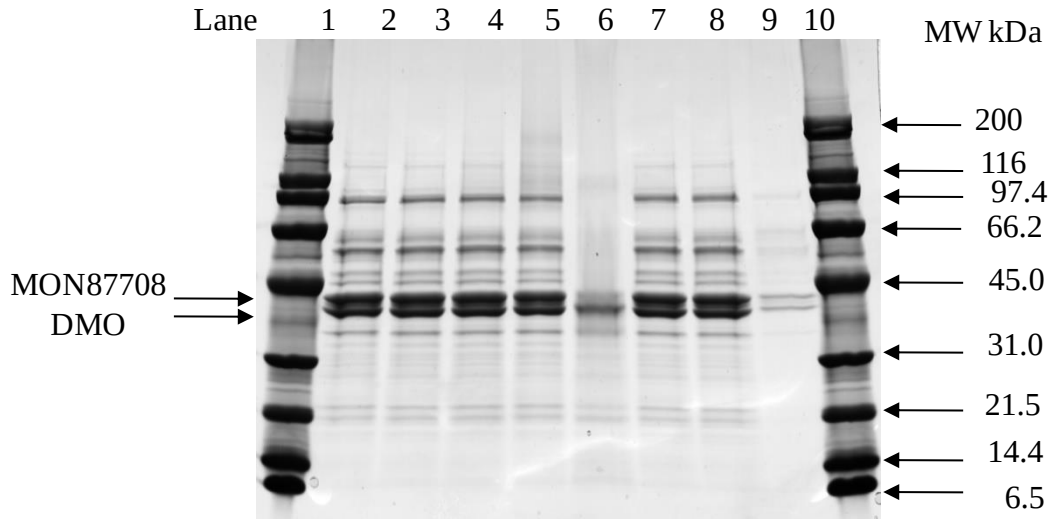

Figure 28. SDS-PAGE of DMO Enzyme Demonstrating the Effect After 15 Minutes at Elevated Temperatures on Protein Structural Stability

Heat-treated samples of DMO enzyme (2.8 µg total protein) separated on a Tris-glycine 4-20 % polyacrylamide gel under denaturing and reducing conditions. Gel was stained with Brilliant Blue G-Colloidal. Approximate molecular weights (kDa) are shown on the right and correspond to molecular weight markers in lanes 1 and 10.

Lane	Description	Total Amount
1	Broad Range Molecular Weight Markers	40.5 µg
2	DMO Enzyme 25 ºC	2.8 µg
3	DMO Enzyme 37 ºC	2.8 µg
4	DMO Enzyme 55 ºC	2.8 µg
5	DMO Enzyme 75 ºC	2.8 µg
6	DMO Enzyme 95 ºC	2.8 µg
7	DMO Enzyme Control Substance	2.8 µg
8	DMO Enzyme Reference 100 % Equivalence	2.8 µg
9	DMO Enzyme Reference 10 % Equivalence	0.28 µg
10	Broad Range Molecular Weight Markers	40.5 µg

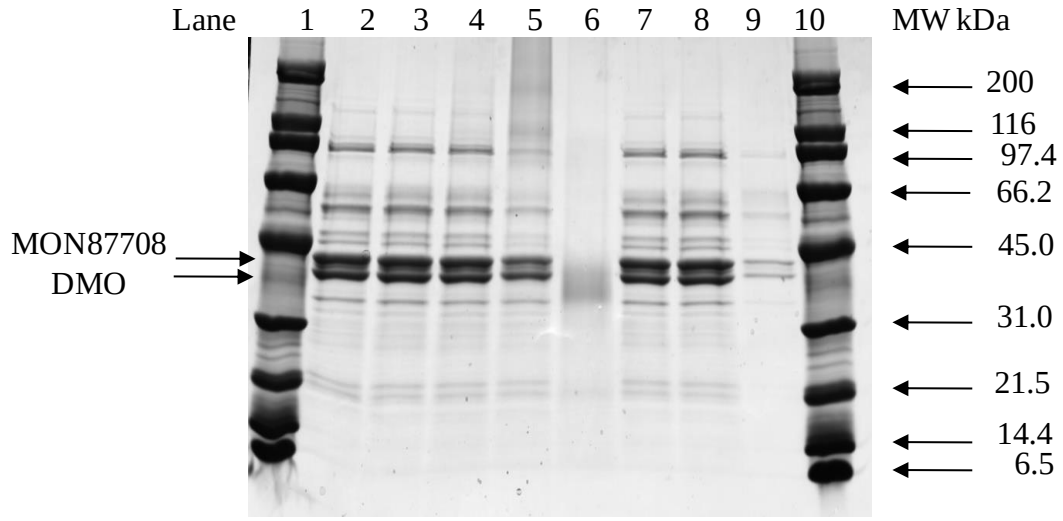

Figure 29. SDS-PAGE of DMO Enzyme Demonstrating the Effect After 30 Minutes at Elevated Temperatures on Protein Structural Stability

Heat-treated samples of DMO enzyme (2.8 µg total protein) separated on a Tris-glycine 4-20 % polyacrylamide gel under denaturing and reducing conditions. Gel was stained with Brilliant Blue G-Colloidal. Approximate molecular weights (kDa) are shown on the right and correspond to molecular weight markers in lanes 1 and 10.

Lane	Description	Total Amount
1	Broad Range Molecular Weight Markers	40.5 µg
2	DMO Enzyme 25 ºC	2.8 µg
3	DMO Enzyme 37 ºC	2.8 µg
4	DMO Enzyme 55 ºC	2.8 µg
5	DMO Enzyme 75 ºC	2.8 µg
6	DMO Enzyme 95 ºC	2.8 µg
7	DMO Enzyme Control Substance	2.8 µg
8	DMO Enzyme Reference 100 % Equivalence	2.8 µg
9	DMO Enzyme Reference 10 % Equivalence	0.28 µg
10	Broad Range Molecular Weight Markers	40.5 µg

B.2(e)(iii) Degradation and heat susceptibility of the MON 94100 DMO protein – Conclusions

The susceptibility of a protein to heat or its degradation in the presence of pepsin and pancreatin is a factor in the assessment of its potential toxicity. The degradation of MON 94100 DMO protein was evaluated by incubation with solutions containing pepsin and pancreatin, and the results show that MON 94100 DMO protein was readily degraded (Section B.2(e)(i)). Exposure to heat during feed processing, and to digestive fluids is likely to have a profound effect on the structure and function of proteins.

The effect of heat treatment on the activity of MON 94100 DMO protein was evaluated using functional assays to assess the impact of temperature on enzymatic activity, and using SDS-PAGE to assess the impact of temperature on protein integrity. The results show that MON 94100 DMO protein was completely deactivated by heating at 55 ºC or higher for 15 min or more (Section B.2(e)(ii)). Therefore, it is anticipated that exposure to functionally active MON 94100 DMO protein from the consumption of feed derived from MON 94100 is unlikely.

B.2(e)(iv) Acute oral toxicity study with the DMO protein

Most known protein toxins act through acute mechanisms to exert toxicity (Hammond and Fuchs, 1998; Pariza and Johnson, 2001; Sjoblad *et al.*, 1992). The primary exceptions to this rule consist of certain anti-nutritional proteins such as lectins and protease inhibitors, which manifest toxicity in a short term (few weeks) feeding study (Liener, 1994). The amino acid sequences of the DMO protein produced in MON 94100 is not similar to any of these anti-nutritional proteins or to any other known protein toxin. In addition, this protein is heat labile and readily degraded by gastrointestinal enzymes. Based on this weight of the evidence and the non-toxic mode of action for these proteins, no further assessment of potential toxicity for these proteins is necessary in accordance with the tiered protein safety assessment paradigm (Codex Alimentarius, 2009; Delaney *et al.*, 2008). Despite this weight of evidence, an acute oral mouse toxicity study was conducted as confirmatory evidence to support the safety of the DMO protein in MON 94100.

DMO+27 and DMO produced from MON 87708 grain was administered by oral gavage to 5 male and 5 female CD-1 mice at a dose of 140 mg/kg body wt (bw). Additional groups of mice were administered a comparable volume of the buffer or a comparable amount (mg/kg bw) of bovine serum albumin (BSA) to serve as vehicle or protein controls, respectively. Following dosing, all mice were observed daily for mortality or signs of toxicity. Body weights and food consumption were measured weekly. All animals were sacrificed on day 14 and subjected to a gross necropsy. There were no treatment-related effects on survival, clinical observations, body weight gain, food consumption or gross pathology. Therefore, under the conditions of this study, the No Observable Adverse Effect Level (NOAEL) for MON 94100 DMO was considered to be 140 mg/kg bw.

B.2(f) Assessment of Potential Allergenicity

History of safe use of the introduced protein is a key consideration in assessing the potential for allergenicity and toxicity and overall assessment of dietary safety. The history of safe use of DMO protein has been previously addressed in Section B.2(c).

Additionally, following the guidelines adopted by the Codex Alimentarius Commission, an assessment of potential allergenicity of introduced proteins has been conducted by comparing the characteristics of the introduced protein to characteristics of known allergens (Codex Alimentarius, 2009). A protein is not likely to be associated with allergenicity if: 1) the protein is from a nonallergenic source, 2) the protein represents only a very small portion of the total plant protein, 3) the protein does not share structural similarities to known allergens based on the amino acid sequence, 4) the protein is rapidly degraded in mammalian gastrointestinal systems, and 5) the protein is not stable to heat treatment. The DMO protein in MON 94100 has been assessed for potential allergenicity according to these safety assessment guidelines.

The assessment of the potential toxicity of an introduced protein is based on comparing the biochemical characteristics of the introduced protein to characteristics of known toxins. These biochemical characteristics are assessed by determining: 1) if the protein has structural similarity to known toxins or other biologically-active proteins that could cause adverse effects in humans or animals; 2) if the protein is rapidly degraded by pepsin and pancreatin; 3) if the protein is stable to heat treatment; 4) if the protein exerts any acute toxic effects in mammals; and 5) the anticipated exposure levels for humans and animals. The DMO protein in MON 94100 has been assessed for potential toxicity based on these criteria.

B.2(f)(i) Source of introduced protein

The dmo gene is derived from the bacterium *Stenotrophomonas maltophilia* strain DI-6, isolated from soil at a dicamba manufacturing plant (Krueger *et al.*, 1989). *S. maltophilia* is ubiquitously present in the environment (Mukherjee and Roy, 2016), including in water and dairy products (An and Berg, 2018; Okuno *et al.*, 2018; Todaro *et al.*, 2011). These bacteria have been used as effective biocontrol agents in plant and animal pathogenesis (Mukherjee and Roy, 2016), and have antibacterial activity against both gram-positive and gram-negative bacteria (Dong *et al.*, 2015). These bacteria can form biofilms that become resistant to antibiotics (Berg and Martinez, 2015; Brooke *et al.*, 2017). Several alternative compounds have been shown to be effective against S. maltophilia antibiotic resistance, such as immunoglobulin, epigallocatechine-3-gallate from green tea, and essential oils (Mukherjee and Roy, 2016). *S. maltophilia* has been found in healthy individuals without any hazard to human health (Heller *et al.*, 2016; Lira *et al.*, 2017). The opportunistic pathogenicity of S. maltophilia is mainly associated with hosts with compromised immune systems rather than with any specific virulence genes of these bacteria. Thus, documented occurrences of S. maltophilia infections have been limited to immunocompromised individuals in hospital settings (Lira *et al.*, 2017).

Other than the potential to become an opportunist pathogen in immunocompromised hosts, *S. maltophilia* is not known for human or animal pathogenicity. *S. maltophilia* history of safe use has been extensively reviewed during the evaluation of several dicamba-tolerant events with no safety or allergenicity issues identified by FSANZ or other regulatory agencies (e.g., MON 87419 maize in 2016 (A118), MON 88701 cotton in 2014 (A1080) and MON 87708 soybean in 2012 (A1063)).

B.2(f)(ii) Bioinformatic comparison (aa) of novel protein(s) to allergens

Structural similarity of the DMO protein to known allergens

The Codex guidelines for the evaluation of the allergenicity potential of introduced proteins (Codex Alimentarius, 2009) are based on the comparison of amino acid sequences between introduced proteins and allergens, where allergenic cross-reactivity may exist if the introduced protein is found to have at least 35% amino acid identity with an allergen over any segment of at least 80 amino acids. The Codex guideline also suggests that a sliding window search with a scientifically justified peptide size be used to identify immunologically relevant peptides in otherwise unrelated proteins. Therefore, the extent of sequence similarities between the DMO protein sequence and known allergens, gliadins, and glutenins was assessed using the FASTA sequence alignment tool along with an eight-amino acid sliding window search (Codex Alimentarius, 2009; Thomas *et al.*, 2005). The methods used are summarized below and detailed in Appendix 8 ([redacted] 2019 (MSL0030271)). The data generated from these analyses confirm that the DMO protein does not share amino acid sequence similarities with known allergens, gliadins, or glutenins.

Periodically, the databases used to evaluate proteins are updated. Since the most recent reports were completed, the allergen (AD_2019) database has been revised and updated. In order to determine if the DMO protein shares significant sequence similarity to new sequences contained in the updated allergen database, protein sequences were used as a query for a FASTA and Sliding Window search of the AD_2019 database.

The FASTA program directly compares amino acid sequences (i.e., primary, linear protein structure). This alignment data may be used to infer shared higher order structural similarities between two sequences (i.e., secondary and tertiary protein structures). Proteins that share a high degree of similarity throughout the entire sequence are often homologous. By definition, homologous proteins have common secondary structures, and three-dimensional configuration, and, consequently, may share similar functions. The allergen, gliadin, and glutenin protein sequence database (AD_2019) was obtained as the "COMprehensive Protein Allergen REsource" (COMPARE) database from the Health and Environmental Sciences Institute (HESI) and was used for the evaluation of sequence similarities shared between the DMO protein and all proteins in the database. The AD_2019 database contains 2,081 sequences. When used to align the sequence of the introduced protein to each protein in the database, the FASTA algorithm produces an E-score (expectation score) for each alignment. The E-score is a statistical measure of the likelihood that the observed similarity score could have occurred by chance in a search. A larger E-score indicates a low degree of similarity between the query sequence and the sequence from the database. Typically, alignments between two sequences which have an E-score of less than or equal to 1×10-5 are considered to have meaningful homology. Results indicate that the DMO protein sequence does not share meaningful similarity with sequences in the allergen database. No alignment met or exceeded the threshold of 35% identity over 80 amino acids recommended by Codex Alimentarius (2009) or had an *E*-score of less than or equal to 1×10^{-5}.

A second bioinformatic tool, an eight-amino acid sliding window search, was used to specifically identify short linear polypeptide matches to known allergens. It is possible that proteins structurally unrelated to allergens, gliadins, and glutenins may contain smaller immunologically meaningful epitopes. An amino acid sequence may have allergenic potential if it has an exact sequence identity of at least eight linearly contiguous amino acids with a potential allergen epitope (Hileman *et al.*, 2002; Metcalfe *et al.*, 1996). Using a

sliding window of less than eight amino acids can produce matches containing considerable uncertainty depending on the length of the query sequence ([redacted] 2006), and is not useful to the allergy assessment process (Thomas *et al.*, 2005). No eight contiguous amino acid identities were detected when the DMO protein sequence was compared to the proteins in the AD_2019 sequence database.

The bioinformatic results demonstrated there were no biologically relevant sequence similarities to allergens when the DMO protein sequence was used as a query for a FASTA search of the AD_2019 database. Furthermore, no short (eight amino acid) polypeptide matches were shared between the DMO protein sequence and proteins in the allergen database. These data show that DMO protein sequence lacks both structurally and immunologically relevant similarities to known allergens, gliadins, and glutenins.

For details, please refer to Appendix 8 ([redacted] 2019, (MSL0030271)).

Structural properties, including digestion by pepsin, heat treatment

The susceptibility of a protein to heat or its degradation in the presence of pepsin and pancreatin is a factor in the assessment of its potential toxicity. The degradation of MON 94100 DMO protein was evaluated by incubation with solutions containing pepsin and pancreatin, and the results show that MON 94100 DMO protein was readily degraded (Section B.2(e)(i)). Exposure to heat during feed processing, and to digestive fluids is likely to have a profound effect on the structure and function of proteins.

The effect of heat treatment on the activity of MON 94100 DMO protein was evaluated using functional assays to assess the impact of temperature on enzymatic activity, and using SDS-PAGE to assess the impact of temperature on protein integrity. The results show that MON 94100 DMO protein was completely deactivated by heating at 55 ºC or higher for 15 min or more (Section B.2(e)(ii)). Therefore, it is anticipated that exposure to functionally active MON 94100 DMO protein from the consumption of feed derived from MON 94100 is unlikely.

B.2(f)(iii) Protein as a proportion of total protein

The MON 94100 DMO protein was detected in all plant tissue types assayed (Section B.2(b), Table 15). Harvested grain is the most relevant tissue analyzed for an allergenicity assessment because feed derived from canola grain can be consumed directly by animals. The primary food uses for canola is refined canola oil in which protein content is negligible (OECD, 2011). The mean level of MON 94100 DMO protein in grain of MON 94100 is 0.64 µg/g dw. The minimum percent dry weight of total protein in grain of MON 94100 is approximately 36% (or 360,000 µg/g). The percentage of MON 94100 DMO protein in MON 94100 grain is calculated as follows:

(0.64 µg/g ÷ 360,000 µg/g) × 100% ≈ 0.00018% or 1.8 ppm of total grain protein

Therefore, the MON 94100 DMO protein represents a very small portion of the total protein in the grain of MON 94100. This low percent of MON 94100 DMO in relation to the total protein, along with the very minimal consumption of DMO via refined canola oil, greatly reduces the potential risk of allergenicity from this protein in MON 94100.

B.3 Other (non-protein) new substances

Not applicable.

B.4 Novel Herbicide Metabolites in GM Herbicide-Tolerant Plants

B.4(a) Novel Herbicide Use of Dicamba and its Metabolites

Herbicide-tolerant canola (*Brassica napus*), MON 94100, was developed, which is tolerant to the herbicide dicamba (3,6-dichloro-2-methoxybenzoic acid). MON 94100 contains a demethylase gene from *Stenotrophomonas maltophilia* that expresses a dicamba mono-oxygenase (DMO) protein to confer tolerance to dicamba herbicide. DMO is an enzyme that catalyzes the demethylation of dicamba to the non-herbicidal compound 3,6-dichlorosalicylic acid (DCSA) and formaldehyde (Chakraborty *et al.*, 2005).

DCSA is a known soybean, soil, and livestock metabolite whose safety has been evaluated by the US EPA (U.S. EPA, 2009a). DCSA is also the primary degradate in soil from dicamba aerobic soil metabolism and is therefore not new to the environment; it is not persistent in the environment and has low potential for leaching to ground water (EFSA, 2007b). DCSA has been evaluated for its toxicity to organisms in the environment. Based on studies using Rainbow trout (*Oncorhynchus mykiss*), *Daphnia*, green algae (*Selenastrum caprinornutum*), *Lemna* and earthworm (*Eisenia fetida*), it was concluded that "the metabolite 3,6-dichlorosalicylic acid (DCSA) was not found to give rise to unacceptable risks" (EFSA, 2007a).

Formaldehyde is a metabolite when dicamba is sprayed on MON 94100 canola. However, formaldehyde is not considered a relevant metabolite in the demethylation of dicamba by U.S. EPA. According to the guidelines published by Office of Prevention, Pesticides and Toxic Substances, United States Environmental Protection Agency (U.S. EPA, 1996), the methoxy side chain that is cleaved from dicamba to form formaldehyde would specifically not be chosen to be labeled in a metabolism study (U.S. EPA, 1996). This is because it is not metabolically stable and would not be considered a significant moiety as it would be readily metabolized and incorporated into the 1-carbon pool of the plant through known pathways. Therefore, formaldehyde was not measured in the residue study when dicamba was applied to MON 94100.

Plants have a large capacity to metabolize formaldehyde naturally produced from internal processes (Hanson and Roje, 2001), and any additional amount of formaldehyde that could be theoretically produced in the plant by dicamba treatment in MON 87419 would be metabolized very quickly. Thus the incremental increase in formaldehyde over and above the levels already presumed to be present in the canola plant would be small and transient and associated with an outdoor application of dicamba herbicide. Further, since current literature supports that formaldehyde is only emitted from foliage under certain conditions (Cojocariu *et al.*, 2005; Cojocariu *et al.*, 2004; Nemecek-Marshall *et al.*, 1995) and that emission rates are low (Nemecek-Marshall *et al.*, 1995), little opportunity exists for formaldehyde to be released from MON 87419 after dicamba treatment. Therefore human safety concerns of formaldehyde released from dicamba-treated MON 87419 are considered to be negligible and the most relevant route of exposure is from repeated inhalation of concentrated levels associated with indoor or occupational environments. USHHS-NTP has already stated that there is no evidence to suggest that dietary intake of formaldehyde is important, despite NTP's 12th Report on Carcinogens reclassifying formaldehyde as a known human carcinogen (USHHS-NTP, 2011). Therefore, the potential for human exposure to any formaldehyde in dicamba-treated MON 94100 canola is highly unlikely.

Formaldehyde is ubiquitous in the environment; plants and animals are constantly exposed to low levels already present in the environment and the atmosphere from a variety of biogenic (e.g., plant and animal) and anthropogenic (e.g., automotive or industrial emissions) sources.

In water, formaldehyde dissipates through biodegradation to low levels in a few days (USHHS-ATSDR, 1999). Aerobic biodegradation half-lives are estimated to be 1-7 days for surface water and 2-14 days for ground water (U.S. EPA, 2008). The half-life of formaldehyde in air is dependent on a number of factors (light intensity, temperature, and location). Through reaction with hydroxyl radical, the half-life of formaldehyde in air varies from 7 to 70 hours (U.S. EPA, 2008) . The photolytic half-life of formaldehyde in air (e.g., in the presence of sunlight) is estimated to be 1.6-6 hours (U.S. EPA, 2008; USHHS-ATSDR, 1999). Formaldehyde is rapidly consumed in the atmosphere through direct photolysis or by oxidation with hydroxyl or nitrate radicals (USHHS-ATSDR, 1999).

Humans are constantly exposed to low levels of formaldehyde. Human exposure to formaldehyde is primarily due to indoor air exposures (USHHS-ATSDR, 1999). Formaldehyde is found in a variety of consumer products such as cosmetics and paints, often as an antimicrobial agent, and is used extensively in urea-formaldehyde "slow-release" fertilizer formulations and adhesives (USHHS-ATSDR, 1999). Indoor formaldehyde air concentrations are generally significantly higher than outdoor air concentrations (USHHS-ATSDR, 1999) as a result of combustion (cooking, heating, tobacco use) and the emission of formaldehyde from a variety of construction materials (e.g., particle board, plywood or foam insulation) as well as permanent press fabrics (e.g., clothing or draperies) (U.S. CPSC, 1997). Formaldehyde present in outdoor air results from a number of sources, and levels of formaldehyde are generally higher in urban areas than in rural areas (USHHS-ATSDR, 1999). Direct contributions of formaldehyde to the atmosphere (i.e., those in the form of formaldehyde itself) from man-made sources are present, but are generally considered to be small relative to natural sources or indirect production of formaldehyde in the atmosphere (WHO, 2002).

B.4(b) Dicamba Residue Study in MON 94100

A study was conducted in 2018 in the U.S. and Canada to determine the magnitude of residues of dicamba in MON 94100 raw agricultural commodities (RAC) resulting from the use of a formulation of dicamba herbicide.

Combined maximum application rate in is proposed to be 1.0 lb a.e./A (1.1 kg a.e./ha) in Canada and 2.0 lb a.e./A (2.2 kg a.e./ha) in the U.S. The proposed maximum application rates and corresponding application growth stages of dicamba to MON 94100 in Canada and the U.S. are summarized below. Any combination of application rates and timings may be used within the allowed limits for individual rates and timings as specified on the label.

Maximum Application Rates	
Combined maximum of all applications per year	Canada: 1.0 lb a.e./A (1.1 kg a.e./ha) U.S.: 2.0 lb a.e./A (2.2 kg a.e./ha)
Total of all burndown, early pre-plant, at-planting, and pre-emergence applications	U.S.: 1.0 lb a.e./A (0.6 kg a.e./ha)
Total in-crop applications from emergence to harvest	Canada: 1.0 lb a.e./A (1.1 kg a.e./ha) U.S.: 1.0 lb a.e./A (1.1 kg a.e./ha)
Maximum single in-crop application	Canada: 0.5 lb a.e./A (0.6 kg a.e./ha) U.S.: 0.5 lb a.e./A (0.6 kg a.e./ha)

The purpose of this summary is to report the residue levels of dicamba and its major metabolites, 2,5-dichloro-3-hydroxy-6-methoxybenzoic acid (5-OH dicamba), 3,6-dichloro-2-hydroxybenzoic acid (DCSA), and 2,5-dichloro-3,6-dihydroxy-benzoic acid (DCGA) in MON 94100 canola seed that resulted from applications of MON 76980, a water soluble herbicide containing 2.9 lb a.e. of dicamba per gallon.

The field trials for the study were conducted in the U.S. at seven sites in five states: Iowa, Idaho, North Dakota, Nebraska, and Washington and in Canada at six sites in two provinces: Manitoba and Saskatchewan. These states and provinces were typical of the major canola producing regions of the U.S. and Canada and accounted for approximately 81 % and 67% of the total canola acreage in the U.S. (USDA-NASS, 2017) and Canada (Statistics Canada, 2018), respectively.

Control (Treatment 1) and two treated (Treatments 2 and 3) plots were established at each site for production of canola RAC seed. Two other treatments were established at four sites for other purposes. Plots for Treatments 2 and 3 measured between 450 and 3,000 square feet in area. The untreated control plot was a minimum distance of 50 ft from any treated plot.

The anticipated labeled rate and timing for applications of dicamba to MON 94100 in the United States are summarized in the following table. The treatment regimen consisted of two post-emergence applications of MON 76980 up to the 6th leaf stage through bolting, but prior to flowering for Treatment 2 and one pre-emergence application followed by two post-emergence applications of MON 76980 up to the 6th leaf stage through bolting, but prior to flowering for Treatment 3. The combined rate of both applications was 1.0 lb a.e./acre for Treatment 2 and 2.0 lb a.e./acre for Treatment 3.

The target application timings and rates are summarized in the following table.

Target Application of Dicamba Formulation MON 76980 to MON 94100 Canola

Treatment	Rate as Dicamba Acid (a.e.)		
	Pre-emergence	**Post-emergence 4-6 leaf**	**Post-emergence 6 leaf through bolting, prior to flowering**
1	–	–	–
2	–	0.5 lb/A (0.6 kg/ha)	0.5 lb/A (0.6 kg/ha)
3	1.0 lb/A (1.1 kg/ha)	0.5 lb/A (0.6 kg/ha)	0.5 lb/A (0.6 kg/ha)

Actual application rates across all applications at all sites for MON 76980 ranged from 96.4% to 145.5% of target rate, with a mean rate of 103.7%. Spray volumes ranged from 12.5 to 20.1 gallons per acre (GPA) and were within ±5% of the target spray volumes for all applications at all sites.

Canola seed samples were collected at full maturity for normal harvest. Samples were harvested by hand or with a mechanical harvester from the interior of the plots. One composite sample from the untreated plot was harvested first, followed by two replicate samples from Treatment 2, and then two replicate samples from Treatment 3.

B.4(c) Results and Conclusions

The metabolic pathways for dicamba are well characterized in soil, animals, and plants, demonstrating commonalities in the metabolic pathways for each. Among plants, the proposed metabolic pathways for dicamba-tolerant crops (cotton, soybean, and corn) are similar to the proposed pathways in non-transgenic crops. DCSA glucoside is the only metabolite that is formed in significant quantities, while minor metabolites identified include unchanged dicamba parent, free and conjugated forms of 5-OH dicamba, DCGA glucoside, DCGA malonyl glucoside, DCGA pentosylglucoside, DCSA pentoside, DCSA succinylglucoside and 3-hydroxy-3-methylglutaryl (HMG) glucoside of DCSA. The weight of evidence supports that the expected metabolic profile of dicamba-tolerant canola is comparable to that previously evaluated in three dicamba-tolerant crops, including soybean, cotton, and corn. Consistent with the expected dicamba metabolism, the following analytes were quantified in dicamba-tolerant canola RACs: dicamba, DCSA, 5-OH dicamba, and DCGA.

Residue levels of dicamba, 5-OH dicamba, DCSA, and DCGA were determined by the current version of Monsanto analytical method ME-1869, "Determination of Dicamba and Major Metabolites in Raw Agricultural Commodities by LC-MS/MS" (Riter, 2018). Analytes were quantitated using LC-MS/MS with electrospray ionization in negative ion mode. The limit of quantitation (LOQ) was determined to be 0.010 ppm (mg/kg).

For this study, one untreated control and two treated mature MON 94100 seed samples from each site were analyzed. Additional untreated seed samples were fortified with known amounts of dicamba, 5-OH dicamba, DCSA, and DCGA and were included for analysis. Untreated samples were fortified at two levels, the limit of quantitation (LOQ) (0.010 ppm) and 10X LOQ (0.100 ppm), with solutions containing dicamba, 5-OH dicamba, DCSA, and DCGA. Average dicamba, 5-OH dicamba, DCSA, and

DCGA recoveries across both fortification levels were 108-110%, 93-98%, 92-93%, and 86-88%, respectively.

The residues in samples collected from Treatment 2 and Treatment 3 are summarized in the following table.

Table 18. Dicamba, 5-OH Dicamba, DCSA, and DCGA Residues in MON 94100 RAC Seed

Analyte	Average PHI (days)[1]	Treatment 2		Treatment 3	
		Median (ppm)[2,3]	Min. – Max. (ppm) [2,3]	Median (ppm)[2,3]	Min. – Max. (ppm)[2,3]
Dicamba	72	<0.010	<0.010-<0.010	<0.010	<0.010-<0.010
5-OH Dicamba	72	<0.010	<0.010-<0.010	<0.010	<0.010-<0.010
DCSA	72	0.015	<0.010-0.070	0.016	<0.010-0.080
DCGA	72	<0.010	<0.010-<0.010	<0.010	<0.010-<0.010
Total[4]	-	<0.045	<0.040-<0.100	<0.046	<0.040-<0.110

[1]PHI - Preharvest Interval - Interval between last application and sampling.
[2]Median of site averaged dicamba, 5-OH dicamba, DCSA, and DCGA values and range of individual field sample values.
[3]The limit of quantitation (LOQ) of dicamba and its metabolites (5-OH Dicamba, DCSA, and DCGA) in MON 94100 canola is 0.010 ppm (parent equivalents). Values below 0.010 ppm are shown as <0.010.
[4]Calculated as follows: dicamba + 5-OH dicamba + DCSA + DCGA ppm (mg/kg)

The residue results indicate that the existing EPA dicamba MRL of 0.05 ppm in canola seed (EFSA, 2013) is sufficient to account for the use of dicamba on MON 94100 tolerant canola.

For details, please also refer to Appendix 9 ([redacted], (MSL0030924))

B.5 Compositional Assessment

Safety assessments of biotechnology-derived crops follow the comparative safety assessment process (Codex Alimentarius, 2009) in which the composition of grain and/or other raw agricultural commodities of the biotechnology-derived crop are compared to the appropriate conventional control that has a history of safe use. For canola, assessments are performed using the general principles outlined in the OECD consensus document for canola composition (OECD, 2011).

A previous review of compositional assessments conducted according to OECD guidelines, that encompassed a total of seven biotechnology-derived crop varieties, nine countries, and eleven growing seasons, concluded that incorporation of biotechnology-derived agronomic traits has had little impact on crop composition compared to other sources of variation. Rather, most compositional variation is attributable to growing region, agronomic practices, and genetic background (Harrigan *et al.*, 2010). Numerous scientific publications have further documented the extensive variability in the concentrations of crop components that reflect the influence of environmental and genetic factors as well as extensive conventional breeding efforts to improve nutrition, agronomics, and yield (Ridley *et al.*, 2011; Taylor *et al.*, 2017; Venkatesh *et al.*, 2014; Zhou *et al.*, 2011).

Compositional equivalence between biotechnology-derived and conventional crops supports an "equal or increased assurance of the safety of foods derived from genetically modified plants" (OECD, 2002). OECD consensus documents on compositional considerations for new crop varieties emphasize quantitative measurements of essential nutrients and known anti-nutrients or toxicants. These quantitative measurements effectively discern compositional changes that imply potential nutritional or safety (e.g., anti-nutritional) concerns. Levels of the components in grain and/or other raw agricultural commodities of the biotechnology-derived crop product are compared to: 1) corresponding levels in a conventional comparator, a genetically similar conventional line, grown concurrently under similar field conditions, and 2) natural ranges from data published in the scientific literature or in publicly available databases (e.g. ILSI Crop Composition Database, (ILSI, 2019)). This second comparison places any potential differences between the assessed biotechnology-derived crop and its comparator in the context of the well-documented variation in the concentrations of crop nutrients and anti-nutrients.

This section provides analyses of concentrations of key nutrients and anti-nutrients in grain of MON 94100 compared to that of a conventional control canola grown and harvested under similar conditions. It is important to note that grain is the only canola tissue that is consumed to any meaningful level by animals (OECD, 2011). The production of materials for compositional analyses used a sufficient variety of field trial sites (five sites in the United States and Canada), reflecting a range of environmental conditions under which MON 94100 is expected to be grown and robust field designs (randomized complete block design with four replicates). Samples were subjected to sensitive analytical methods that allow quantitative and accurate measurements of key components. The information provided in this section addresses relevant factors in Codex Plant Guidelines, Section 4, paragraphs 44 and 45 for compositional analyses (Codex Alimentarius, 2009).

B.5(a) Levels of key nutrients, toxicants and anti-nutrients

Grain samples were harvested from MON 94100 and a conventional control grown at a total of five sites (Bonneville County, Idaho (IDDO); Jerome County, Idaho (IDJE); Portage la Prairie Rural Municipality, Manitoba (MBPS); Brookings County, South Dakota (SDTO); and Grant County, Washington (WAEP) in the United States and Canada during 2018. The field sites were planted in a randomized complete block design with four replicates per site. MON 94100 and the conventional control were grown under agronomic field conditions typical for each of the different growing regions. MON 94100 plots were treated with dicamba to generate samples under conditions of the intended use of the product.

The compositional analysis provided a comprehensive comparative assessment of the levels of key nutrients and anti-nutrients in grain of MON 94100 and the conventional control. The evaluation of MON 94100 followed considerations relevant to the compositional quality of canola as defined by the OECD consensus document (OECD, 2011). Harvested grain samples were assessed for moisture and levels of key nutrients including proximates (protein, total fat and ash), amino acids (18 components), fatty acids (21 components), carbohydrates by calculation, fiber (acid detergent fiber (ADF) and neutral detergent fiber (NDF)), minerals (calcium and phosphorus) and vitamins (vitamin E and vitamin K_1). Grain samples were also assessed for levels of anti-nutrients (phytic acid, tannins, sinapine, total glucosinolates, total alkyl glucosinolates and total indolyl glucosinolates). Of the 56 measured components, 10 components (caproic acid, caprylic acid, capric acid, lauric acid, myristic acid, heptadecanoic acid, heptadecenoic acid, eicosadienoic acid, erucic acid and docosadienoic acid) had more than 50% of the observations fall below the assay limit of quantitation (LOQ) and were excluded from statistical analyses. Moisture values for grain were measured for conversion of components from fresh to dry weight, but were not statistically analyzed. Therefore, 45 components were statistically analyzed.

The statistical comparison of MON 94100 and the conventional control was based on compositional data combined across all field sites. Statistically-significant differences were identified at the 5% level ($\alpha = 0.05$). A statistically-significant difference between MON 94100 and the conventional control does not necessarily imply biological relevance from a food and feed perspective. Therefore, statistically-significant differences observed between MON 94100 and the conventional control were evaluated further to determine whether the detected difference indicated a biologically relevant compositional change or supported a conclusion of compositional equivalence, as follows:

Step 1 – Determination of the Magnitude of Difference between Test (MON 94100) and Conventional Control Means

The difference in means between MON 94100 and the conventional control was determined for use in subsequent steps.

Step 2 – Assessment of the Difference in the Context of Natural Variation within the Conventional Control across Multiple Sites

The relative impact of MON 94100 was evaluated in the context of variation within the conventional control germplasm grown across multiple sites (i.e., variation due to environmental influence). This assesses the mean difference between MON 94100 and the conventional control in the context of the individual replicate values for the conventional control (maximum value minus the minimum value). When a mean difference is less than the variability seen due to natural environmental variation within the single, closely related germplasm, the difference is typically not a food or feed safety concern (Venkatesh *et al.*, 2014).

Step 3 – Assessment of the Difference in the Context of Natural Variation Due to Multiple Sources

The relative impact of MON 94100 on composition was evaluated in the context of sources of natural variation such as environmental and germplasm influences. This assessment determined whether the mean value of MON 94100 was within the natural variability defined by the literature values or the ILSI Crop Composition Database (ILSI-CCDB) values. This naturally occurring variability is important in assessing the biological relevance of statistically-significant differences in composition between MON 94100 and the conventional control.

These evaluations of natural variation are important as crop composition is known to be greatly influenced by environment and variety (Harrigan *et al.*, 2010). Although used in the comparative assessment process, detection of statistically-significant differences between MON 94100 and the conventional control mean values does not necessarily imply a meaningful contribution by MON 94100 to compositional variability. Only if the impact of MON 94100 on levels of components was large relative to natural variation inherent to conventional canola would further assessments be required to establish whether the change in composition would have an impact from a food and feed safety and nutritional perspective. Any differences between MON 94100 and the conventional control that are within the observed natural variation for canola are not meaningful, therefore the results support a conclusion of compositional equivalence.

B.5(b) Compositional equivalence of MON 94100 grain to that of conventional canola

There were no statistically-significant differences ($p<0.05$) for 44 of the 45 components analyzed from MON 94100 grain (Table 19 to Table 24). There was one component (sinapine) that showed a statistically-significant difference ($p<0.05$) between MON 94100 and the conventional control (Table 24). For sinapine, the mean value was 0.75 % dw for MON 94100 and 0.73 % dw for the conventional control, a difference of 0.021 % dw. For this component, the mean difference between MON 94100 and the conventional control was less than the conventional control range and the MON 94100 mean component value was also within the range of values observed in the ILSI-CCDB values (Table 25).

These data indicated that the statistically-significant difference observed in sinapine in grain was not biologically-meaningful from a food and feed safety perspective. These results support the conclusion that MON 94100 was not a major contributor to variation in component levels in canola grain and confirmed the compositional equivalence of MON 94100 to the conventional control in levels of key nutrients and anti-nutrients in grain.

For details, please refer to Appendix 10 ([redacted](MSL0030455)).

Table 19. Summary of Canola Grain Protein and Amino Acids for MON 94100 and Conventional Control

Component (% dw)[1]	MON 94100 Mean (S.E.)[2] Range	Control Mean (S.E.) Range	Control Range Value[3]	Difference (Test minus Control) Mean (S.E.)	*p*-Value	% Relative[4]
Protein	28.13 (1.15) 22.67 - 32.56	27.71 (1.15) 23.30 - 32.09	8.79	0.42 (0.22)	0.066	1.52
Alanine	1.24 (0.048) 1.07 - 1.44	1.22 (0.048) 1.03 - 1.39	0.36	0.018 (0.018)	0.388	1.44
Arginine	1.90 (0.10) 1.54 - 2.43	1.88 (0.10) 1.44 - 2.59	1.15	0.019 (0.040)	0.626	1.03
Aspartic acid	2.06 (0.11) 1.66 - 2.41	2.05 (0.11) 1.55 - 2.35	0.81	0.013 (0.027)	0.657	0.63
Cystine	0.69 (0.022) 0.57 - 0.79	0.68 (0.022) 0.60 - 0.81	0.21	0.016 (0.012)	0.194	2.39
Glutamic acid	4.97 (0.23) 4.06 - 5.95	4.85 (0.23) 4.00 - 5.75	1.74	0.12 (0.060)	0.064	2.41

Table 19. Summary of Canola Grain Protein and Amino Acids for MON 94100 and Conventional Control (Continued)

Component (% dw)[1]	MON 94100 Mean (S.E.)[2] Range	Control Mean (S.E.) Range	Control Range Value[3]	Difference (Test minus Control) Mean (S.E.)	*p*-Value	% Relative[4]
Glycine	1.39 (0.057) 1.20 - 1.61	1.37 (0.057) 1.13 - 1.57	0.44	0.016 (0.019)	0.447	1.16
Histidine	0.68 (0.023) 0.58 - 0.78	0.68 (0.023) 0.59 - 0.79	0.20	-0.0016 (0.013)	0.904	-0.23
Isoleucine	1.16 (0.054) 0.93 - 1.36	1.15 (0.054) 0.94 - 1.33	0.39	0.013 (0.017)	0.508	1.09
Leucine	2.01 (0.094) 1.61 - 2.36	1.99 (0.094) 1.62 - 2.31	0.69	0.020 (0.028)	0.520	1.00
Lysine	1.45 (0.051) 1.29 - 1.72	1.46 (0.051) 1.26 - 1.75	0.50	-0.0021 (0.027)	0.940	-0.14
Methionine	0.52 (0.021) 0.41 - 0.62	0.51 (0.021) 0.46 - 0.59	0.13	0.0064 (0.0098)	0.548	1.24

Table 19. Summary of Canola Protein and Amino Acids for MON 94100 and Conventional Control (Continued)

Component (% dw)[1]	MON 94100 Mean (S.E.)[2] Range	Control Mean (S.E.) Range	Control Range Value[3]	Difference (Test minus Control) Mean (S.E.)	*p*-Value	% Relative[4]
Phenylalanine	1.16 (0.057) 0.92 - 1.37	1.15 (0.057) 0.90 - 1.33	0.43	0.014 (0.017)	0.473	1.18
Proline	1.73 (0.068) 1.40 - 2.06	1.69 (0.068) 1.49 - 2.02	0.53	0.039 (0.022)	0.090	2.32
Serine	1.19 (0.049) 1.00 - 1.38	1.17 (0.049) 0.97 - 1.34	0.37	0.019 (0.013)	0.217	1.66
Threonine	1.17 (0.042) 1.03 - 1.34	1.16 (0.042) 0.98 - 1.30	0.32	0.010 (0.016)	0.558	0.90
Tryptophan	0.39 (0.018) 0.30 - 0.46	0.38 (0.018) 0.30 - 0.45	0.15	0.0080 (0.0053)	0.148	2.10
Tyrosine	0.85 (0.034) 0.73 - 0.97	0.84 (0.034) 0.70 - 0.95	0.25	0.0045 (0.010)	0.675	0.54
Valine	1.41 (0.058) 1.18 - 1.65	1.40 (0.058) 1.15 - 1.58	0.43	0.014 (0.021)	0.542	1.00

[1]dw=dry weight
[2] Mean (S.E.) = least-square mean (standard error)
[3]Maximum value minus minimum value for the control canola variety
[4]The relative magnitude of the difference in mean values between MON 94100 (treated with dicamba) and the control, expressed as a percent of the control.

Table 20. Summary of Canola Grain Total Fat and Fatty Acids for MON 94100 and Conventional Control

				Difference (Test minus Control)	
Component	MON 94100 Mean (S.E.)[1] Range	Control Mean (S.E.) Range	Control Range Value[2]	Mean (S.E.)	*p*-Value
Total fat (% dw)[3]	43.22 (1.41) 37.28 - 48.43	43.30 (1.41) 38.73 - 47.87	9.14	-0.080 (0.30)	0.791
Palmitic acid (% Total FA)[4]	4.29 (0.070) 3.98 - 4.68	4.28 (0.070) 3.98 - 4.55	0.57	0.0050 (0.064)	0.941
Palmitoleic acid (% Total FA)	0.24 (0.0066) 0.22 - 0.27	0.25 (0.0066) 0.22 - 0.29	0.063	-0.0048 (0.0034)	0.167
Stearic acid (% Total FA)	1.75 (0.060) 1.55 - 1.96	1.74 (0.060) 1.50 - 2.00	0.50	0.0063 (0.024)	0.793
Oleic acid (% Total FA)	65.29 (0.39) 63.18 - 67.57	65.11 (0.39) 63.31 - 66.74	3.43	0.18 (0.33)	0.608
Linoleic acid (% Total FA)	18.87 (0.36) 17.06 - 20.43	18.95 (0.36) 17.65 - 20.52	2.87	-0.075 (0.22)	0.754

Table 20. Summary of Canola Grain Total Fat and Fatty Acids for MON 94100 and Conventional Control (Continued)

			Difference (Test minus Control)		
Component	MON 94100 Mean (S.E.)[1] Range	Control Mean (S.E.) Range	Control Range Value[2]	Mean (S.E.)	*p*-Value
Linolenic acid (% Total FA)	7.23 (0.24) 6.35 - 8.22	7.32 (0.24) 6.42 - 8.19	1.77	-0.085 (0.11)	0.500
Arachidic acid (% Total FA)	0.55 (0.017) 0.50 - 0.63	0.56 (0.017) 0.48 - 0.61	0.13	-0.0025 (0.0065)	0.700
Eicosenoic acid (% Total FA)	1.16 (0.016) 1.07 - 1.23	1.18 (0.016) 1.12 - 1.24	0.13	-0.019 (0.011)	0.096
Behenic acid (% Total FA)	0.27 (0.0089) 0.23 - 0.30	0.27 (0.0089) 0.24 - 0.31	0.072	-0.0037 (0.0034)	0.295
Lignoceric acid (% Total FA)	0.17 (0.011) 0.13 - 0.22	0.18 (0.011) 0.14 - 0.23	0.091	-0.0036 (0.0054)	0.542
Nervonic acid (% Total FA)	0.18 (0.025) 0.090 - 0.31	0.18 (0.025) 0.098 - 0.28	0.18	-0.0019 (0.013)	0.893

[1] Mean (S.E.) = least-square mean (standard error)
[2]Maximum value minus minimum value for the control canola variety
[3]dw=dry weight
[4]FA=Fatty Acid
The following components with more than 50% of observations below the assay LOQ were excluded from statistical analysis: caproic acid, caprylic acid, capric acid, lauric acid, myristic acid, heptadecanoic acid, heptadecenoic acid, eicosadienoic acid, erucic acid and docosadienoic acid.

Table 21. Summary of Canola Grain Carbohydrates by Calculation and Fiber for MON 94100 and Conventional Control

				Difference (Test minus Control)	
Component (% dw)[1]	MON 94100 Mean (S.E.)[2] Range	Control Mean (S.E.) Range	Control Range Value[3]	Mean (S.E.)	*p*-Value
Carbohydrates by calculation	24.79 (0.46) 23.13 - 26.42	24.82 (0.46) 23.26 - 26.59	3.33	-0.035 (0.18)	0.845
ADF	13.92 (0.79) 11.37 - 18.28	13.93 (0.79) 10.94 - 18.31	7.37	-0.0097 (0.35)	0.977
NDF	18.86 (0.93) 15.31 - 23.84	18.96 (0.93) 15.24 - 23.50	8.26	-0.10 (0.39)	0.796

[1]dw=dry weight

[2] Mean (S.E.) = least-square mean (standard error)

[3]Maximum value minus minimum value for the control canola variety

Table 22. Summary of Canola Grain Ash and Minerals for MON 94100 and Conventional Control

Component (% dw)[1]	MON 94100 Mean (S.E.)[2] Range	Control Mean (S.E.) Range	Control Range Value[3]	Difference (Test minus Control) Mean (S.E.)	*p*-Value
Ash	3.86 (0.26) 2.99 - 4.56	3.95 (0.26) 3.18 - 5.00	1.82	-0.084 (0.076)	0.335
Calcium	0.36 (0.036) 0.28 - 0.47	0.39 (0.036) 0.30 - 0.63	0.33	-0.027 (0.018)	0.204
Phosphorus	0.80 (0.066) 0.56 - 1.00	0.80 (0.066) 0.59 - 1.01	0.42	-0.00025 (0.011)	0.981

[1]dw=dry weight

[2] Mean (S.E.) = least-square mean (standard error)

[3]Maximum value minus minimum value for the control canola variety

Table 23. Summary of Canola Grain Vitamins for MON 94100 and Conventional Control

Component	MON 94100 Mean (S.E.)[2] Range	Control Mean (S.E.) Range	Control Range Value[3]	Difference (Test minus Control) Mean (S.E.)	*p*-Value
Vitamin E (mg/g dw)[1]	0.10 (0.0076) 0.067 - 0.14	0.096 (0.0076) 0.066 - 0.13	0.068	0.0066 (0.0032)	0.105
Vitamin K_1 (µg/g dw)[1]	0.70 (0.081) 0.47 - 1.00	0.77 (0.081) 0.54 - 1.12	0.58	-0.074 (0.034)	0.097

[1]dw=dry weight; Common names of vitamins: E=α-Tocopherol; K_1=phylloquinone.

[2] Mean (S.E.) = least-square mean (standard error)

[3]Maximum value minus minimum value for the control canola variety

Table 24. Summary of Canola Grain Anti-Nutrients for MON 94100 and Conventional Control

				Difference (Test minus Control)	
Component	MON 94100 Mean (S.E.)[1] Range	Control Mean (S.E.) Range	Control Range Value[2]	Mean (S.E.)	*p*-Value
Total glucosinolates (µmol/g dw)[3]	11.49 (0.67) 8.49 - 14.68	10.98 (0.67) 8.02 - 12.96	4.95	0.51 (0.30)	0.104
Total alkyl glucosinolates (µmol/g dw)	5.14 (0.53) 2.62 - 8.61	4.85 (0.53) 2.65 - 6.99	4.34	0.29 (0.19)	0.140
Total indolyl glucosinolates (µmol/g dw)	5.93 (0.23) 4.72 - 6.85	5.75 (0.23) 4.73 - 7.10	2.37	0.18 (0.16)	0.254
Phytic acid (% dw)	1.80 (0.16) 1.09 - 2.59	1.78 (0.16) 0.86 - 2.34	1.48	0.019 (0.081)	0.813
Sinapine (% dw)	0.75 (0.017) 0.67 - 0.82	0.73 (0.017) 0.63 - 0.81	0.18	0.021 (0.0099)	0.043
Tannins (% dw)	0.054 (0.0029) 0.019 - 0.065	0.055 (0.0029) 0.043 - 0.071	0.028	-0.0014 (0.0036)	0.716

[1]Mean (S.E.) = least-square mean (standard error)
[2]Maximum value minus minimum value for the control canola
[3]dw=dry weight

Table 25. Literature and ILSI-CCDB Database Ranges for Components in Canola Grain

Tissue Components[1]	Literature Range[2]	ILSI Range[3]
Grain Nutrients		
Proximates		
protein (% dw)	21.234-28.662[a]	15.6-35.7
total fat (% dw)	34.368-44.954[a]	24.6-55.2
ash (% dw)	3.362-6.02[a]	2.6-10.6
Amino Acids		
alanine (% dw)	0.71-1.09[b]	0.73-1.45
arginine (% dw)	0.93-1.55[b]	0.97-2.34
aspartic acid (% dw)	1.20-2.03[b]	1.15-2.68
cystine (% dw)	0.32-0.52[b]	0.19-0.96
glutamic acid (% dw)	3.23-4.35[b]	2.37-7.31
glycine (% dw)	0.82-1.29[b]	0.86-1.75
histidine (% dw)	0.41-0.68[b]	0.47-1.05
isoleucine (% dw)	0.62-1.02[b]	0.65-1.40
leucine (% dw)	1.07-1.77[b]	1.14-2.42
lysine (% dw)	0.96-1.50[b]	1.07-2.09
methionine (% dw)	0.27-0.52[b]	0.19-0.71
phenylalanine (% dw)	0.64-1.07[b]	0.69-1.52
proline (% dw)	0.85-1.53[b]	1.01-2.28
serine (% dw)	0.69-1.12[b]	0.66-1.53
threonine (% dw)	0.74-1.17[b]	0.72-1.40
tryptophan (% dw)	0.20-0.37[b]	0.166-0.499
tyrosine (% dw)	NA	0.41-1.03
valine (% dw)	0.80-1.33[b]	0.82-1.70
Fatty Acids		
palmitic acid (% Total FA)	2.5-7.0[c]	3.53-5.70
palmitoleic acid (% Total FA)	NA-0.6[c]	0.16-0.40
stearic acid (% Total FA)	0.8-3.0[c]	1.50-2.89
oleic acid (% Total FA)	51.0-70.0[c]	53.19-69.45
linoleic acid (% Total FA)	15.0-30.0[c]	14.13-25.68
linolenic acid (% Total FA)	5.0-14.0[c]	5.79-13.07
arachidic acid (% Total FA)	0.2-1.2[c]	0.49-0.95
eicosenoic acid (% Total FA)	0.1-4.3[c]	0.93-3.33
behenic acid (% Total FA)	NA-0.6[c]	0.19-0.52
lignoceric acid (% Total FA)	NA-0.3[c]	0.09-0.32
nervonic acid (% Total FA)	NA-0.4[c]	0.08-0.40
Carbohydrates By Calculation		
carbohydrates by calculation (% dw)	NA	17.7-47.4
Fiber		
ADF (% dw)	12.405-28.379[a]	8.94-42.30
NDF (% dw)	18.964-37.861[a]	10.93-53.70
Minerals		
calcium (% dw)	0.361-0.728[a]	0.248-1.410
phosphorus (% dw)	0.544-0.896[a]	0.41-1.85

Table 25. Literature and ILSI-CCDB Database Ranges for Components in Canola Grain (Continued)

Tissue Components[1]	Literature Range[2]	ILSI Range[3]
Grain Nutrients		
Vitamins		
vitamin E (mg/g dw)	NA	0.0096-0.1796
vitamin K_1 (µg/g dw)	0.40-2.39[d]	0.40-5.63
Grain Other		
Anti-Nutrients		
total glucosinolates (µmol/g dw)	38.42-NA[e]	0.41-31.98
total alkyl glucosinolates (µmol/g dw)	NA	0.24-28.33
total indolyl glucosinolates (µmol/g dw)	NA	0.06-7.18
phytic acid (% dw)	NA	0.94-3.88
sinapine (% dw)	NA	0.19-1.36
tannins (% dw)	NA	0.05-1.27

[1]dw=dry weight; FA=Fatty Acid

[2]Literature range references: [a](Dairy One Forage Lab, 2011);[b](OECD, 2011);[c](Codex Alimentarius, 2011);[d](Claussen *et al.*, 2015);[e](Bell, 1995)

[3]ILSI range is from ILSI Crop Composition Database, 2019 (Accessed January 15, 2019).

B.5(c) Compositional assessment of MON 94100 conclusion

Compositional analysis was conducted on grain of MON 94100 and the conventional control grown at five sites in the United States and Canada during the 2018 field season. There were no statistically-significant differences ($p<0.05$) for 44 of the 45 components analyzed from MON 94100 grain. There was one component (sinapine) that showed a statistically-significant difference ($p<0.05$) between MON 94100 and the conventional control (Table 24). For sinapine, the mean value was 0.75 % dw for MON 94100 and 0.73 % dw for the conventional control, a difference of 0.021 % dw. For this component, the mean difference between MON 94100 and the conventional control was less than the conventional control range and the MON 94100 mean component value was also within the range of values observed in the ILSI-CCDB values.

These data indicated that the statistically-significant difference observed in sinapine in grain was not biologically-meaningful from a food and feed safety perspective. These results support the conclusion that MON 94100 was not a major contributor to variation in component levels in canola grain and confirmed the compositional equivalence of MON 94100 to the conventional control in levels of key nutrients and anti-nutrients in grain.

C. NUTRITIONAL IMPACT of GM FOOD

There are no impacts on nutirion of MON 94100. This product is developed to confer dicamba tolerance to canola. It is not a nutritionally altered product.

D. OTHER INFORMATION

The data and information presented in this submission demonstrate that the food and feed derived from MON 94100 are as safe and nutritious as those derived from commercially-available, conventional canola for which there is an established history of safe consumption. No additional studies will be required to add value to the safety of MON 94100.

PART 3 STATUTORY DECLARATION – AUSTRALIA

I, Nina McCormick, declare the following points in this application:

1. The information provided in this application fully sets out the matters required.
2. The information provided in this application is true to the best of my knowledge and belief.
3. No information has been withheld that might prejudice this application, to the best of my knowledge and belief.

Signature: [redacted]

Declared before me ..... [redacted] .....

This 6 day of .....October..... 2020.

PART 4 REFERENCES

[redacted] 2019. Rationale for Bridging Existing Dicamba-Tolerant Oilseed Crops Metabolism Data to Fulfil the Requirements for Dicamba-Tolerant Canola MON 94100. Monsanto Technical Report MSL0029450. Chesterfield, Missouri.

Adrian-Romero, M., G. Blunden, B.G. Carpenter and E. Tyihák. 1999. HPLC quantification of formaldehyde, as formaldemethone, in plants and plant-like organisms. Chromatographia 50:160-166.

An, S.-q. and G. Berg. 2018. *Stenotrophomonas maltophilia*. Trends in Microbiology 26:637-638.

Anderson, J.E., J.-M. Michno, T.J.Y. Kono, A.O. Stec, B.W. Campbell, S.J. Curtin and R.M. Stupar. 2016. Genomic variation and DNA repair associated with soybean transgenesis: A comparison to cultivars and mutagenized plants. BMC Biotechnology 16:41.

Anthony, K., V. Arechavala-Gomeza, L.E. Taylor, A. Vulin, Y. Kaminoh, S. Torelli, L. Feng, N. Janghra, G. Bonne, M. Beuvin, R. Barresi, M. Henderson, S. Laval, A. Lourbakos, G. Campion, V. Straub, T. Voit, C.A. Sewry, J.E. Morgan, K.M. Flanigan and F. Muntoni. 2014. Dystrophin quantification: Biological and translational research implications. Neurology 83:2062-2069.

ASA. 2019. 2019 SoyStats: A reference guide to soybean facts and figures. American Soybean Association, St. Louis, Missouri. http://soystats.com/wp-content/uploads/2019-SoyStats-Web.pdf [Accessed May 1, 2020].

Astwood, J.D., J.N. Leach and R.L. Fuchs. 1996. Stability of food allergens to digestion in vitro. Nature Biotechnology 14:1269-1273.

Axelos, M., C. Bardet, T. Libox, A. Le Van Thai, C. Curie and B. Lescure. 1989. The gene family encoding the *Arabidopsis thaliana* translation elongation factor EF-1α: Molecular cloning, characterization and expression. Molecular and General Genetics 219:106-112.

Barker, R.F., K.B. Idler, D.V. Thompson and J.D. Kemp. 1983. Nucleotide sequence of the T-DNA region from the *Agrobacterium tumefaciens* octopine Ti plasmid pTi15955. Plant Molecular Biology 2:335-350.

Bäumlein, H., W. Boerjan, I. Nagy, R. Bassüner, M. Van Montagu, D. Inzé and U. Wobus. 1991. A novel seed protein gene from *Vicia faba* is developmentally regulated in transgenic tobacco and *Arabidopsis* plants. Molecular and General Genetics 225:459-467.

Bautista-Zapanta, J.-n., K. Suzuki and K. Yoshida. 2002. Characterization of four ribosomal RNA operons in the genome of *Agrobacterium tumefaciens* MAFF301001. Nucleic Acids Research S2:91-92.

Beck, E., G. Ludwig, E.A. Auerswald, B. Reiss and H. Schaller. 1982. Nucleotide sequence and exact localization of the neomycin phosphotransferase gene from transposon Tn*5*. Gene 19:327-336.

Beckie, H.J., S.I. Warwick, H. Nair and G. Séguin-Swartz. 2003. Gene flow in commercial fields of herbicide-resistant canola (*Brassica napus*). Ecological Applications 13:1276-1294.

Behrens, M.R., N. Mutlu, S. Chakraborty, R. Dumitru, W.Z. Jiang, B.J. LaVallee, P.L. Herman, T.E. Clemente and D.P. Weeks. 2007. Dicamba resistance: Enlarging and preserving biotechnology-based weed management strategies. Science 316:1185-1188.

Bell, J.M. 1995. Meal and by-product utilization in animal nutrition. Pages 301-337 in *Brassica* Oilseeds: Production and Utilization. D.S. Kimber and D.I. McGregor (eds.). CAB International, Wallingford, United Kingdom.

Berg, G. and J.L. Martinez. 2015. Friends or foes: Can we make a distinction between beneficial and harmful strains of the *Stenotrophomonas maltophilia* complex? Frontiers in Microbiology 6:241.

Bevan, M., W.M. Barnes and M.-D. Chilton. 1983. Structure and transcription of the nopaline synthase gene region of T-DNA. Nucleic Acids Research 11:369-385.

Biron, D.G., C. Brun, T. Lefevre, C. Lebarbenchon, H.D. Loxdale, F. Chevenet, J.-P. Brizard and F. Thomas. 2006. The pitfalls of proteomics experiments without the correct use of bioinformatics tools. Proteomics 6:5577-5596.

Boyles, M., J. Criswell, F. Epplin, K. Giles, C. Godsey, W. Heer, G. Hergert, J. Holman, D. Jardine, C. Jones, V. Martin, D. Mengel, T. Peeper, D. Peterson, K. Roozeboom, T. Royer, H. Sanders, P. Sloderbeck, M. Stamm and C. Thompson. 2009. Great Plains canola production handbook. Kansas State University Agricultural Experiment Station and Cooperative Extension Service, Manhattan, Kansas.

Bradshaw, R.A., W.W. Brickey and K.W. Walker. 1998. N-terminal processing: The methionine aminopeptidase and N^{α}-acetyl transferase families. Trends in Biochemical Sciences 23:263-267.

Breyton, C. 2000. The cytochrome b_6f complex: Structural studies and comparison with the bc_1 complex. Biochimica et Biophysica Acta 1459:467-474.

Brooke, J.S., G. Di Bonaventura, G. Berg and J.-L. Martinez. 2017. Editorial: A multidisciplinary look at *Stenotrophomonas maltophilia*: An emerging multi-drug-resistant global opportunistic pathogen. Frontiers in Microbiology 8:1511.

Brown, J., J.B. Davis, M. Lauver and D. Wysocki. 2009. U.S. Canola Association: Canola growers manual. University of Idaho, Oregon State University, Boise, Idaho.

Cade, R., K. Burgin, K. Schilling, T.-J. Lee, P. Ngam, N. Devitt and D. Fajardo. 2018. Evaluation of whole genome sequencing and an insertion site characterization method for molecular characterization of GM maize. Journal of Regulatory Science 6:1-14.

Caetano-Anollés, G., M. Wang, D. Caetano-Anollés and J.E. Mittenthal. 2009. The origin, evolution and structure of the protein world. Biochemical Journal 417:621-637.

CCC. 2016. Comparison of dietary fats. Canola Council of Canada, Winnipeg, Manitoba.

CCC. 2019. Canola encyclopedia - Weeds. Canola Council of Canada, Winnipeg, Manitoba. www.canolacouncil.org [Accessed September 13, 2019].

CCC. 2020. Canola grower's manual. Canola Council of Canada, Winnipeg, Manitoba. https://www.canolacouncil.org/crop-production/canola-grower's-manual-contents#top [Accessed March 19, 2020].

CFIA. 2019. Plant Breeders' Rights: Crop Reports -. Canola Variety 65037. Canadian Food Inspection Agency, Ottawa, Ontario. https://inspection.gc.ca/english/plaveg/pbrpov/cropreport/can/app00006351e.sht [Accessed November 12, 2019].

Chakraborty, S., M. Behrens, P.L. Herman, A.F. Arendsen, W.R. Hagen, D.L. Carlson, X.-Z. Wang and D.P. Weeks. 2005. A three-component dicamba *O*-demethylase from *Pseudomonas maltophilia*, strain DI-6: Purification and characterization. Archives of Biochemistry and Biophysics 437:20-28.

Clark, S.E. and G.K. Lamppa. 1992. Processing of the precursors for the light-harvesting chlorophyll-binding proteins of photosystem II and photosystem I during import and in an organelle-free assay. Plant Physiology 98:595-601.

Claussen, F.A., M.L. Talor, M.L. Breeze and K. Liu. 2015. Measurement of vitamin K_1 in commercial canola cultivars from growing locations in North and South America using high-performance liquid chromatography - tandem mass spectrometry. Journal of Agricultural and Food Chemistry 63:1076-1081.

Codex Alimentarius. 2005. Codex standard for named vegetable oils. Pages 1-13 in *Codex-STAN 210*. Codex Alimentarius Commission, Joint FAO/WHO Food Standards Programme, Food and Agriculture Organization of the United Nations, Rome, Italy.

Codex Alimentarius. 2009. Foods derived from modern biotechnology. Second Edition. Codex Alimentarius Commission, Joint FAO/WHO Food Standards Programme, Food and Agriculture Organization of the United Nations, Rome, Italy.

Codex Alimentarius. 2011. Codex standard for named vegetable oils. Codex-Stan 210-1999. Codex Alimentarius Commission, Joint FAO/WHO Food Standards Programme, Food and Agriculture Organization of the United Nations, Rome, Italy.

Cojocariu, C., P. Escher, K.-H. Häberle, R. Matyssek, H. Rennenberg and J. Kreuzwieser. 2005. The effect of ozone on the emission of carbonyls from leaves of adult *Fagus sylvatica*. Plant Cell and Environment 28:603-611.

Cojocariu, C., J. Kreuzwieser and H. Rennenberg. 2004. Correlation of short-chained carbonyls emitted from *Picea abies* with physiological and environmental parameters. New Phytologist 162:717-727.

Coruzzi, G., R. Broglie, C. Edwards and N.-H. Chua. 1984. Tissue-specific and light-regulated expression of a pea nuclear gene encoding the small subunit of ribulose-1, 5-bisphosphate carboxylase. EMBO Journal 3:1671-1679.

D'Ordine, R.L., T.J. Rydel, M.J. Storek, E.J. Sturman, F. Moshiri, R.K. Bartlett, G.R. Brown, R.J. Eilers, C. Dart, Y. Qi, S. Flasinski and S.J. Franklin. 2009. Dicamba monooxygenase: Structural insights into a dynamic Rieske oxygenase that catalyzes an exocyclic monooxygenation. Journal of Molecular Biology 392:481-497.

Dairy One Forage Lab. 2011. Dairy One Forage Lab Database: Canola seed. Dairy One, Ithaca, New York. http://www.dairyone.com [Accessed October 25, 2011].

Darrouzet, E., J.W. Cooley and F. Daldal. 2004. The cytochrome bc_1 complex and its homologue the b_6f complex: Similarities and differences. Photosynthesis Research 79:25-44.

Delaney, B., J.D. Astwood, H. Cunny, R.E. Conn, C. Herouet-Guicheney, S. MacIntosh, L.S. Meyer, L. Privalle, Y. Gao, J. Mattsson, M. Levine and ILSI. 2008. Evaluation of protein safety in the context of agricultural biotechnology. Food and Chemical Toxicology 46:S71-S97.

della-Cioppa, G., S.C. Bauer, B.K. Klein, D.M. Shah, R.T. Fraley and G.M. Kishore. 1986. Translocation of the precursor of 5-enolpyruvylshikimate-3-phosphate synthase into chloroplasts of higher plants *in vitro*. Proceedings of the National Academy of Sciences of the United States of America 83:6873-6877.

Depicker, A., S. Stachel, P. Dhaese, P. Zambryski and H.M. Goodman. 1982. Nopaline synthase: Transcript mapping and DNA sequence. Journal of Molecular and Applied Genetics 1:561-573.

Dong, H., C. Zhu, J. Chen, X. Ye and Y.-P. Huang. 2015. Antibacterial activity of *Stenotrophomonas maltophilia* endolysin P28 against both gram-positive and gram-negative bacteria. Frontiers in Microbiology 6:1299.

Dumitru, R., W.Z. Jiang, D.P. Weeks and M.A. Wilson. 2009. Crystal structure of dicamba monooxygenase: A Rieske nonheme oxygenase that catalyzes oxidative demethylation. Journal of Molecular Biology 392:498-510.

EFSA. 2007a. Ecotoxicology. Draft assessment report: Initial risk assessment provided by the rapporteur Member State Denmark for the existing active substance dicamba of the third stage (part B) of the review programme referred to in Article 8(2) of Council Directive 91/414/EEC. European Food Safety Authority, Brussels, Belgium.

EFSA. 2007b. Environmental fate and behaviour. Draft assessment report: Initial risk assessment provided by the rapporteur Member State Denmark for the existing active substance dicamba of the third stage (part B) of the review programme referred to in Article 8(2) of Council Directive 91/414/EEC. European Food Safety Authority, Brussels, Belgium.

EFSA. 2013. Reasoned opinion on the modification of the MRL for dicamba in genetically modified soybean. EFSA Journal 11:3440.

FAO-WHO. 2011a. Pesticide residues in food 2010: Joint FAO/WHO meeting on pesticide residues. FAO Plant Production and Protection Paper 200. Food and Agriculture Organization of the United Nations, World Health Organization, Rome, Italy.

FAO-WHO. 2011b. Summary report: Acceptable daily intakes, acute reference doses, short-term and long-term dietary intakes, recommended maximum residue limits and supervised trials median residue values recorded by the 2011 meeting. Food and Agriculture Organization of the United Nations, World Health Organization, Geneva, Switzerland.

Ferraro, D.J., L. Gakhar and S. Ramaswamy. 2005. Rieske business: Structure-function of Rieske non-heme oxygenases. Biochemical and Biophysical Research and Communications 338:175-190.

Fling, M.E., J. Kopf and C. Richards. 1985. Nucleotide sequence of the transposon Tn*7* gene encoding an aminoglycoside-modifying enzyme, 3"(9)-*O*-nucleotidyltransferase. Nucleic Acids Research 13:7095-7106.

Fluhr, R., C. Kuhlemeier, F. Nagy and N.-H. Chua. 1986. Organ-specific and light-induced expression of plant genes. Science 232:1106-1112.

Fraley, R.T., S.G. Rogers, R.B. Horsch, P.R. Sanders, J.S. Flick, S.P. Adams, M.L. Bittner, L.A. Brand, C.L. Fink, J.S. Fry, G.R. Galluppi, S.B. Goldberg, N.L. Hoffmann and S.C. Woo. 1983. Expression of bacterial genes in plant cells. Proceedings of the National Academy of Sciences of the United States of America 80:4803-4807.

Fu, T.-J., U.R. Abbott and C. Hatzos. 2002. Digestibility of food allergens and nonallergenic proteins in simulated gastric fluid and simulated intestinal fluid - A comparative study. Journal of Agricultural and Food Chemistry 50:7154-7160.

Giza, P.E. and R.C.C. Huang. 1989. A self-inducing runaway-replication plasmid expression system utilizing the Rop protein. Gene 78:73-84.

Gray, J., E. Wardzala, M. Yang, S. Reinbothe, S. Haller and F. Pauli. 2004. A small family of LLS1-related non-heme oxygenases in plants with an origin amongst oxygenic photosynthesizers. Plant Molecular Biology 54:39-54.

Hammond, B.G. and R.L. Fuchs. 1998. Safety evaluation for new varieties of food crops developed through biotechnology. Pages 61-79 in Biotechnology and Safety Assessment. Second Edition. J.A. Thomas (ed.). Taylor & Francis, Philadelphia, Pennsylvania.

Hammond, B.G. and J.M. Jez. 2011. Impact of food processing on the safety assessment for proteins introduced into biotechnology-derived soybean and corn crops. Food and Chemical Toxicology 49:711-721.

Hanson, A.D. and S. Roje. 2001. One-carbon metabolism in higher plants. Annual Review of Plant Physiology and Plant Molecular Biology 52:119-137.

Harayama, S., M. Kok and E.L. Neidle. 1992. Functional and evolutionary relationships among diverse oxygenases. Annual Review of Microbiology 46:565-601.

Harrigan, G.G., D. Lundry, S. Drury, K. Berman, S.G. Riordan, M.A. Nemeth, W.P. Ridley and K.C. Glenn. 2010. Natural variation in crop composition and the impact of transgenesis. Nature Biotechnology 28:402-404.

Heller, D., E.J. Helmerhorst, A.C. Gower, W.L. Siqueira, B.J. Paster and F.G. Oppenheim. 2016. Microbial diversity in the early *in vivo*-formed dental biofilm. Applied and Enviornmental Microbiology 82:1881-1888.

Helm, R.M. 2001. Topic 5: Stability of known allergens (digestive and heat stability). Joint FAO/WHO expert consultation on foods derived from biotechnology., Food and Agriculture Organization of the United Nations, Rome, Italy.

Herman, P.L., M. Behrens, S. Chakraborty, B.M. Chrastil, J. Barycki and D.P. Weeks. 2005. A three-component dicamba *O*-demethylase from *Pseudomonas maltophilia*, strain DI-6: Gene isolation, characterization, and heterologous expression. Journal of Biological Chemistry 280:24759-24767.

Herrmann, K.M. 1995. The shikimate pathway: Early steps in the biosynthesis of aromatic compounds. The Plant Cell 7:907-919.

Hibino, T., R. Waditee, E. Araki, H. Ishikawa, K. Aoki, Y. Tanaka and T. Takabe. 2002. Functional characterization of choline monooxygenase, an enzyme for betaine synthesis in plants. Journal of Biological Chemistry 277:41352-41360.

Hileman, R.E., A. Silvanovich, R.E. Goodman, E.A. Rice, G. Holleschak, J.D. Astwood and S.L. Hefle. 2002. Bioinformatic methods for allergenicity assessment using a comprehensive allergen database. International Archives of Allergy and Immunology 128:280-291.

Hochuli, E., W. Bannwarth, H. Döbeli, R. Gentz and D. Stüber. 1988. Genetic approach to facilitate purification of recombinant proteins with a novel metal chelate adsorbent. Nature Biotechnology 6:1321-1325.

Hunt, A.G. 1994. Messenger RNA 3' end formation in plants. Annual Review of Plant Physiology and Plant Molecular Biology 45:47-60.

Illergård, K., D.H. Ardell and A. Elofsson. 2009. Structure is three to ten times more conserved than sequence - A study of structural response in protein cores. Proteins 77:499-508.

ILSI. 2019. Crop composition database, Version 7.0. International Life Sciences Institute, Washington, D.C. https://www.cropcomposition.org/query/index.html.

Klee, H.J., Y.M. Muskopf and C.S. Gasser. 1987. Cloning of an *Arabidopsis thaliana* gene encoding 5-enolpyruvylshikimate-3-phosphate synthase: Sequence analysis and manipulation to obtain glyphosate-tolerant plants. Molecular and General Genetics 210:437-442.

Kovalic, D., C. Garnaat, L. Guo, Y. Yan, J. Groat, A. Silvanovich, L. Ralston, M. Huang, Q. Tian, A. Christian, N. Cheikh, J. Hjelle, S. Padgette and G. Bannon. 2012. The use of next generation sequencing and junction sequence analysis bioinformatics to achieve molecular

characterization of crops improved through modern biotechnology. The Plant Genome 5:149-163.

Krause, E., H. Wenschuh and P.R. Jungblut. 1999. The dominance of arginine-containing peptides in MALDI-derived tryptic mass fingerprints of proteins. Analytical Chemistry 71:4160-4165.

Krueger, J.P., R.G. Butz, Y.H. Atallah and D.J. Cork. 1989. Isolation and identification of microorganisms for the degradation of dicamba. Journal of Agricultural and Food Chemistry 37:534-538.

Liener, I.E. 1994. Implications of antinutritional components in soybean foods. Critical Reviews in Food Science and Nutrition 34:31-67.

Lira, F., G. Berg and J.L. Martínez. 2017. Double-faced meets the bacterial world: The opportunistic pathogen *Stenotrophomonas maltopilia*. Frontiers in Mircobiology 8:2190.

Maiti, I.B. and R.J. Shepperd. 1998. Isolation and expression analysis of peanut chlorotic streak caulimovirus (PClSV) full-length transcript (FLt) promoter in transgenic plants. Biochemical and Biophysical Research Communications 244:440-444.

Metcalfe, D.D., J.D. Astwood, R. Townsend, H.A. Sampson, S.L. Taylor and R.L. Fuchs. 1996. Assessment of the allergenic potential of foods derived from genetically engineered crop plants. Critical Reviews in Food Science and Nutrition 36:S165-S186.

Moreno, F.J., F.A. Mellon, M.S.J. Wickham, A.R. Bottrill and E.N.C. Mills. 2005. Stability of the major allergen Brazil nut 2S albumin (Ber e 1) to physciologically relevant *in vitro* gastrointestinal digestion. FEBS Journal 272:341-352.

Mukherjee, P. and P. Roy. 2016. Genomic potential of *Stenotrophomonas maltophilia* in bioremediation with an assessment of its multifaceted role in our environment. Frontiers in Mircobiology 7:967.

Nam, J.-W., H. Nojiri, T. Yoshida, H. Habe, H. Yamane and T. Omori. 2001. New classification system for oxygenase components involved in ring-hydroxylating oxygenations. Bioscience, Biotechnology, and Biochemistry 65:254-263.

NDSU. 2005. Canola production field guide. A-1280. North Dakota State University Extension Service, Fargo, North Dakota.

Nemecek-Marshall, M., R.C. MacDonald, J.J. Franzen, C.L. Wojciechowski and R. Fall. 1995. Methanol emission from leaves: Enzymatic detection of gas-phase methanol and relation of methanol fluxes to stomatal conductance and leaf development. Plant Physiology 108:1359-1368.

Niepel, M. and D.R. Gallie. 1999. Identification and characterization of the functional elements within the tobacco etch virus 5' leader required for cap-independent translation. Journal of Virology 73:9080-9088.

OECD. 1997. Consensus document on the biology of *Brassica napus* L. (oilseed rape). Series on Harmonization of Regulatory Oversight in Biotechnology No. 7. Organisation for Economic Co-operation and Development, Paris, France.

OECD. 2001. Consensus document on key nutrients and key toxicants in low erucic acid rapeseed (Canola). ENV/JM/MONO(2001)13. Organisation for Economic Co-operation and Development, Paris, France.

OECD. 2002. Report of the OECD workshop on the toxicological and nutritional testing of novel foods. SG/ICGB(1998)1/FINAL. Organisation for Economic Co-operation and Development, Paris, France.

OECD. 2011. Revised consensus document on compositional considerations for new varieties of low erucic acid rapeseed (canola): Key food and feed nutrients, anti-nutrients and toxicants. ENV/JM/MONO(2011)55. Organisation for Economic Co-operation and Development, Paris, France.

OECD. 2012. Consensus document on the biology of the *Brassica* crops (*Brassica* spp.). ENV/JM/MONO(2012)41. Series on Harmonisation of Regulatory Oversight in Biotechnology No. 54. Organisation for Economic Co-operation and Development, Paris, France.

OGTR. 2008. The biology of *Brassica napus* L. (canola). Australian Government, Department of Health and Ageing, Office of the Gene Technology Regulator, Canberra, ACT, Australia.

OGTR. 2011. The biology of *Brassica napa* L. (canola). Australian Government, Department of Health and Ageing, Office of the Gene Technology Regulator, Canberra, Australia.

Okuno, N.T., I.R. Freire, R.T.R.S. Segundo, C.R. Silva and V.A. Marin. 2018. Polymerase chain reaction assay for detection of *Stenotrophomonas maltophilia* in cheese samples based on the *sme*T gene. Current Mircobiology 75:1555-1559.

Okunuki, H., R. Techima, T. Shigeta, J. Sakushima, H. Akiyama, Y. Goda, M. Toyoda and J. Sawada. 2002. Increased digestibility of two products in genetically modified food (CP4 EPSPS and Cry1Ab) after preheating. Journal of the Food Hygienic Society of Japan 43:68-73.

Palleroni, N.J. and J.F. Bradbury. 1993. *Stenotrophomonas*, a new bacterial genus for *Xanthomonas maltophilia* (Hugh 1980) Swings et al. 1983. International Journal of Systematic Bacteriology 43:606-609.

Pariza, M.W. and E.A. Johnson. 2001. Evaluating the safety of microbial enzyme preparations used in food processing: Update for a new century. Regulatory Toxicology and Pharmacology 33:173-186.

Piper, K.R., S.B. von Bodman, I. Hwang and S.K. Farrand. 1999. Hierarchical gene regulatory systems arising from fortuitous gene associations: Controlling quorum sensing by the opine regulon in *Agrobacterium*. Molecular Microbiology 32:1077-1089.

Prado, J.R., G. Segers, T. Voelker, D. Carson, R. Dobert, J. Phillips, K. Cook, C. Cornejo, J. Monken, L. Grapes, T. Reynolds and S. Martino-Catt. 2014. Genetically engineered crops: From idea to product. Annual Review of Plant Biology 65:769-790.

Rademacher, T.W., R.B. Parekh and R.A. Dwek. 1988. Glycobiology. Annual Review of Biochemistry 57:785-838.

Radke, S.E., J.C. Turner and D. Facciotti. 1992. Transformation and regeneration of *Brassica rapa* using *Agrobacterium tumefaciens*. Plant Cell Reports 11:499-505.

Rathinasabapathi, B., M. Burnet, B.L. Russell, D.A. Gage, P.-C. Liao, G.J. Nye, P. Scott, J.H. Golbeck and A.D. Hanson. 1997. Choline monooxygenase, an unusual iron-sulfur enzyme catalyzing the first step of glycine betaine synthesis in plants: Prosthetic group characterization and cDNA cloning. Proceedings of the National Academy of Sciences of the United States of America 94:3454-3458.

Richins, R.D., H.B. Scholthof and R.J. Shepherd. 1987. Sequence of figwort mosaic virus DNA (caulimovirus group). Nucleic Acids Research 15:8451-8466.

Ridley, W.P., G.G. Harrigan, M.L. Breeze, M.A. Nemeth, R.S. Sidhu and K.C. Glenn. 2011. Evaluation of compositional equivalence for multitrait biotechnology crops. Journal of Agricultural and Food Chemistry 59:5865-5876.

Riter, L.S. 2018. Monsanto Method: ME-1869-03. "Determination of Dicamba and Major Metabolites in Raw Agricultural Commodities by LC-MS/MS". April 6, 2018.

Rogers, S.G. 2000. Promoter for transgenic plants. Patent 6,018,100, U.S. Patent Office, Washington, D.C.

Rosche, B., B. Tshisuaka, B. Hauer, F. Lingens and S. Fetzner. 1997. 2-oxo-1,2-dihydroquinoline 8-monooxygenase: Phylogenetic relationship to other multicomponent nonheme iron oxygenases. Journal of Bacteriology 179:3549-3554.

Russell, B.L., B. Rathinasabapathi and A.D. Hanson. 1998. Osmotic stress induces expression of choline monooxygenase in sugar beet and amaranth. Plant Physiology 116:859-865.

Ryan, R.P., S. Monchy, M. Cardinale, S. Taghavi, L. Crossman, M.B. Avison, G. Berg, D. van der Lelie and J.M. Dow. 2009. The versatility and adaptation of bacteria from the genus *Stenotrophomonas*. Nature Reviews Microbiology 7:514-525.

Salomon, S. and H. Puchta. 1998. Capture of genomic and T-DNA sequences during double-strand break repair in somatic plant cells. EMBO Journal 17:6086-6095.

Schmidt, C.L. and L. Shaw. 2001. A comprehensive phylogenetic analysis of Rieske and Rieske-type iron-sulfur proteins. Journal of Bioenergetics and Biomembranes 33:9-26.

Silvanovich, A., M.A. Nemeth, P. Song, R. Herman, L.Tagliani and G.A. Bannon. 2006. The value of short amino acid sequence matches for prediction of protein allergenicity. Toxicological Sciences 90:252-258.

Sjoblad, R.D., J.T. McClintock and R. Engler. 1992. Toxicological considerations for protein components of biological pesticide products. Regulatory Toxicology and Pharmacology 15:3-9.

Statistics Canada. 2018. Production of principal field crops, November 2018. Statistics Canada, Ottawa, Canada. https://www150.statcan.gc.ca/n1/daily-quotidien/181206/dq181206b-eng.htm [Accessed January 27, 2020].

Sutcliffe, J.G. 1979. Complete nucleotide sequence of the *Escherichia coli* plasmid pBR322. Cold Spring Harbor Symposia on Quantitative Biology 43:77-90.

Tashkov, W. 1996. Determination of formaldehyde in foods, biological media and technological materials by headspace gas chromatography. Chromatographia 43:625-627.

Taylor, M., A. Bickel, R. Mannion, E. Bell and G.G. Harrigan. 2017. Dicamba-tolerant soybeans (*Glycine max* L.) MON 87708 and MON 87708 × MON 89788 are compositionally equivalent to conventional soybean. Journal of Agricultural and Food Chemistry 65:8037-8045.

Thomas, K., M. Aalbers, G.A. Bannon, M. Bartels, R.J. Dearman, D.J. Esdaile, T.J. Fu, C.M. Glatt, N. Hadfield, C. Hatzos, S.L. Hefle, J.R. Heylings, R.E. Goodman, B. Henry, C. Herouet, M. Holsapple, G.S. Ladics, T.D. Landry, S.C. MacIntosh, E.A. Rice, L.S. Privalle, H.Y. Steiner, R. Teshima, R. van Ree, M. Woolhiser and J. Zawodny. 2004. A multi-laboratory evaluation of a common in vitro pepsin digestion assay protocol used in assessing the safety of novel proteins. Regulatory Toxicology and Pharmacology 39:87-98.

Thomas, K., G. Bannon, S. Hefle, C. Herouet, M. Holsapple, G. Ladics, S. MacIntosh and L. Privalle. 2005. In silico methods for evaluating human allergenicity to novel proteins: International Bioinformatics Workshop Meeting Report, 23-24 February 2005. Toxicological Sciences 88:307-310.

Todaro, M., N. Francesca, S. Reale, G. Moschetti, F. Vitale and L. Settanni. 2011. Effect of different salting technologies on the chemical and microbiological characteristics of PDO Pecorino Siciliano cheese. European Food Research and Technology 233:931-940.

U.S. CPSC. 1997. An update on formaldehyde. U.S. Consumer Product Safety Commission, Washington, D.C.

U.S. EPA. 1996. Residue chemistry test guidelines: Nature of the residue - Plants, livestock. OPPTS 860.1300. U.S. Environmental Protection Agency, Washington, D.C.

U.S. EPA. 2008. Reregistration eligibility decision for formaldehyde and paraformaldehyde. EPA 739-R-08-004. U.S. Environmental Protection Agency, Washington, D.C.

U.S. EPA. 2009a. Memorandum: Correction to the amendments to the dicamba RED. U.S. Environmental Protection Agency, Washington, D.C.

U.S. EPA. 2009b. Reregistration eligibility decision for dicamba and associated salts. U.S. Environmental Protection Agency, Washington, D.C.

U.S. FDA. 2006. Qualified health claims: Letter of enforcement discretion - Unsaturated fatty acids from canola oil and reduced risk of coronary heart diesease (Docket No. 2006Q-0091). U.S. Food and Drug Administration, Washington, D.C. http://wayback.archive-it.org/7993/20171114183734/https:/www.fda.gov/Food/IngredientsPackagingLabeling/LabelingNutrition/ucm072958.htm [Accessed May 1, 2020].

USDA-FAS. 2019. Oilseeds: World markets and trade. U.S. Department of Agriculture, Foreign Agricultural Service, Washington, D.C. https://downloads.usda.library.cornell.edu/usda-esmis/files/tx31qh68h/7d2797406/cj82kp34g/oilseeds.pdf [Accessed May 1, 2020].

USDA-NASS. 2017. 2017 Census of Agriculture: United States Summary and State Data. U.S. Department of Agriculture, National Agricultural Statistics Service, Washington, D.C.

USHHS-ATSDR. 1999. Toxicological profile for formaldehyde. U.S. Department of Health and Human Services, Agency for Toxic Substances and Disease Registry, Washington, D.C.

USHHS-NTP. 2011. Report on carcinogens. U.S. Department of Health and Human Services, National Toxicology Program, Washington, D.C.

Vassilopoulou, E., N. Rigby, F.J. Moreno, L. Zuidmeer, J. Akkerdaas, I. Tassios, N.G. Papadopoulos, P. Saxoni-Papageorgiou, R. van Ree and C. Mills. 2006. Effect of *in vitro* gastric and duodenal digestion on the allergenicity of grape lipid transfer protein. Journal of Allergy and Clinical Immunology 118:473-480.

Venkatesh, T.V., M.L. Breeze, K. Liu, G.G. Harrigan and A.H. Culler. 2014. Compositional analysis of grain and forage from MON 87427, an inducible male sterile and tissue selective glyphosate-tolerant maize product for hybrid seed production. Journal of Agricultural and Food Chemistry 62:1964-1973.

Vieths, S., J. Reindl, U. Müller, A. Hoffmann and D. Haustein. 1999. Digestibility of peanut and hazelnut allergens investigated by a simple in vitro procedure. European Food Research and Technology 209:379-388.

Wang, C., K.C. Glenn, C. Kessenich, E. Bell, L.A. Burzio, M.S. Koch, B. Li and A. Silvanovich. 2016. Safety assessment of dicamba mono-oxygenases that confer dicamba tolerance to various crops. Regulatory Toxicology and Pharmacology 81:171-182.

Wang, X.-Z., B. Li, P.L. Herman and D.P. Weeks. 1997. A three-component enzyme system catalyzes the O demethylation of the herbicide dicamba in *Pseudomonas maltophilia* DI-6. Applied and Environmental Microbiology 63:1623-1626.

Werlen, C., H.-P.E. Kohler and J.R. van der Meer. 1996. The broad substrate chlorobenzene dioxygenase and *cis*-chlorobenzene dihydrodiol dehydrogenase of *Pseudomonas* sp. strain P51 are linked evolutionarily to the enzymes for benzene and toluene degradation. Journal of Biological Chemistry 271:4009-4016.

WHO. 2002. Concise international chemical assessment document 40: Formaldehyde. World Health Organization, Geneva, Switzerland.

Yagami, T., Y. Haishima, A. Nakamura, H. Osuna and Z. Ikezawa. 2000. Digestibility of allergens extracted from natural rubber latex and vegetable foods. Journal of Allergy and Clinical Immunology 106:752-762.

Yang, L., C. Wang, A. Holst-Jensen, D. Morisset, Y. Lin and D. Zhang. 2013. Characterization of GM events by insert knowledge adapted re-sequencing approaches. Scientific Reports 3:2839.

Ye, X., E.J. Williams, J. Shen, S. Johnson, B. Lowe, S. Radke, S. Strickland, J.A. Esser, M.W. Petersen and L.A. Gilbertson. 2011. Enhanced production of single copy backbone-free transgenic plants in multiple crop species using binary vectors with a pRi replication origin in *Agrobacterium tumefaciens*. Transgenic Research 20:773-786.

Zambryski, P., A. Depicker, K. Kruger and H.M. Goodman. 1982. Tumor induction by *Agrobacterium tumefaciens*: Analysis of the boundaries of T-DNA. Journal of Molecular and Applied Genetics 1:361-370.

Zastrow-Hayes, G.M., H. Lin, A.L. Sigmund, J.L. Hoffman, C.M. Alarcon, K.R. Hayes, T.A. Richmond, J.A. Jeddeloh, G.D. May and M.K. Beatty. 2015. Southern-by-sequencing: A robust screening approach for molecular characterization of genetically modified crops. The Plant Genome 8:1-15.

Zhou, J., G.G. Harrigan, K.H. Berman, E.G. Webb, T.H. Klusmeyer and M.A. Nemeth. 2011. Stability in the composition equivalence of grain from insect-protected maize and seed from glyphosate-tolerant soybean to conventional counterparts over multiple seasons, locations, and breeding germplasms. Journal of Agricultural and Food Chemistry 59:8822-8828.